THE ROLE OF OXYGEN DELIVERY IN MEDIATING VOLUNTARY EXCITATION-CONTRACTION COUPLING: AN OXYGEN CONFORMING RESPONSE OF MUSCLE CONTRACTION FORCE

by

Patrick Jonathan Drouin

A thesis submitted to the School of Kinesiology and Health Studies

In conformity with the requirements for

the degree of Doctor of Philosophy

Queen's University

Kingston, Ontario, Canada

(September 2023)

Abstract

As we exercise long and/or hard enough, exercise related metabolites impair the ability of muscle excitation to cause muscle contraction – reflecting an impairment of excitation-contraction coupling. Like metabolite mediated impairment, a decrease in oxygen delivery can also impair excitation-contraction coupling. During electrically stimulated exercise (i.e., maintained muscle excitation), when muscle oxygen delivery decreases, muscle contraction force decreases to protect the metabolic environment (i.e., muscle metabolites). What's interesting about this phenomenon, and what distinguishes it from metabolite mediated impairment of excitation-contraction coupling, is that when normal oxygen delivery is restored, muscle contraction force per excitation is rapidly reversed back to normal levels. Because muscle contraction force conforms to oxygen delivery, we have termed this phenomenon the oxygen conforming response. To date this oxygen conforming response has only been demonstrated under electrically stimulated exercise designs where key characteristics of voluntary muscle recruitment are violated. Therefore, the general purpose of this dissertation was to assess whether the key characteristics of this oxygen conforming response exist during voluntary exercise in humans. In thesis study 1, we developed a model enabling forearm muscle excitation targeted exercise and then we used brachial artery compression to reversibly reduce forearm blood flow by ~50%. By doing so, we demonstrated that muscle contraction force rapidly follows changes in oxygen delivery at or above 75% critical force exercise intensities – demonstrating the existence and exercise intensity dependence of the oxygen conforming response. Next, thesis study 2 used a remote skeletal metaboreflex to reversibly increase forearm blood flow. By doing so we demonstrated that an increase in oxygen delivery above 'normal' can reversibly improve excitation-contraction coupling. Finally, thesis study 3 used arm position to alter forearm perfusion pressure during maximal effort exercise. By doing so we demonstrated that oxygen conforming can (a) modify the progressive decline of muscle contraction force and (b) rapidly shift the stabilized muscle contraction critical force. Combined, these key findings highlight the underappreciated cellular disturbance

independent role oxygen delivery can play in modifying excitation-contraction coupling. Critically, this dissertation has only begun to shed light on this oxygen conforming phenomenon that – like skeletal muscle fatigue – deserves continued attention.

Co-Authorship

This dissertation is the work of Patrick Jonathan Drouin in collaboration with his supervisor Dr. Michael E. Tschakovsky.

Chapter 3 is published as:

Drouin PJ, Forbes SPA, Liu T, Lew LA, McGarity-Shipley E & Tschakovsky ME. Muscle contraction force conforms to muscle oxygenation during constant-activation voluntary forearm exercise. Exp Physiol 107, 1360-1374, 2020. P.J.D. and M.E.T. conceived and designed research; P.J.D., S.P.A.F., T.L., L.L. and E.M.S. performed experiments; P.J.D. analyzed data; P.J.D. and M.E.T. interpreted results of experiments; P.J.D. prepared figures and tables; P.J.D. drafted manuscript; P.J.D., S.P.A.F., T.L., L.L., E.M.S. and M.E.T. edited and revised manuscript; P.J.D., S.P.A.F., T.L., L.L., E.M.S. and M.E.T. approved final version of manuscript. P.J.D., S.P.A.F., T.L., L.L., E.M.S. and M.E.T. agree to be accountable for all aspects of the work in ensuring that questions related to accuracy or integrity of any part of the work are appropriately investigated and resolved. P.J.D., S.P.A.F., T.L., L.L., E.M.S. and M.E.T. qualify for authorship, and all those who qualify for authorship are listed.

Chapter 4 is published as:

Drouin PJ, Liu T, Lew LA, McGarity-Shipley E & Tschakovsky ME. The 'normal' adjustment of oxygen delivery to small muscle mass exercise is not optimized for muscle contractile function. J Physiol 601, 783-799, 2023. P.J.D. and M.E.T. conceived and designed research; P.J.D., T.L., L.L. and E.M.S. performed experiments; P.J.D. analyzed data; P.J.D. and M.E.T. interpreted results of experiments; P.J.D. prepared figures and tables; P.J.D. drafted manuscript; P.J.D., T.L., L.L., E.M.S. and M.E.T. edited and revised manuscript; P.J.D., T.L., L.L., E.M.S. and M.E.T. approved final version of manuscript. P.J.D., T.L., L.L., E.M.S. and M.E.T. agree to be accountable for all aspects of the work in ensuring that questions related to accuracy or integrity of any part of the work are appropriately investigated and resolved. P.J.D., T.L., L.L., E.M.S. and M.E.T. qualify for authorship, and all those who qualify for authorship are listed.

Chapter 5 is under review as:

P.J. Drouin, S.P.S. Mladen, S.P.A. Forbes, A.K. Zedic, S.P.B Inouye, E.N. Beaudette & M.E. Tschakovsky. Effect of altering oxygen delivery on excitation contraction-coupling during maximal effort forearm exercise: role of oxygen conforming response. JP-RP-2023-285215. P.J.D. and M.E.T. conceived and designed research; P.J.D., S.P.S.M., S.P.A.F., A.K.Z., S.P.B.I., and E.N.B. performed experiments; P.J.D. analyzed data; P.J.D. and M.E.T. interpreted results of experiments; P.J.D. prepared figures and tables; P.J.D. drafted manuscript; P.J.D., S.P.S.M., S.P.A.F., A.K.Z., S.P.B.I., E.N.B. and M.E.T. edited and revised manuscript; P.J.D., S.P.S.M., S.P.A.F., A.K.Z., S.P.B.I., E.N.B. and M.E.T. approved final version of manuscript. P.J.D., S.P.S.M., S.P.A.F., A.K.Z., S.P.B.I., E.N.B. and M.E.T. agree to be accountable for all aspects of the work in ensuring that questions related to accuracy or integrity of any part of the work are appropriately investigated and resolved. P.J.D., S.P.S.M., S.P.A.F., A.K.Z., S.P.B.I., E.N.B. and M.E.T. qualify for authorship, and all those who qualify for authorship are listed.

Acknowledgements

Like the ability of an oxygen conforming response to act positively in opposition of on-going negative cellular disturbance mediated force depression, a leader is able counteract our own negativity with their supportive leadership. Dr. T, it is the extra effort that you have put into recognizing my efforts and highlighting the positive aspects of my work that, to me, makes you more than just a 'supervisor'. You are a true leader and someone that I will always look up to as I continue to develop as a person and professional. I am very fortunate to have had your guidance and support over the past 7+ years. Thank you for helping me learn to think, listen, write and, of course, fish. I will never forget that day we both snorkeled with and caught 77 bass offshore of Main Duck Island. Proof of your 50th catch of the day (yes… you out fished me by almost double):

To my wife, Désirée, thank you for being my biggest supporter and for celebrating my academic successes when I have been hesitant to do so myself. To Dr. McGarity-Shipley and Lindsay Lew, thank you for stepping up in a time of need to help me get my first two thesis studies completed. I would, no doubt, still be in data collection if it weren't for your selfless assistance. To my HVCL colleagues, thank you for putting up with my many hours of data collection, I could not have done this without you all. In particular, thank you to Emma Beaudette for stepping up and being my unofficial HVCL guinea pig, helping me to develop, somewhat, tolerable methodologies. Cheers!

Table of Contents

List of Figures

List of Tables

List of Abbreviations

ADP	Adenosine Diphosphate
AMP	Adenosine Monophosphate
ANOVA	Analysis of Variance
ATP	Adenosine Triphosphate
BAC	Brachial Artery Compression
Ca^{2+}	Calcium
CI	Critical Impulse
CI	Confidence Interval
CP	Critical Power
EMG	Electromyography
EPSP	Excitatory Postsynaptic Potential
ETC	Electron Transport Chain
FAD	Flavin Adenine Dinucleotide
$FADH_2$	Flavin Adenine Dinucleotide + Hydrogen
FBF	Forearm Blood Flow
FDP	Flexor Digitorum Profundus
FDS	Flexor Digitorum Superficialis
FVC	Forearm Vascular Conductance
GTP	Guanosine Triphosphate
H^+	Hydrogen Ions

H_2O Water

HPP High Perfusion Pressure

IPSP Inhibitory Postsynaptic Potential

LPP Low Perfusion Pressure

MAP Mean Arterial Blood Pressure

MAUI Measurements from Arterial Ultrasound Imaging

MBV Mean Blood Velocity

MVC Maximal Voluntary Contraction

NAD^+ Nicotinamide Adenine Dinucleotide

NADH Nicotinamide Adenine Dinucleotide + Hydrogen

NIRS Near Infrared Spectroscopy

NSERC Natural Sciences and Engineering Research Council

O_2 Oxygen

PCr Phosphocreatine

PFK Phosphofructokinase

P_i Inorganic Phosphate

PK Pyruvate Kinase

RMS Root Mean Square

SC Sham Compression

SD Standard Deviation

SENIAM Surface ElectroMyoGraphy for the Non-Invasive Assessment of Muscles

SNARE Soluble N-ethylmaleimide-sensitive factor activating protein receptor

TCA Tricarboxylic Acid Cycle

VO_2 Rate of Oxygen Consumption

Chapter 1

General Introduction

There is no debating the importance of oxygen for continued human life on earth. Though many of us may not understand the physiology behind the difficulties of living at high altitude (where the partial pressure of oxygen is low) most of us are familiar with the idea that there is an oxygen limitation making sustained life difficult or even impossible. Although this example of high altitude living makes the point that oxygen is important for sustained life, high altitude living is not relevant to most human beings (Beall, 2014). Many of us are fortunate to live under circumstances where we are less concerned about survival, and instead we are more concerned about how we can improve our physical and mental wellbeing. A well accepted method of improving physical and mental wellbeing is through physical activity (unstructured) or exercise (structured) (Fontaine, 2000; Ganjeh et al., 2021; Ho et al., 2015; Knapen et al., 2015; Thorsteinsdottir et al., 2018; Wasserman, 2019). Unfortunately, our ability to benefit from exercise is limited firstly by our willingness to perform it, and secondly, by our ability to tolerate it (Crewe et al., 2008; Eston et al., 2007; Nakamura et al., 2008; Venhorst et al., 2018a, 2018b). Critically, our ability to tolerate exercise will directly impact our willingness to continue performing it (Venhorst et al., 2018a, 2018b). Therefore, understanding contributors to exercise tolerance is critical to supporting improved exercise adherence. Although this dissertation will focus on basic physiological mechanisms, the direction of this dissertation stems from a desire to understand the contribution of oxygen to exercise tolerance.

During exercise, oxygen needs to be delivered at adequate rates to support the production of adenosine triphosphate (ATP) through oxidative phosphorylation. To support the delivery of oxygen to the muscle, there is (a) an increased dilation of exercising muscle arterioles (i.e., increased conductance), (b) a maintenance or increase in arterial blood pressure, and (c) a maintenance of normal arterial blood oxygen content. Combined, muscle oxygen delivery reflects the product of blood flow (arteriole conductance x blood pressure) multiplied by arterial blood oxygen content.

In apparently healthy humans, our bodies are generally very good at matching oxygen delivery to demand (Gonzalez-Alonso et al., 2002; Gonzalez-Alonso et al., 2001; Hogan et al., 1983; Radegran, 1997; Richardson et al., 1995). Even with this apparently good matching of oxygen delivery to demand, if the exercise intensity is high enough or continues for long enough, we experience a decline in exercise performance – termed performance fatiguability (Black et al., 2017; Hunter, 2018). Although performance fatiguability will occur during most physical tasks (Hunter, 2018), most of us are unaware of the specific mechanisms occurring in the muscle while exercise is ongoing, rather, we experience a subjective increase in effort to maintain the same exercise intensity – termed perceived fatigability (Venhorst et al., 2018a, 2018b). Although most of us can relate more to the experience of altered perceived fatigability during exercise, it is primarily the changes to performance fatigability that contribute to these subjective perceptions and therefore this dissertation focuses on measures of performance rather than perceived fatigability.

For exercise to occur, the brain sends an excitatory electrical signal via the spinal cord to the muscle. This excitatory electrical signal leads to a chain of events causing muscle contraction – this process is referred to as excitation-contraction coupling. As exercise continues, there is a build-up of metabolites (the byproduct of metabolic reactions), and these metabolites interfere with excitation-contraction coupling. As exercise intensity increases there is an increasing build-up of these metabolites exacerbating the compromise to the efficacy of excitation-contraction coupling (Debold, 2016; Parsons et al., 1997). Importantly, unless you stop exercising or reduce the exercise intensity, you cannot reverse the metabolite associated compromise to excitation-contraction coupling (Pitcher & Miles, 1997; Romer et al., 2006). Even once exercise is terminated, excitation-contraction coupling remains compromised for some time (e.g., several minutes to days).

Like the metabolite-mediated compromise, a reduction in oxygen delivery can also impair excitation-contraction coupling. To eliminate the variability associated with voluntary human exercise, this phenomenon has been typically demonstrated under models that bypass the natural excitation of the muscle. That is, many experimental designs have used an electrical stimulator over the muscle belly or nerve to create muscle contraction (Fitzpatrick et al., 1996; Luu & Fitzpatrick, 2013). With this electrical stimulation model, several authors have demonstrated that muscle contraction force (the outcome of excitation-contraction coupling) decreases along with oxygen delivery (Fitzpatrick et al., 1996; Hobbs & McCloskey, 1987; Hogan et al., 1996; Luu & Fitzpatrick, 2013). This decrease in muscle contraction force with oxygen delivery is objectively negative, however, it is occurring for a good cause. By allowing muscle contraction force to decrease with reduced oxygen delivery, disturbance of the muscle's metabolic environment is prevented (metabolites in the muscle) (Hogan et al., 1996). These observations highlight the muscles inherent response to a decrease in muscle oxygen delivery; metabolic demand decreases (the negative) to protect the metabolic environment (the positive). As opposed to metabolite-mediated compromise to excitation-contraction coupling, muscle contraction force is rapidly reversable with oxygen delivery (Fitzpatrick et al., 1996; Hobbs & McCloskey, 1987; Luu & Fitzpatrick, 2013). Critically, this modulation of muscle contraction force at a given muscle excitation can occur while exercise is ongoing. Given that muscle contraction force conforms to oxygen delivery, we have termed this phenomenon the oxygen conforming response of muscle contraction force.

In summary, from electrically stimulated exercise models, we can describe the oxygen conforming response as having the following key characteristics: (a) muscle contraction force at a given muscle excitation rapidly conforms to oxygen delivery, (b) muscle contraction force rapidly recovers upon restoration of normal oxygen delivery, and (c) muscle contraction force alterations at a maintained muscle excitation occur without disturbance to the metabolic environment. Although this electrical stimulation work has been important in characterizing the oxygen conforming response, electrical stimulation violates characteristics of voluntarily activated muscle and neither muscle blood flow nor oxygenation has been concomitantly measured. Therefore, it remained to be determined whether muscle contraction force follows changes in oxygen delivery during voluntary muscle contractions in humans. Accordingly, the general objective of this dissertation was to assess whether the key characteristics of this oxygen conforming response exist during voluntary exercise in humans.

In line with the aforementioned general objective, the order of thesis experiments was planned to inform methodological design for subsequent thesis experiments. In the first thesis experiment, by designing an experimental model that would permit human participants to voluntarily target a given level of muscle excitation, we could assess whether muscle contraction force would follow changes in muscle oxygen delivery. Furthermore, to inform subsequent experimental designs, we assessed whether the oxygen conforming response is exercise intensity dependent. In the second thesis experiment, we assessed whether an increase in oxygen delivery above normal levels could reversibly improve the relationship between muscle contraction force and excitation. In the third thesis experiment, we assessed whether changes in oxygen delivery could rapidly alter muscle contraction force during maximal effort exercise.

The importance of herein thesis experiments stems from an underappreciation of oxygen conforming contributions to performance fatigability. Although it is appreciated that reduced oxygen delivery can impair excitation-contraction coupling (Poole et al., 2016), the specific methods by which oxygen can affect excitation-contraction coupling are left out of focus. Critically, given that oxygen delivery is compromised with age (Betik & Hepple, 2008; Proctor et al., 2004; Proctor et al., 1998) and disease (Dean, 1997), understanding the role oxygen delivery can play in altering excitation-contraction coupling is vital to understanding the difficulties associated with being physically active. Significantly, the work herein, examining the role of oxygen conforming during voluntary human exercise, will set the stage for important future work into understanding

(a) what its mechanisms are, (b) whether it exists and how it might affect exercise in age and disease, and (c) whether it can feasibly be improved with interventions.

Chapter 2

Literature Review

2.1 Essential neurophysiology and biochemistry of exercise

Beginning in the cerebral cortex, a motor program is generated from the combined activity of the premotor, supplementary motor, and primary motor cortices. An excitatory signal travels along the corticospinal tract where upon arrival at the junction between the medulla and the spinal cord, 75-90% of corticospinal fibers decussate forming the lateral corticospinal tract (Holodny et al., 2005). Most of these fibers will then terminate at spinal interneurons that will then synapse with lower motoneurons.

When an excitatory signal arrives at an excitatory synapse on the dendrites (i.e., part of the receptive segment) of the lower motoneuron – located within the anterior horn of the spinal cord – a synaptic potential is propagated along the motoneuron cell body (i.e., soma) (Larkum et al., 1998). A single excitatory postsynaptic potential (EPSP) is insufficient to cause an action potential – summation of several EPSP's is necessary and it must work against inhibitory post-synaptic potentials (IPSP). The integration of EPSP's and IPSP's occurs at the initial segment of the motoneuron and if there is sufficient excitatory input (i.e., exceeds the initial segment motoneuron threshold: ~ -45 mV) at the initial segment, an action potential is generated along the axon. Smaller motoneurons (usually measured through axon thickness) are more excitable (i.e., have a lower excitation threshold) and therefore require less excitatory input at the initial segment for action potential generation – resulting in smaller motoneurons being recruited first (Henneman, 1985; Henneman et al., 1965; Milner-Brown et al., 1973; Olson et al., 1968; Zajac & Faden, 1985). The integrated potential activates voltage gated channels – causing sodium channels to open first (Larkum et al., 1998; Magee & Johnston, 1995). Upon allowing sodium to enter the neuron cytosol, the membrane potential goes from ~ -60-70 mV to +30 mV – this voltage spike is called the action potential. Within 1-ms the sodium channels close, and potassium channels open, thereby stopping sodium from entering the cell and allowing potassium to exit the cell (Magee & Johnston, 1995), causing a rapid repolarization or even hyperpolarization. As quickly as they opened, potassium channels close again. Sodium potassium ATPase help restore the resting potential (Pivovarov et al., 2018).

The action potential continues to propagate – in an all or none fashion – along the axon taking advantage of myelination to rapidly (through saltatory conduction) – and more efficiently (i.e., reduced ATP cost) – reach the synaptic segment of the neuron (Cohen et al., 2020; Hartline & Colman, 2007). Upon arrival of the action potential at the synaptic segment of the motoneuron, voltage gated calcium channels are activated at the terminal of the presynaptic membrane – this causes calcium to enter the presynaptic terminal (Mochida, 2019). This increase in cytosolic calcium is sensed by synaptotagmin 1 and undergoes a change with the SNARE (Soluble N-ethylmaleimide-sensitive factor activating protein receptor) complex causing fusion of synaptic vesicles to the nerve terminal of the presynaptic membrane (Mochida, 2019). Through exocytosis, these synaptic vesicles release their contents (i.e., ~10,000 acetylcholine molecules) into the synaptic cleft (Mochida, 2019). Acetylcholine binds to the two sites on a single nicotinic acetylcholine receptor on the motor endplate (postsynaptic membrane) causing ligand-gated ion channels to open – making the endplate equally permeable to sodium and potassium ions (Hogg et al., 2003). Much sodium enters the muscle cytosol, and some potassium exits the cytosol. Combined with the opening of voltage-gated sodium channels, the endplate potential shifts from -90 mV to -45 mV causing action potential propagation along the skeletal muscle membrane (i.e., sarcolemma) and into the muscle fiber via transverse tubules. Like in the neuron, to repolarize the muscle cell, voltage-gated potassium channels open shortly after voltage-gated sodium channels open and close. Simultaneously, sodium potassium ATPase restores the resting potential. The resetting of the resting potential is necessary before a new endplate potential can be generated (Therien & Blostein, 2000). Therefore, ATP availability will determine the rate of sodium potassium ATPase mediated resetting of the endplate resting potential. This reflects the <u>**first site**</u>

of ATP demand in the muscle. Electromyography is the technique used to detect changes in muscle fiber membrane voltages – reflecting muscle excitation (Vigotsky et al., 2017).

Within the transverse tubules an action potential activates the calcium release unit – formed of ryanodine and dihydropyridine receptors. The sarcoplasmic reticulum then releases calcium into the cytosol (100-fold concentration increase). These high concentrations of calcium create a favourable environment for calcium to bind to troponin C on tropomyosin filaments – causing a conformation change. This conformation change causes troponin I to detach from F-actin thereby allowing tropomyosin to move out of the binding site of myosin on F-actin. Simultaneously, myosin ATPase hydrolyzes ATP and then binds to the open F-actin binding site. Myosin ATPase is the **second site** of ATP demand in the muscle. The power stroke then occurs, moving the thin filament in relation to the thick filament while simultaneously liberating the myosin ATPase of ADP and Pi. ATP will then enter the active site causing actin and myosin to detach – restarting the muscle contraction cycle. Between muscle contractions it is necessary for the calcium ATPase to sequester calcium from the cytosol back to the sarcoplasmic reticulum (2 calcium per ATP) so that (a) the muscle can relax and (b) calcium concentrations in the sarcoplasmic reticulum are restored – preparing for another volley of action potentials. Calcium ATPase mediated calcium sequestering reflects the **third site** of ATP demand in the muscle. Importantly, it is thought that calcium sequestering (back into the sarcoplasmic reticulum) by calcium ATPase accounts for one third of the ATP cost of skeletal muscle – with the rest accounted for by myosin ATPase activity (Mougios, 2020). The cost of resetting the endplate potential by sodium potassium ATPase in this total is not clear. Next, we will summarize how ATP is generated to support the three key sites of ATP demand within the muscle during continuous exercise.

2.2 Oxygen dependence in metabolism

The release of energy through metabolism is required to support the production of adenosine triphosphate (ATP) necessary for exercise. The production of ATP is firstly dependent on macromolecules which are consumed as food and broken down into their smaller constituents (i.e., carbohydrates, lipids, proteins). Once carbohydrates (i.e., one source of energy) are broken down into glucose, glycogen can be synthesized, or glucose can continue to circulate in the blood until it is required for energy production. Glucose is firstly converted to glucose 6-phosphate whereas glycogen is converted to glucose 1-phosphate and then glucose 6-phosphate. Once converted to glucose 6-phosphate, glycolysis (i.e., conversion of glucose to pyruvate) continues through the remaining nine steps to produce 2 pyruvates as well as 2 NADH (converted to 2 $FADH_2$ in the mitochondria) and 2 ATP. The 2 pyruvates enter the mitochondrial matrix where they are then oxidized into 2 acetyl-CoA, yielding 2 CO_2 and 2 NADH. Following the conversion of pyruvate to acetyl-CoA, in the mitochondrion, the 2 acetyl-CoA enter the citric acid cycle where a number of high energy molecules are produced, yielding 4 CO_2, 2 GTP (nearly equivalent to ATP), 6 NADH and 2 $FADH_2$ (Mougios, 2006, 2020). In the inner mitochondrial membrane the NADH and $FADH_2$ yielded from the citric acid cycle donates a pair of electrons to NADH-Q oxidoreductase and ubiquinone, respectively (Mougios, 2006, 2020). The donated electrons continue to be passed forward until they are donated to O_2. The aforementioned donation process is known as the electron transport chain and provides a considerable amount of energy (sum $\Delta G^o = -100.6\ \text{kcal} \cdot \text{mol}^{-1}$) required for oxidative phosphorylation (Mougios, 2006, 2020). Additionally, the electron transport chain yields 2 H_2O, 1 NAD^+ and 1 FAD needed for the citric acid cycle to continue. During the electron transport process, hydrogen ions (H^+) are actively pumped from the mitochondrial matrix into the intermembrane space. These H^+ are required for oxidative phosphorylation. Oxidative phosphorylation is the process of synthesizing ATP and H_2O from ADP, P_i and H^+ through its endergonic reaction requiring energy released from the oxygen dependent electron transport chain. Ultimately, for every NADH and $FADH_2$ oxidized, it is thought that 2.5 and 1.5 ATP are synthesized, respectively (Mougios, 2006, 2020).

To summarize, through carbohydrate oxidation a total of 8 NADH and 4 $FADH_2$ are formed. Through the oxygen dependent electron transport chain and oxidative phosphorylation 26 ATP are synthesized (6 O_2 required). Summed with the 2 ATP produced during glycolysis and 2 ATP produced during the citric acid cycle, 30 ATP are produced from a single glucose molecule (Mougios, 2006, 2020). Ultimately then, ~87% of ATP produced during glucose metabolism is dependent on oxygen availability. Next, we will discuss how the metabolic environment determines exercise intensity domains.

2.3 Metabolic environment across exercise intensity domains

2.3.1 Moderate vs. heavy exercise intensities

Now that (a) we understand where ATP is needed in the muscle to support continuous exercise and (b) we appreciate the importance of oxygen availability for ATP production, I can describe exercise intensity domains in regard to their differences in metabolic environment. As exercise intensity increases, an exercise mediated decrease in ATP and phosphocreatine (PCr) activates phosphofructokinase (PFK) and pyruvate kinase (PK), while an increase in AMP and ADP activates PFK and PK, respectively (Mougios, 2006, 2020). Combined, an increase in PFK and PK contribute to an increased glycolytic flux. By increasing glycolytic flux, the rate of pyruvate and NADH production is increased. When exercise becomes more severe, the increased glycolytic flux can cause NAD^+ utilization to exceed the rate of NAD^+ regeneration – causing an increase in the [NADH]/[NAD^+] ratio and therefore slowing the conversion of pyruvate to acetyl CoA. Importantly, if NAD^+ becomes limited, glycolysis can slow or even stop if NAD^+ becomes depleted. This phenomenon is thought to occur as a result of the rate of glycolysis exceeding the rate of NADH electron donation to O_2. Due to the slower rate of NAD^+ regeneration via the electron transport chain, the higher concentrations of NADH and pyruvate will favour the conversion of pyruvate to lactate (Mougios, 2006, 2020). Importantly, lactate dehydrogenase uses NADH as the oxidant for this reaction and therefore NAD^+ is regenerated to continue glycolysis and the citric acid cycle. This process is critical because although anaerobic glucose catabolism (i.e., conversion of glucose to lactate) is an inefficient use of glucose, it is rapid, producing close to three times the amount of ATP produced via aerobic metabolism in the same time span (Mougios, 2006, 2020). Therefore, when ATP demand is high, the rate of anaerobic glucose catabolism increases to maintain the rate of ATP production. Ultimately then, when exercise becomes more severe – stimulating increased glycolytic flux – the rate of anaerobic glucose catabolism increases and lactate concentrations increase. The lactate threshold – reflecting the exercise intensity at which blood lactate concentrations increase by 1 mmol · L above resting levels – is therefore used to separate moderate from heavy exercise intensity domains. Critically, despite an accumulation of lactate above the lactate threshold, a steady state of the metabolic environment can be achieved during heavy intensity exercise (Black et al., 2017). In summary then, despite an increase in lactate accumulation, indicating an increase in the rate of ATP produced via anaerobic carbohydrate catabolism, during heavy exercise, ATP production can meet ATP demand (see Appendix B).

2.3.2 Heavy vs. severe exercise intensities

To demarcate heavy from severe intensity exercise, it is common practice to identify the target muscle(s) critical power or critical force output – critical force will be used here on out. Critical force refers to the maximal force output at which a steady state in ATP production and ATP demand can be achieved (Black et al., 2017; Poole et al., 2016). Above critical force, ATP production cannot meet ATP demand for extended periods, relying heavily on anaerobic sources of ATP production (Black et al., 2017; Poole et al., 2016). Therefore, when exercise is performed above critical force, the mismatch between ATP demand and ATP production, in association with an increase in exercise related metabolites, ultimately contributes to task failure. Importantly, the accumulation of exercise related metabolites is involved in the development of skeletal muscle fatigue. Specifically, by precipitating calcium in the sarcoplasmic reticulum, increased levels of inorganic phosphate impair excitation-contraction coupling by reducing the release of free Ca^{2+} from the sarcoplasmic reticulum (Allen & Trajanovska, 2012; Dutka et al., 2005; Westerblad & Allen, 1996; Westerblad et al., 1993). Furthermore, increased accumulation of P_i and H^+ contributes to decreased affinity of calcium binding to troponin C on tropomyosin filaments – causing reduced calcium binding and therefore reduced thin filament activation (Debold, 2016). Finally, an accumulation of P_i – by reducing the number of strongly bound actin-myosin heads – is thought to reduce thin filament activation (Parsons et al., 1997). Combined the increased accumulation of P_i

and H^+ at higher exercise intensities, in addition to the reduced sarcoplasmic reticulum release of free calcium is thought to cause the majority of force depression seen during exercise (Debold, 2016).

In addition to metabolically-mediated skeletal muscle fatigue, an increase in exercise intensity can contribute to skeletal muscle damage, thereby impairing the calcium release unit and reducing the calcium released for a given action potential (Carson et al., 2002). Together, the aforementioned fatigue mechanisms impair the skeletal muscle's ability to generate force. It is the rate of this skeletal muscle fatigue development that demarcates heavy from severe exercise. Below critical force, skeletal muscle fatigue develops slowly, eventually contributing to task failure, whereas above critical force, skeletal muscle fatigue develops much more quickly thereby contributing to a more rapid time to task failure (Burnley et al., 2010; Burnley et al., 2012).

In summary then, exercise intensities below the lactate threshold are moderate where limited accumulation of lactate occurs (Black et al., 2017). Above the lactate threshold and below critical force, exercise intensities are heavy where lactate accumulates, indicating an increased contribution of ATP production through anaerobic carbohydrate catabolism (Black et al., 2017; Mougios, 2006, 2020). Despite the accumulation of lactate during heavy exercise, steady state exercise (i.e., levels of metabolites stabilize) can be achieved, thereby indicating that during heavy exercise, ATP supply can meet ATP demand (Black et al., 2017). Above critical force – reflecting severe exercise intensities – a steady state in the rate of ATP supply matching ATP demand cannot be achieved (Black et al., 2017). Therefore, the identification of a critical force plateau is essential for the prescription of exercise work rates between the high (i.e., steady state achievable) and severe (i.e., steady state unachievable) exercise intensity domains.

2.4 How do changes in local oxygen delivery affect muscle excitation-contraction coupling?

In section 2.1 I identified where ATP is needed in the exercising muscle, in section 2.2 I have demonstrated the importance of oxygen availability for continued ATP production during continuous exercise and in section 2.3 I demonstrated how differences in metabolic environment determine exercise intensity domains. Now I will discuss the impact of changes in local oxygen delivery during maintained muscle excitation or force of contraction maintenance exercise. Considered studies will only be those that directly manipulated local oxygen delivery and not those manipulating fraction of oxygen in the inspired air. Importantly, although many studies have used local perfusion pressure changes to manipulate exercising muscle oxygen delivery, very few have simultaneously measured muscle blood flow, oxygenation, or oxygen delivery. Therefore, as I describe the effect of changes in oxygen delivery on muscle excitation contraction-coupling, I will clearly point out if oxygen delivery was or was not measured.

2.4.1 Common electrical stimulation methods and limitations

Although voluntary exercise necessitates that a motor command be generated in the brain to excite the desired muscle(s) to cause movement, electrical stimulation can be used to either (a) create muscle contraction in participants you cannot direct to complete a task (e.g., animals) or (b) to eliminate the variability of human motor control. In electrical stimulation models, muscle excitation is controlled by the electrical stimulator and therefore, muscle excitation is maintained constant. However, for electrical stimulation to mimic voluntary exercise, three key characteristics must be achieved. First, motor unit recruitment should follow the size principle – recruiting from smaller less fatigable to larger more fatigable fibers (Henneman, 1985; Henneman et al., 1965; Milner-Brown et al., 1973; Olson et al., 1968; Zajac & Faden, 1985). Second, individual motor unit firing frequencies should be within physiological ranges (i.e., <20 Hz) (Bellemare et al., 1983; Dalton et al., 2009; Lou et al., 2017; Van Cutsem et al., 1997). Third, motor unit recruitment should be asynchronous and variable (Lou et al., 2017). Depending on the type of electrical stimulation method used, there can be violations to the aforementioned key characteristics of voluntarily activated muscle.

When neuromuscular electrical stimulation is completed over the nerve trunk, there is orderly recruitment of motor units (Barss et al., 2018; Bergquist et al., 2012). This is achieved by stimulating sensory axons that contribute to an H-reflex – causing recruitment of motor units through central rather than peripheral pathways (Bergquist et al., 2012). Nerve trunk stimulation however does not allow for asynchronous motor unit recruitment, and as a result, higher stimulation frequencies are required to achieve smooth muscle contraction – contributing to increased rates of neuromuscular fatigue (Lou et al., 2017). To overcome the synchronous high frequency limitation of nerve trunk stimulation, muscle belly and nerve trunk electrical stimulation can be combined – this technique is referred to as interleaved neuromuscular electrical stimulation. Muscle belly electrical stimulation randomly recruits (more superficial) motor units through peripheral pathways. Although this method violates the orderly recruitment of motor unit recruitment (and it targets more superficial motor units), when combined with nerve trunk electrical stimulation, it is possible to recruit motor units in an asynchronous manner. This approach helps to lower individual motor unit firing frequencies to more physiological levels – reducing motor unit fatigability (Lou et al., 2017).

This interleaved electrical stimulation approach, however, does not eliminate all limitations. First, because two stimulators (one over the nerve trunk and another over the muscle belly) are required for the interleaved approach, the stimulators must be effectively coordinated to achieve smooth muscle contraction – this is not easily accomplished (Lou et al., 2017). Second, muscle belly electrical stimulation use violates the orderly recruitment of motor units – this does not mimic voluntary muscle excitation (Bergquist et al., 2012). Therefore, although there are methods to more closely mimic voluntary recruitment through electrical stimulation, none of these methods can fully replicate voluntary motor unit recruitment. Accordingly, in discussing electrical stimulation studies, I will point out the type(s) of neuromuscular stimulation being used in the study design.

2.4.2 Changes in oxygen delivery during maintained muscle excitation exercise

An important aspect of maintained muscle excitation exercise is that muscle contraction force is free to fluctuate. The fluctuation of muscle contraction force with changes in perfusion pressure has been repeatedly demonstrated in animal (Barclay et al., 1979; Hirvonen & Sonnenschein, 1962; Hobbs & McCloskey, 1987) and human models (Fitzpatrick et al., 1996; Luu & Fitzpatrick, 2013; Wright et al., 1999). By decreasing perfusion pressure in the electrically stimulated muscle, muscle contraction force decreases (Fitzpatrick et al., 1996; Hirvonen & Sonnenschein, 1962; Hobbs & McCloskey, 1987; Luu & Fitzpatrick, 2013; Wright et al., 1999). Importantly, Hogan et al. (1996) demonstrated that muscle contraction force decreases with changes in muscle oxygen delivery without compromise to the metabolic milieu (see Appendix B for more details). In surgically isolated canine gastrocnemius muscle, these authors slowly decreased muscle oxygen delivery – either via a decrease in blood flow or blood oxygen content – during sciatic nerve electrical stimulation. The slow reduction in oxygen delivery, independent of blood flow, led to a gradual reduction in muscle contraction force, and therefore ATP demand. Importantly, the downregulation of muscle contraction force with reduced oxygen delivery protected the metabolic milieu – this is evident from the maintained levels of muscle lactate, [ATP] and [PCr]. Therefore, under conditions of maintained muscle excitation, the muscles inherent response to a decrease in muscle oxygen delivery is to decrease metabolic demand, thereby protecting the metabolic milieu. Accordingly, under conditions of reduced oxygen delivery at a maintained muscle excitation, protection of the metabolic milieu is the benefit whereas reduced excitation-contraction coupling efficacy is the consequence. Additionally, by lowering muscle oxygen delivery separately, through reductions in blood flow vs. arterial oxygen content, Hogan et al. (1996) have demonstrated that in electrically stimulated dog muscle, the downregulation to muscle contraction force with reduced oxygen delivery is specifically oxygen delivery rather than blood flow mediated.

In the same year, Fitzpatrick et al. (1996) demonstrated that, in humans, changes in muscle contraction force, with changes in perfusion pressure (no measure of oxygen delivery), are rapidly reversible. These authors used electrical stimulation of the ulnar nerve in human participants to cause thumb adduction. Under these conditions of maintained muscle excitation, Fitzpatrick et al. (1996) moved the exercising arm from at to above heart level. By doing so, these authors reduced forearm perfusion pressure, therefore, without a compensatory increase in arterial blood pressure or forearm vasodilation, exercising blood flow should be reduced compared to at heart level (Perrey et al., 2001; Tschakovsky & Hughson, 1999; Walker et al., 2007). Upon decreasing perfusion pressure, like in the work of Hogan et al. (1996), muscle contraction force decreased at a maintained muscle excitation. Fitzpatrick et al. (1996) added to our understanding of perfusion pressure changes on muscle excitation contraction coupling by demonstrating the reversibility of this response. That is, upon movement of the exercising arm from above back to heart level, muscle contraction force was rapidly restored to normal levels. These data from Fitzpatrick et al. (1996) therefore demonstrate that muscle contraction force rapidly (within 60-sec) conforms to a decrease in perfusion pressure.

Later, Hogan, Kohin, et al. (1999) produced another elegant study design in which they demonstrated that the reversibility of muscle contraction force is oxygen delivery dependent. For 2-min, in surgically isolated canine gastrocnemius muscle, these authors cut off blood flow to the electrically stimulated (sciatic nerve) muscle. Under ischemic conditions, muscle contraction force dropped drastically. The authors then restored blood flow, but they kept oxygen delivery low by keeping PO_2 low. Under these conditions of restored flow but maintained low oxygen delivery, muscle contraction force remained compromised. Upon restoration of normal PO_2 – and therefore oxygen delivery – muscle contraction force rapidly (within 30-sec) recovered. By adjusting PO_2 independent of blood flow, Hogan, Kohin, et al. (1999) were able to demonstrate that muscle contraction force recovery can occur during exercise and that this response is oxygen delivery rather than blood flow dependent.

Combined, the work of Fitzpatrick et al. (1996) and Hogan and colleagues (Hogan, Kohin, et al., 1999; Hogan et al., 1996) has demonstrated four key attributes of electrically stimulated skeletal muscle to a decrease in oxygen delivery. First, muscle contraction force rapidly conforms to a decrease in muscle oxygen delivery (see Appendix B for more details). Second, muscle contraction force is rapidly recovered upon restoring muscle oxygen delivery. Third, these changes in muscle contraction force appear to occur without affecting the metabolic milieu. Fourth, muscle contraction force conforms to changes in oxygen delivery and not simply muscle blood flow. Given the apparent conformation of muscle contraction force to oxygen delivery, we termed this phenomenon the oxygen conforming response of muscle contraction force.

2.4.3 Changes in oxygen delivery during maintained muscle contraction force exercise

As opposed to electrically stimulated muscle exercise designs, where muscle excitation is controlled, voluntary exercise at a target muscle contraction force necessitates muscle excitation modulation. This phenomenon has been repeatedly demonstrated such that in humans, during fatiguing submaximal exercise contractions, muscle excitation must increase to protect muscle contraction force from dropping (Amann et al., 2007; Broxterman et al., 2015; Egana et al., 2010; Fulco et al., 1996; Vanhatalo et al., 2011). Importantly, like during fatiguing exercise necessitating an increase in muscle excitation to maintain muscle contraction force, a decrease in muscle perfusion pressure can also necessitate an increase in muscle excitation. This phenomenon was demonstrated by Hobbs and McCloskey (1987). These authors had human participants complete rhythmic plantar flexion exercise at varying levels of local perfusion pressure (no measure of muscle oxygen delivery). As perfusion pressure decreased (by increasing the height of the exercising leg above the heart), muscle excitation needed to increase to maintain the target muscle contraction force. Like in the electrically stimulated exercise models, upon restoring muscle perfusion pressure, muscle excitation at a target muscle contraction force returned to normal levels. The work of Hobbs and McCloskey (1987) is the first evidence of an oxygen conforming response existing in voluntary human exercise.

Despite these important findings, Hobbs and McCloskey (1987) did not measure blood flow, muscle oxygenation, nor did they report the amount of time taken for muscle excitation to be restored upon restoring normal perfusion pressure. Accordingly, Drouin et al. (2019) completed a study to overcome the limitations in the work of Hobbs and McCloskey (1987). In the study completed by Drouin et al. (2019) participants were asked to complete handgrip exercise at a previously determined work rate known not to cause progressive skeletal muscle fatigue development. During this handgrip exercise, two 2-min bouts of brachial artery compression were completed to reduce exercising muscle blood flow by 50%. After both 2-min bouts of brachial artery compression, blood flow was restored, and the muscle excitation response was observed. In the model created by Drouin et al. (2019), when exercising muscle blood flow was decreased, muscle excitation increased to maintain muscle contraction force. However, only when blood flow was restored, following the second bout of decreased blood flow, was there a significant rapid (< 2min) decrease in muscle excitation required to maintain the same muscle contraction force. The rapid increase in muscle excitation required to maintain the same muscle contraction force with compromised blood flow followed by a rapid restoration of muscle excitation – when blood flow was restored – supported the existence of the oxygen conforming response in voluntary human exercise. In summary, the work completed by Hobbs and McCloskey (1987) and Drouin et al. (2019) are interpreted to suggest that the oxygen conforming response exists in voluntary human exercise. Importantly, when blood flow is decreased, the amount of muscle excitation required to maintain the same muscle contraction force increases. When blood flow is restored, the muscle excitation required to maintain the same muscle contraction force is also rapidly restored (< 2min) (Drouin et al., 2019).

Although Haseler et al. (1998) did not measure muscle excitation, nor did they specifically control muscle oxygen delivery, these authors did demonstrate that the metabolic environment is dependent on inspired oxygen concentrations. Haseler et al. (1998) demonstrated that, in 6 healthy men, when muscle contraction force was maintained during a 10-min bout of exercise, percent PCr followed changes in inspired oxygen concentrations. Specifically, when oxygen delivery was reduced, %PCr also decreased and reached a new steady state. Alternatively, when oxygen delivery levels started low during exercise, PCr levels began low, then upon an increase in oxygen delivery, PCr levels increased and stabilized at a new steady state. Upon ending exercise, PCr levels rapidly returned to normal. The findings of Haseler et al. (1998) demonstrate the disturbance caused by a maintenance of muscle contraction force when oxygen delivery is reduced. Specifically, as a result of reduced oxygen delivery, the rate of ATP being produced via oxidative phosphorylation is reduced thereby necessitating an increase in the rate of ATP produced via anaerobic sources of ATP (i.e., the phosphocreatine cycle, glycolysis and TCA) until the concentrations of ADP, H^+ and NADH are increased to restore the rate of ETC and oxidative phosphorylation necessary to support exercise (Erecinska & Wilson, 1982; Hogan, Arthur, et al., 1992; Hogan et al., 1998; Hogan et al., 1996; Wilson & Erecinska, 1985; Wilson et al., 1979). Therefore, the benefit of increasing muscle excitation under conditions of reduced oxygen delivery is maintained muscle contraction force, however, the consequence is increased accumulation of fatigue-inducing metabolites (see Appendix B for more details).

Considering the increased accumulation of fatigue-inducing metabolites likely to be evident during muscle contraction force targeted exercise, this work from Hobbs and McCloskey

(1987) and Drouin et al. (2019) does not replicate the muscle contraction force conforming to oxygen delivery seen in electrically stimulated exercise models (Fitzpatrick et al., 1996; Hobbs & McCloskey, 1987; Luu & Fitzpatrick, 2013). Therefore, an isolation of potential oxygen-conforming alterations of muscle contraction force under voluntary exercise conditions has yet to be achieved. Furthermore, Fitzpatrick et al. (1996) have provided evidence that the oxygen conforming response in electrically stimulated exercise is exercise intensity dependent, therefore, it remained to be determined if the oxygen conforming response of muscle contraction force is also exercise intensity dependent during voluntary human contractions. Accordingly, the first aim of this thesis was to examine the effect of decreased oxygen delivery on muscle contraction force at a set voluntary muscle excitation at varying exercise intensities. This examination was completed first to inform experimental design for proceeding experiments.

2.5 The current perspective of oxygen delivery demand matching: Is it optimal for excitation-contraction coupling?

Now that I have demonstrated that muscle excitation-contraction coupling is sensitive to a decrease in oxygen delivery, I will now consider whether muscle excitation-contraction coupling can benefit from increased oxygen delivery.

2.5.1 Current perspective of oxygen delivery demand matching.

The current perspective surrounding the adequacy of oxygen delivery is that it is tightly matched to demand at exercise intensities below critical power (Radegran, 1997; Richardson et al., 1995). This interpretation is drawn from the observation that (a) muscle oxygen delivery increases linearly with demand (Hogan et al., 1983; Radegran, 1997; Richardson et al., 1995), (b) there is a counteracting vasoconstriction when arterial oxygen content is increased (Gonzalez-Alonso et al., 2002; Gonzalez-Alonso et al., 2001) and (c) VO_2 is unchanged under conditions of reduced oxygen delivery (Hogan et al., 1983; Pawelczyk et al., 1992). Therefore, the normal adjustment of oxygen delivery to demand appears to be optimized (Nyberg & Jones, 2022). However, this perspective does not consider the adequacy of oxygen delivery demand matching for muscle excitation-contraction coupling. The following section will therefore examine whether there is support for the oxygen delivery demand matching as being optimal for excitation-contraction coupling.

2.5.2 Effect of increased local perfusion pressure on muscle-excitation contraction coupling.

Like muscle contraction force conforming to a decrease in oxygen delivery, muscle contraction force is also subject to conform to an increase in oxygen delivery. This phenomenon has been demonstrated in electrically stimulated exercise models. First, via electrical (ulnar nerve) stimulation mediated human thumb adduction, Fitzpatrick et al. (1996) demonstrated muscle contraction force increases along with perfusion pressure (no measure of oxygen delivery). Compared to a similar percent reduction in perfusion pressure, an increase in perfusion pressure had a smaller effect on muscle contraction force (~8% increase vs. ~22% decrease). Importantly, like the muscle contraction force conformation to reduced perfusion pressure, the increased muscle contraction force with increased perfusion pressure is rapidly reversed when perfusion pressure is restored to normal (i.e., at heart level) (Fitzpatrick et al., 1996). These are the first findings to demonstrate that increased perfusion pressure can improve muscle excitation-contraction coupling during electrically stimulated exercise. Much later, Luu and Fitzpatrick (2013) demonstrated this same phenomenon in the electrically stimulated (tibialis anterior muscle belly) human tibialis anterior muscle. By lowering the leg below heart level, tibialis anterior muscle contraction force increased with perfusion pressure (no measure of oxygen delivery) and then rapidly reversed when perfusion pressure was restored to normal levels. These findings from Fitpatrick's group (Fitzpatrick et al., 1996; Luu & Fitzpatrick, 2013), support the potential for an increase in perfusion pressure to improve muscle excitation-contraction coupling.

2.5.3 Effect of increased systemic arterial blood pressure on muscle-excitation contraction coupling.

Like local perfusion pressure changes, an increase in systemic blood pressure can be utilized to increase blood flow to the exercising muscle. While measuring electrically stimulated adductor pollicis muscle contraction force (ulnar nerve stimulation), Wright et al. (2000) used leg exercise to increase systemic arterial blood pressure. Like local perfusion pressure changes, the systemic arterial blood pressure increase (no measure of local oxygen delivery) led to an increase in muscle contraction force that was rapidly reversed when normal systemic blood pressure was restored. Next, like the work in the adductor pollicis of Wright et al. (2000), Luu and Fitzpatrick (2013) demonstrated that a forearm exercise mediated increase in systemic blood pressure (no measure of local oxygen delivery) led to an attenuated decrease in electrically stimulated tibialis anterior muscle contraction force compared to an extrapolated exponential fit. This comparison to a fit rather than a control condition limits our ability to interpret these data to support the contribution of oxygen delivery on muscle contraction force. This limitation is particularly important given that muscle contraction force was not reversed with a restoration of normal systemic blood pressure. If this were an oxygen conforming mediated effect, I would have expected the increased muscle contraction force to be rapidly reversed when systemic blood pressure was restored to normal levels.

Despite the aforementioned limitations, the work from Fitzpatrick's group has characterized the response of electrically stimulated muscle contraction force to an increase in local perfusion pressure (Fitzpatrick et al., 1996; Luu & Fitzpatrick, 2013) and systemic blood pressure (Luu & Fitzpatrick, 2013; Wright et al., 2000). That is, an increase in perfusion pressure can reversibly improve muscle excitation-contraction coupling. However, an important limitation of these data must be acknowledged – that is, the lack of oxygen delivery measurements. Without measurements of local oxygen delivery, these models assume that the target muscle(s) vasoregulatory response is one that favours increased oxygen delivery rather than one that prevents it. In a scenario where the vasoregulatory response is one that prevents increased oxygen delivery, there would be increased vasoconstriction in the target muscle group. The possibility of counteracting vasoconstriction has been previously demonstrated (Perrey et al., 2001), therefore, measurement of systemic blood pressure alone cannot be used to confirm increased muscle oxygen delivery. Accordingly, it remains unknown whether a systemic blood pressure increase is contributing to an increase in oxygen delivery and therefore increased muscle excitation contraction coupling.

Combined, although the current perspective suggests that muscle oxygen delivery demand is optimized for muscle VO_2 below critical force, the aforementioned evidence in electrically stimulated muscle suggests that there is benefit of increased oxygen delivery for muscle excitation-contraction coupling. Considering that these studies have only been completed under electrically stimulated exercise models and that muscle oxygen delivery has not been measured, the aim of the second thesis study was to determine whether the normal adjustment of oxygen delivery is optimal for muscle excitation-contraction coupling during voluntary exercise.

2.6 Oxygen conforming contribution to critical force?

Up to this point, I have demonstrated that there is evidence to support an oxygen conforming response of muscle contraction force during electrically stimulated exercise below critical force. However, as described in section 2.3, there are considerable differences in the metabolic milieu when comparing exercise intensities below *versus* above critical force. Critically, during maximal effort exercise, (a) a steady state between oxygen delivery and demand cannot be achieved (Black et al., 2017; Poole et al., 2016) and (b) maximal VO_2 (Fenuta et al., 2023; Goulding et al., 2020; Kellawan & Tschakovsky, 2014), oxidative ATP production (Broxterman et al., 2017), and cellular disturbance (i.e., Pi, pH and PCr) are rapidly reached (Burnley et al., 2010; Korzeniewski & Rossiter, 2020). The following section will therefore describe our current understanding of how oxygen delivery can modify muscle contraction force during a maximal effort exercise test.

2.6.1 Methods of critical force identification.

The first method developed to identify the critical force plateau utilizes multiple constant workload exercise tests to exhaustion. During these constant workload tests, time to exhaustion is recorded and plotted relative to the associated power output. By measuring time to exhaustion under three or more constant workloads, a hyperbolic model can be used to fit the data. This hyperbolic fit is then used to identify a 'plateau' in in the power-duration relationship – reflecting critical force (or power) (Hill, 1993; Jones et al., 2010). The second method developed to identify the critical force plateau necessitates that participants complete maximal effort rhythmic contractions until a plateau in muscle contraction force/power is observed (Burnley, 2009; Kellawan & Tschakovsky, 2014; Vanhatalo et al., 2007). Test length for this maximal effort model depends on the exercise mode. Typically, to identify a plateau in muscle contraction force/power, 3-min, 5-min, and 10-

min are adequate for cycling (Vanhatalo et al., 2007), knee extension (Burnley, 2009), and handgrip exercise (Kellawan & Tschakovsky, 2014), respectively.

2.6.2 Effect of local oxygen delivery and varied levels of inspired oxygen percentage on critical force.

The first evidence in support of critical force being oxygen delivery dependent comes from the work of Vanhatalo et al. (2010). These authors measured time to exhaustion during knee extension exercise at four different constant workloads, under both normoxic and hyperoxic conditions. By using a hyperbolic model to fit their data, Vanhatalo et al. (2010) demonstrated that the critical force plateau can be improved under hyperoxic conditions. More recently, Goulding et al. (2020) demonstrated a similar response during cycling exercise under normoxic and hyperoxic conditions. By using the multiple constant workload cycling trial model of critical power identification, Goulding et al. (2020) demonstrated that critical power can be increased under hyperoxic compared to normoxic conditions. Importantly, muscle oxygenation was measured in both the work of Vanhatalo et al. (2010) and Goulding et al. (2020), and muscle oxygenation was shown to be improved in both designs. Combined, these data support the perspective that increased oxygen delivery – via inspired hyperoxic air – can improve critical power.

As opposed to hyperoxic exercise, a decrease in inspired oxygen concentration (i.e., hypoxia) can decrease critical power. Simpson et al. (2015) demonstrated that critical power is reduced under hypoxic compared to normoxic conditions by measuring it in both a constant workload model and an all-out 3-min cycling test. Importantly, the model used did not significantly affect the critical power estimate under either hypoxic or normoxic conditions. Later, using a 3-min all-out exercise test under normoxic and hypoxic conditions, Sousa et al. (2021) confirmed these findings from Simpson et al. (2015) – critical power is reduced under hypoxic exercise conditions. Combined, by examining the critical power plateau under hyperoxic (Goulding et al., 2020; Vanhatalo et al., 2010) and hypoxic (Simpson et al., 2015; Sousa et al., 2021) conditions, these data support a role of inspired oxygen concentration on determining the critical power plateau.

An important limitation of these inspired oxygen concentration data must however be acknowledged – it is not possible to isolate the local (in the muscle) *versus* central (in the brain/spinal cord) oxygenation contribution to the critical force plateau. Therefore, isolation of a local oxygen delivery effect on muscle excitation-contraction coupling is needed. Luckily, prior to most of this inspired oxygen concentration critical force work, Broxterman et al. (2014) cleverly designed a study to assess the effect of local oxygen delivery on the critical force plateau. To create conditions of high *versus* low oxygen delivery, Broxterman et al. (2014) took advantage of the normal mechanical compression mediated occlusion of blood flow. Specifically, during muscle contraction, intramuscular pressure increases, and if the muscle contraction is intense enough, it can occlude blood flow. Therefore, a condition with less relaxation time would contribute to reduced oxygen delivery compared to a condition with more relaxation time. Accordingly, Broxterman et al. (2014) had participants complete exercise with a contraction to relaxation duty cycle of 50% (1.5 sec contraction to 1.5 sec relaxation) reflecting a low oxygen delivery condition *versus* a 20% duty cycle (0.6 sec contraction to 2.4 sec relaxation) reflecting a high oxygen delivery condition. Broxterman et al. (2014) then utilized three constant load rhythmic handgrip trials to exhaustion, both under low (i.e., 50% duty cycle) and high (i.e., 20% duty cycle) oxygen delivery conditions and used a hyperbolic model to identify critical force under both conditions. By doing so, these authors demonstrated that critical power is reduced under low compared to high oxygen delivery conditions (Broxterman et al., 2014) – supporting an oxygen delivery dependence of the critical force plateau.

In summary, by altering inspired oxygen concentration (Goulding et al., 2020; Simpson et al., 2015; Sousa et al., 2021; Vanhatalo et al., 2010) and local oxygen delivery (Broxterman et al., 2014), these authors have demonstrated that the critical force plateau is oxygen delivery dependent.

2.6.3 Evidence for oxygen conforming response contribution to critical force.

Although oxygen delivery appears to affect the critical force plateau, the contribution of an oxygen conforming response of muscle contraction force to this plateau remains unknown. In fact, to date, there is only one study demonstrating one of the key oxygen conforming characteristics during maximal effort exercise. Hammer et al. (2020) utilized cuff occlusion during the first 150-sec of a 300-sec maximal effort handgrip exercise test. As expected, with a complete lack of oxygen delivery, muscle contraction force dropped to critical levels during cuff occlusion. However, as opposed to the authors predictions, upon removal of cuff occlusion, muscle contraction force rapidly (within 60-sec) returned to levels measured under a free flow (control) condition. Such a rapid restoration of muscle contraction force with oxygen delivery restoration is consistent with an oxygen conforming response determining muscle contraction force during maximal effort exercise. The work of Hammer et al. (2020) was not designed to identify an oxygen conforming contribution during maximal effort exercise, therefore, beyond the exciting observation of a rapid restoration of muscle contraction force with cuff occlusion release, their data does not demonstrate other key oxygen conforming characteristics during a maximal effort exercise test. Furthermore, unlike previous oxygen conforming work, these data were measured under conditions not relevant to everyday exercise (i.e., full blood flow occlusion). Accordingly, the aim of the third thesis study was to assess whether relatively small, physiologically relevant, changes in oxygen delivery can affect the muscle contraction force decline and stabilization of critical force during maximal effort exercise. Key to the identification of an oxygen conforming response during maximal effort exercise will be observation of muscle contraction force rapidly following changes in oxygen delivery.

2.7 Summary thesis study 1

2.7.1 Principle proposition

1. During electrically stimulated muscle contractions, the muscle's inherent response to a decrease in oxygen delivery is to reduce muscle contraction force (i.e., the consequence) to prevent metabolic disturbance (i.e., the benefit).
2. During electrically stimulated muscle contractions, the magnitude of muscle contraction force conformation with reduced oxygen delivery appears to be exercise intensity dependent.

2.7.2 Interacting proposition

1. It remains to be determined if – when human participants are asked to maintain a constant level of voluntary muscle excitation – muscle contraction force will decrease when oxygen delivery is reduced and whether muscle contraction force will be rapidly restored upon restoration of muscle oxygen delivery.
2. It remains to be determined whether muscle contraction force conformation with reduced oxygen delivery is exercise intensity dependent during voluntary human exercise.

2.7.3 Speculative proposition

1. We speculate that voluntary muscle contraction force will rapidly decrease and increase when oxygen delivery is decreased and increased, respectively, thereby supporting the existence of an oxygen conforming response in voluntary muscle contractions.
2. We speculate that muscle contraction force will follow muscle oxygen delivery at higher and not lower exercise intensities.

2.7.4 Purpose

The purpose of this study was to test the hypothesis that muscle contraction force at a maintained voluntary muscle excitation follows changes in oxygen delivery.

2.7.5 Hypothesis

We hypothesized that muscle contraction force at a maintained voluntary muscle excitation will follow changes in oxygen delivery at higher but not lower exercise intensities.

2.7.6 Significance

Importantly, this study aimed to improve our understanding of mechanisms involved in oxygen delivery-mediated changes in exercise tolerance by examining the role rapid changes in oxygen delivery can play in modifying muscle excitation-contraction coupling.

2.8 Summary thesis study 2

2.8.1 Principle proposition

Oxygen delivery is viewed as tightly coupled to demand in exercise below critical power because increasing oxygen delivery does not increase the rate of oxygen uptake.

2.8.2 Interacting proposition

Whether the ‘normal’ adjustment of oxygen delivery in small muscle mass exercise below critical power is optimal for excitation-contraction coupling remains unknown.

2.8.3 Speculative proposition

Given the evidence in electrically stimulated models, that increased oxygen delivery can improve muscle excitation-contraction coupling, we speculate that an increase in oxygen delivery above ‘normal’ should improve muscle excitation-contraction coupling during voluntary exercise.

2.8.4 Purpose

The purpose of this study was to test the hypothesis that an increase in oxygen delivery above ‘normal’ will improve muscle excitation-contraction coupling.

2.8.5 Hypothesis

We hypothesized that an increase in oxygen delivery above ‘normal’ will improve muscle excitation-contraction coupling.

2.8.6 Significance

Importantly, this study aimed to highlight the importance in considering the adequacy of oxygen delivery for muscle excitation-contraction coupling and not just the rate of oxygen consumption.

2.9 Summary thesis study 3

2.9.1 Principle proposition

At exercise intensities below critical force – where the cellular environment can achieve stability – muscle contraction force relative to muscle excitation rapidly conforms to changes in oxygen delivery.

2.9.2 Interacting proposition

It remains to be determined whether, during maximal effort exercise – where stabilization of the rate of ATP production and demand cannot be achieved – oxygen conforming can (a) modify the progressive decline of muscle contraction force and (b) rapidly shift the stabilized muscle contraction critical force.

2.9.3 Speculative proposition

Given (a) the observed rapid restoration of muscle contraction force with restoration of blood flow during maximal effort exercise, and (b) the reduced critical force plateau under reduced oxygen delivery conditions, we speculate that the rate of muscle contraction force decline will be increased with reduced oxygen delivery, but that it will be rapidly reversible with restoration of normal oxygen delivery.

2.9.4 Purpose

The purpose of this study was to test the hypothesis that during a maximal effort rhythmic handgrip exercise test the oxygen conforming response can (a) modify the progressive decline of muscle contraction force and (b) rapidly shift the stabilized muscle contraction critical force.

2.9.5 Hypothesis

We hypothesized that during a maximal effort rhythmic handgrip exercise test the oxygen conforming response can (a) modify the progressive decline of muscle contraction force and (b) rapidly shift the stabilized muscle contraction critical force.

2.9.6 Significance

Importantly, this study aimed to demonstrate the cellular-disturbance independent role oxygen delivery can play in modifying exercise tolerance during maximal effort exercise.

Chapter 3 - Muscle contraction force conforms to muscle oxygenation during constant activation voluntary forearm exercise

Chapter 3 is published as:

Drouin PJ, Forbes SPA, Liu T, Lew LA, McGarity-Shipley E & Tschakovsky ME. Muscle contraction force conforms to muscle oxygenation during constant-activation voluntary forearm exercise. Exp Physiol 107, 1360-1374, 2020.

3.1 Abstract

In electrically stimulated skeletal muscle, force production is downregulated when oxygen delivery is compromised and rapidly restored upon oxygen delivery restoration in the absence of cellular disturbance. Whether this "oxygen conforming" response of force occurs and is exercise intensity dependent during stable voluntary muscle activation in humans is unknown. In 12-participants (6-female), handgrip force, forearm muscle activation (electromyography; EMG), muscle oxygenation, and forearm blood flow (FBF) were measured during rhythmic handgrip exercise at forearm EMG achieving 50, 75 or 90% critical impulse (CI). 4-min of brachial artery compression to reduce FBF by ~60% (Hypoperfusion) or sham compression (adjacent to artery; Control) was performed during exercise. Sham compression had no effect. Hypoperfusion rapidly reduced muscle oxygenation at all exercise intensities, resulting in contraction force per muscle activation (force/EMG) progressively declining over 4 min by ~16% in 75 and 90% CI. No force/EMG decline occurred in 50% CI. Rapid restoration of muscle oxygenation post-compression was closely followed by force/EMG such that it was not different from Control within 30-sec for 90% CI and after 90-sec for 75% CI. Our findings reveal an oxygen conforming response does occur in voluntary exercising muscle in humans. Within the exercise modality and magnitude of fluctuation of oxygenation in this study, the oxygen conforming response appears to be exercise intensity dependent. Mechanisms responsible for this oxygen conforming response have implications for exercise tolerance and warrant investigation.

3.2 New findings

- **What is the central question of this study?** In electrically stimulated skeletal muscle, force production is downregulated when oxygen delivery is compromised and rapidly restored upon oxygen delivery restoration. Whether “oxygen conforming” of force production occurs during voluntary muscle activation in humans and whether it is exercise intensity dependent remains unknown.
- **What is the main finding and its importance?** Here we show in humans that force at a given voluntary muscle activation does conform to a decrease in oxygen delivery and rapidly and completely recovers with restoration of oxygen delivery. This oxygen conforming response of contraction force appears to happen only at higher intensities.

3.3 Introduction

Electrically stimulated muscle exhibits an “oxygen conforming” response of force production at a given stimulation in both human (Fitzpatrick et al., 1996; Hobbs & McCloskey, 1987; Luu & Fitzpatrick, 2013) and animal (Hobbs & McCloskey, 1987; Hogan, Kohin, et al., 1999) models. Specifically, muscle force production decreases when oxygen delivery is reduced, but rapidly (within 60-sec) recovers when oxygen delivery is restored. There are two intriguing characteristics of this oxygen conforming response in electrically stimulated muscle. First, force reduction with reduced oxygen delivery at a stable muscle activation occurs without a disturbance to the intracellular environment (Hogan et al., 1996). Second, force production rapidly recovers to normal with restoration of oxygen delivery (Fitzpatrick et al., 1996; Hobbs & McCloskey, 1987; Hogan, Kohin, et al., 1999; Luu & Fitzpatrick, 2013).

These two characteristics are strikingly different from cellular disturbance-mediated compromise to force production under hypoxemic conditions (Amann et al., 2006; Katayama et al., 2007; McKeown et al., 2021; Pitcher & Miles, 1997; Romer & Dempsey, 2006; Romer et al., 2006; Ruggiero et al., 2020; Szubski et al., 2007; Wright et al., 1999) which occurs when the task requires maintaining force production and therefore ATP demand. Specifically, when skeletal muscle is “forced” to achieve a given force production in the face of decreased muscle oxygenation, altered phosphorylation and redox potential to maintain aerobic ATP production is observed (Erecinska & Wilson, 1982; Haseler et al., 1998; Hogan, Arthur, et al., 1992; Hogan et al., 1998; Hogan et al., 1996; Wilson & Erecinska, 1985; Wilson et al., 1979). The result is elevated levels of fatigue-inducing molecules (e.g., Pi and H+) that compromise force production at a given muscle activation (Fulco et al., 1996; Hogan, Arthur, et al., 1992; Hogan, Richardson, et al., 1999). Furthermore, as opposed to the oxygen conforming-mediated compromise to force production (Fitzpatrick et al., 1996; Hogan, Kohin, et al., 1999; Luu & Fitzpatrick, 2013), cellular disturbance-mediated compromise to force production takes longer to recover and necessitates that the fatiguing exercise be discontinued (Amann et al., 2006; Katayama et al., 2007; McKeown et al., 2021; Pitcher & Miles, 1997; Romer & Dempsey, 2006; Romer et al., 2006; Ruggiero et al., 2020; Szubski et al., 2007; Wright et al., 1999). Thus, oxygen conforming mechanisms of skeletal muscle force modulation are likely different from "traditional" cellular disturbance-mediated mechanisms of fatigue.

Although the oxygen conforming response phenomenon is evident in electrically stimulated exercise models, the fundamental differences in motor unit recruitment between electrical stimulation and voluntary activation preclude the external validity of electrical stimulation work to voluntary activation (Barss et al., 2018; Bergquist et al., 2012; Henneman, 1985; Lou et al., 2017). To date, only two studies have reported findings consistent with an oxygen conforming response in voluntary exercise. First, Hobbs & McCloskey (1987) demonstrated that exercising muscle activation must increase to maintain a given force output when the exercising leg is moved from heart level (control) to above heart level (reduced local arterial perfusion pressure) where presumably oxygen delivery is compromised. Importantly, Hobbs & McCloskey (1987) showed that muscle activation returned to control levels when the exercising leg was moved back to heart level. However, Hobbs & McCloskey (1987) did not measure muscle oxygenation or blood flow nor did they report the time required for muscle activation to be restored upon returning the exercising leg to heart level. To build on the work of Hobbs and McCloskey (1987), Drouin *et al.* (2019) measured forearm muscle activation, blood flow and oxygenation during constant force rhythmic voluntary handgrip exercise in response to two episodes of brachial artery compression to create a targeted reduction in exercising muscle blood flow. Drouin *et al.* (2019) found that muscle activation increased with the first episode of decreased muscle oxygen delivery and remained so when blood flow was restored. However, with the second episode of decreased muscle oxygen delivery, muscle activation increased further but was then rapidly restored when muscle oxygen delivery returned to normal.

Although the muscle activation responses to oxygen delivery compromise and restoration observed by Hobbs & McCloskey (1987) and by Drouin *et al.* (2019) are consistent with an oxygen conforming effect requiring elevated muscle activation to maintain force when skeletal muscle oxygenation is reduced, maintained force production would also cause an increase in metabolites contributing to cellular disturbance-mediated fatigue (Erecinska & Wilson, 1982; Haseler et al., 1998; Hogan, Arthur, et al., 1992; Hogan et al., 1998; Hogan et al., 1996; Wilson & Erecinska, 1985; Wilson et al., 1979). Thus, an isolation of potential oxygen conforming alterations in muscle force production in voluntary human skeletal muscle exercise has yet to be achieved. Therefore, the purpose of this study was to create experimental conditions of maintained voluntary activation of skeletal muscle experiencing targeted manipulations of muscle oxygen delivery to test the hypothesis that oxygen conforming modulation of skeletal muscle force production occurs during voluntary exercise in humans. Furthermore, given there is evidence for exercise intensity dependence of oxygen conforming in electrically stimulated muscle contractions (Fitzpatrick et al., 1996), we also tested the hypothesis that oxygen conforming in voluntary human exercise is exercise intensity dependent.

3.4 Methods

3.4.1 Participants and ethical approval

Twelve healthy participants (6 female) were recruited for this study (see Table 1). All experimental procedures were reviewed and approved by the Queen's University Health Sciences and Affiliated Teaching Hospitals Research Ethics Board (6005158 PHE-036-02) and conformed to the standards set by the Declaration of Helsinki except for registration in a data base. Informed written consent of voluntary participation was obtained from all participants prior to participation in the study.

3.4.2 Experimental design

This study was a within- and between-participant design in which participants completed 13 handgrip exercise tests over seven testing days (one maximal effort exercise test to determine critical impulse on day 1 and two constant load handgrip exercise tests on days 2-7). On days where participants completed two handgrip exercise tests, these were always the same intensity and condition. At minimum, a 10-min break was provided between the two exercise tests performed on a single day. Recovery of force at a given electromyography was confirmed before starting the second test on a day. All handgrip exercise was completed in the Human Vascular Control Lab with participants laying supine on a padded table. Participants were asked to abstain from food 4-hrs before, caffeine and alcohol 12-hrs before as well as strenuous upper body exercise 24-h before each testing day.

3.4.3 Exercise modality

Forearm handgrip exercise consisting of rhythmic isometric forearm handgrip contractions with a duty cycle of 2-sec contraction to 4-sec relaxation for all handgrip exercise tests. It is important to note that this means over an absolute amount of elapsed time, only 33% of that time constitutes elevated ATP consumption associated with force production.

3.4.4 Establishing exercise work rates

On the first experimental day, participants completed a 10-min critical impulse test as previously described (Kellawan & Tschakovsky, 2014). As per Kellawan et al. (2014) critical impulse was calculated as the average impulse of the final 30-sec of contractions. From the calculated critical impulse identified on day one, low, moderate, and high intensity conditions were calculated as 50%, 75% and 90% critical impulse, respectively. On the following six experimental days, participants were pseudo-randomly allocated to either a low (i.e., 50%), moderate (i.e., 75%) or high (i.e., 90%) intensity exercise bout.

3.4.5 Establishing a voluntary muscle activation target

To establish a voluntary muscle activation target, participants were asked to complete ten 2-sec handgrip contractions with 30-sec of rest between each at the contraction force for the exercise intensity being tested. The average of these 10 contractions was used to establish the target muscle activation amplitude for the subsequent exercise tests on a given day.

3.5 Experimental conditions

Each exercise protocol consisted of 15-min of handgrip exercise targeting the previously established muscle activation amplitude. To test the oxygen conforming response in voluntary exercise, we created two conditions: Hypoperfusion and Control. *Hypoperfusion condition:* To establish the hypoperfusion condition, at the 7th minute of exercise, 4 minutes of manual brachial artery compression (at the antecubital fossa distal to the site of brachial artery blood velocity measurement) was performed, achieving a targeted ~50% reduction of steady state brachial artery blood velocity – ultimately resulting in a stable and reproducible ~60% reduction of forearm blood flow in all conditions and intensities (see Appendix C for more details). *Control condition:* To establish the Control condition, at the 7th minute of exercise, manual compression was completed immediately adjacent to the brachial artery of participants so that brachial artery blood flow was not affected (see Appendix C for more details). This acted as a sham mimicking the sensation of compression at the site of the artery. To ensure participant blinding to intensity and condition, participants were only able to see their exercising muscle activation. Experimental conditions were pseudo-randomly allocated. See Fig. 1 for a summary of the experimental protocol.

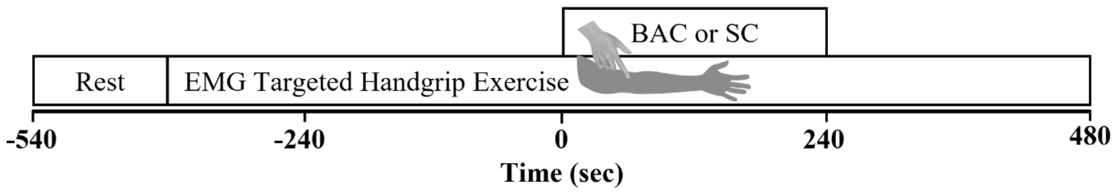

Figure 3-1. Schematic of the experimental design. Electromyography (EMG) targeted handgrip exercise starts at time = -420 sec. At time = 0 sec either 1) manual brachial artery compression (BAC; hypoperfusion condition) was performed, achieving a targeted ~50% reduction of steady state brachial artery blood velocity or 2) sham compression (SC; Control condition) was performed immediately adjacent to the brachial artery so that brachial artery blood velocity was not affected. Two EMG targeted handgrip exercise tests were performed on a day under Hypoperfusion or Control conditions.

3.5.1 Ischemic calibration of near infrared spectroscopy signals.

To calibrate the near infrared spectroscopy (NIRS) signals, ischemic calibration was completed at the end of each session. This ischemic calibration of the NIRS signals was completed according to the guidelines of Thomas Barstow (2019). First, the participants forearm was maintained in a horizontal position. Second, a wide blood pressure cuff was wrapped around the upper arm proximal to the NIRS probe on the forearm. Third, the blood pressure cuff was inflated to and maintained at 250-mmHg until the NIRS signals had plateaued. Fourth, pressure was released from the blood pressure cuff and measurement continued for another 2-min. Participants were asked to remain still throughout the procedure.

3.5.2 Instrumentation and data acquisition

3.5.2.1 Flexor digitorum superficialis muscle activation.

Flexor digitorum superficialis muscle activation was recorded with either a single Trigno electromyography (EMG) Sensor (Delsys, Natick, MA) placed according to “Anatomical guide for the electromyographer: the limbs and trunk” guidelines (Perotto & Delagi, 1994) or via four mini wireless bipolar electrodes placed according to guidelines reported elsewhere (Drouin et al., 2019) with guidance from the work of Bickerton et al. (1997). Within a participant, the same EMG sensors and placement were used for all experimental procedures. EMG activity was recorded by wirelessly sending a voltage signal to the Delsys Trigno Base (Delsys, Natick, MA), where it was then transmitted through a Trigno EMG 1-16 adapter (ADInstruments, Colorado Springs, CO) and PowerLab interface cable (ADInstruments, Colorado Springs, CO). The EMG signal was then displayed and recorded in Labchart 7 software (ADInstruments, Colorado Springs, CO) where EMG data were collected at 2000 Hz/channel. A calculated channel was created to calculate the root mean square (RMS) of the raw EMG signal. When using the four mini-EMG sensors, a separate channel was created to calculate the mean EMG RMS of all four sensors combined. The single (when using a single Trigno EMG sensor) or mean (when using four mini wireless bipolar electrodes) EMG RMS signal was used as the voluntary muscle activation target throughout handgrip exercise.

3.5.2.2 Flexor digitorum superficialis muscle oxygenation.

Flexor digitorum superficialis muscle oxygenation was recorded via near infrared spectroscopy (NIRS, Oxymon MK III, Artinis Medical Systems, Netherlands) next to the EMG sensor(s) placed on the forearm. The NIRS device provided measurements of change in oxygenated [haem] (oxy[haem]) and deoxygenated [haem] (deoxy[haem]). This study used a single channel consisting of one optical fiber operating at three wavelengths (874, 761, and 803 nm), where the light is transmitted into the muscle and received by an avalanche photodiode. NIRS data were collected at a sample rate of 10 Hz with an interoptode distance of 25-mm and a constant differential path length factor of 3.59, with participant-specific power and gain settings, ensuring optimal signal performance.

3.5.2.3 Handgrip force output.

Force of handgrip contraction was recorded via a force transducer connected to a PowerLab/8SP (ADInstruments, Colorado Springs, CO), collected at 2000 Hz. The force transducer was calibrated using a calibration curve created using known weights and measuring the associated voltage. The force transducer was then calibrated using a two-point calibration calculated from the calibration curve.

3.5.2.4 Forearm blood flow.

During the 17-min experimental protocol, brachial artery blood velocity and diameter were measured continuously. Brachial artery blood velocity was measured with a flat 4-MHz pulsed Doppler probe (model 500V 131 Transcranial Doppler; Multigon industries, Mt. Vernon, NY) attached to the skin over the brachial artery proximal to the antecubital fossa of the exercising forearm. Brachial artery blood velocity data were collected in volts by analog connection to a Powerlab/8_{SP} (ADInstruments, Colorado Springs, CO) and converted to cm/s in Labchart 7 software (ADInstruments, Colorado Springs, CO). Brachial artery diameter was measured with a linear echo ultrasound probe positioned over the brachial artery ~5cm proximal to the Doppler probe, operating at 13 MHz in 2D mode (Vivid I; GE Medical Systems, London, ON, Canada).

3.5.3 Data analysis

3.5.3.1 Flexor digitorum superficialis muscle activation and handgrip force output.

Flexor Digitorum Superficialis muscle activation and handgrip force was analyzed with MATLAB 2020b software (MathWorks, Natick, MA). First, the resting (i.e., no forearm contraction) EMG RMS value was subtracted from the calculated EMG RMS signal. Second, the onset and offset of each handgrip contraction was identified using the EMG signal. Third, within the onset and offset of each contraction, the area under the curve of both EMG RMS and force were calculated using the 'trapz' function in MATLAB. The mean time at each contraction was calculated and aligned with the calculated EMG RMS and force area under the curve values. Force per EMG (force/EMG) was then calculated to control for inevitable contraction to contraction variation in muscle activation during the voluntary exercise task. To compare the effect of hypoperfusion on the decline in force/EMG between exercise intensities we calculated the percent change in force/EMG from steady state (i.e., 30-sec before compression; mean time = -15-sec).

3.5.3.2 Flexor digitorum superficialis muscle oxygenation: ischemic calibration.

Successful ischemic calibration permitted the following analysis of NIRS signals. First, the 5-min of ischemia helped us obtain a 100% deoxy[haem] signal (i.e., maximal measured deoxy[haem] value) as well as a 0% oxy[haem] signal (i.e., minimal measured oxy[haem] value). Second, upon release of pressure from the blood pressure cuff, we were able to obtain a 100% oxy[haem] signal (i.e., maximal measured oxy[haem] value) and a 0% deoxy[haem] signal (i.e., minimal measured deoxy[haem] value) – this approach has a reported excellent within-subject reproducibility (Ryan et al., 2012). Both oxy[haem] and deoxy[haem] were then calculated as a percent change from steady state (i.e., 30-sec before compression; mean time = -15-sec).

3.5.3.3 Forearm blood flow.

Brachial artery blood velocity data were analyzed with MATLAB 2020b software (MathWorks, Natick, MA). The brachial artery blood velocity data were averaged into 30-sec time bins to reflect the length of five duty cycles. Brachial artery diameters were quantified with Measurements from Arterial Ultrasound Imaging (MAUI, Hedgehog Medical) automated edge detection software and averaged over the same time as blood velocity values. Forearm blood flow (FBF) was calculated as MBV (cm/s) · 60 s/min · π · [brachial artery diameter (cm)/2]2. Where MBV is mean blood velocity in cm/s. FBF was then calculated as a percent change from steady state (i.e., 30-sec before compression; mean time = -15-sec).

3.5.3.4 General methods.

Following the above data analysis approaches, the two trials completed on a single day were averaged to yield a single mean response for each intensity and condition combination.

3.5.4 Statistical analysis

A two-way repeated measures ANOVA was used to test for exercise intensity and condition effects on steady state exercise responses prior to brachial artery or sham compression, (mean time = -15-sec). To assess the effect of brachial artery compression-mediated hypoperfusion (i.e., hypoperfusion condition) compared to the Control condition (i.e., sham compression) over time, two-way repeated measures ANOVAs were run on FBF, oxy[haem], deoxy[haem], force/EMG, perceived mental and physical strain data. To test for an effect of intensity over time within the hypoperfusion condition, two-way repeated measures ANOVAs were run on FBF, oxy[haem], deoxy[haem] and force/EMG. Statistical tests were run using SigmaStat 4.0 (Systat Software, Palo Alto, CA). All pairwise multiple comparisons were adjusted using the Holm-Sidak method. Statistical significance was assumed at $P < 0.05$.

3.6 Results

3.6.1 Participant's completion of protocols.

Of the 12 recruited participants (see Table 1 for anthropometric data), two males (ID: OCR22, OCR10) did not complete the 50% intensity and one female (ID: OCR06) did not complete the 75% intensity. Therefore, all statistical tests were completed on 12 participants (6 female) at 90%, 11 participants (5 female) at 75% and 10 participants (6 female) at 50% intensities on all measures except muscle oxygenation. The NIRS system malfunctioned on one occasion resulting in data loss for one female participant at the 75% intensity (ID: OCR12). Muscle oxygenation values at the 75% intensity were therefore analyzed on 10 participants (4 female).

Table 3-1. Age, anthropometric measures, force, critical impulse (CI) and percent maximal voluntary contraction (MVC).

Variable (unit)	Female Mean (n=6)	Male Mean (n=6)	Group Mean (n=12)
Age (years)	20.0 ± 1.1	21.7 ± 3.4	20.8 ± 2.7
Height (cm)	169.8 ± 3.2*	177.7 ± 5.6	173.7 ± 6.0
Weight (Kg)	61.5 ± 9.3	75.2 ± 11.8	68.3 ± 12.6
Force of MVC (N)	276.3 ± 33.4*	474.5 ± 76.5	375.4 ± 115.4
Force at CI (N)	112.3 ± 13.9*	182.0 ± 39.0	147.1 ± 45.5
Force at 90% CI (N)	101.2 ± 12.5*	164.3 ± 35.3	132.8 ± 41.2
Force at 75% CI (N)	86.1 ± 10.5*	136.9 ± 29.4	113.8 ± 34.1
Force at 50% CI (N)	56.2 ± 6.9*	91.3 ± 21.5	72.1 ± 23.2
%MVC at CI	41.7 ± 9.4	38.1 ± 4.1	39.9 ± 7.5
%MVC at 90% CI	37.6 ± 8.5	34.4 ± 3.7	36.0 ± 6.7
%MVC at 75% CI	33.1 ± 6.5	28.7 ± 3.1	30.6 ± 5.4
%MVC at 50% CI	20.9 ± 4.7	18.8 ± 2.2	20.0 ± 3.9

*Significantly different from Male, $P<0.05$. Values are means ± SD.

3.6.2 Steady state exercise prior to compression.

Forearm blood flow: There was a main effect of intensity *[F(2,18) = 13.827, P<0.001]* but not condition *[F(1,9) = 0.276, P=0.612]*, nor was there an intensity by condition interaction *[F(2,18) = 2.050, P=0.158]*. FBF was not different between 75 and 90% intensities, but both 75 and 90% intensities resulted in higher blood flow compared to the 50% intensity (see Table 2 for significant post-hoc comparisons). *Muscle oxygenation:* There was no main effect of intensity for oxy[haem] *[F(2,16) = 1.316, P=0.295]* and deoxy[haem] *[F(2,16) = 1.298, P=0.299]* or condition for oxy[haem] *[F(1,8) = 0.364, P=0.562]* and deoxy[haem] *[F(1,8) = 0.375, P=0.557]* nor was there an intensity by condition interaction for oxy[haem] *[F(2,15) = 1.865, P=0.189]* and deoxy[haem] *[F(2,15) = 0.066, P=0.936]*. Therefore, oxygenation in steady state exercise was similar across exercise intensities and conditions. *Force at a given electromyography:* There was no main effect of intensity *[F(2,18) = 0.908, P=0.421]* or condition *[F(1,9) = 0.386, P=0.550]*, nor was there an intensity by condition interaction *[F(2,18) = 0.463, P=0.636]*. Therefore, force at a given electromyography in steady state exercise was similar across exercise intensities and conditions. Given that there are no statistically significant differences in baseline starting values between conditions within intensities and between intensities, we have chosen to report all data as a percent change from steady state values prior to brachial artery or sham compression.

Table 3-2. Steady state measures of force at a given electromyography (force/EMG), oxy[haem], deoxy[haem] and forearm blood flow (FBF).

Intensity	Condition	Force/EMG (N.s/V.s)	Oxy[haem] (%)	Deoxy[haem] (%)	FBF (ml/min)
90%	Hypo.	1211.0 ± 756.2	61.5 ± 8.9	31.5 ± 8.6	232.4 ± 145.0
90%	Con.	1132.1 ± 752.1	70.5 ± 9.1	31.0 ± 12.8	208.5 ± 126.3
90%	Hypo. & Con.	1171.5 ± 735.1	66.0 ± 9.9	31.3 ± 10.6	220.4 ± 132.9*
75%	Hypo.	1249.4 ± 1125.6	68.3 ± 8.7	28.4 ± 11.4	198.1 ± 110.4
75%	Con.	1121.0 ± 946.1	64.5 ± 11.5	36.4 ± 8.2	230.6 ± 142.2
75%	Hypo. & Con.	1185.2 ± 1014.2	66.7 ± 9.9	27.4 ± 9.8	214.0 ± 125.0*
50%	Hypo.	1372.1 ± 832.0	71.4 ± 11.0	29.5 ± 5.7	142.1 ± 96.5
50%	Con.	1391.2 ± 1000.8	72.0 ± 15.0	28.6 ± 6.0	150.4 ± 89.0
50%	Hypo. & Con.	1381.6 ± 895.8	71.7 ± 12.8	29.0 ± 5.7	146.2 ± 90.5

*Significantly different from 50%, P<0.05. Con., Control; Hypo., Hypoperfusion.

3.6.3 What was the effect of manual compression on FBF?

There was a time by condition interaction at 90% [$F\ (16, 176) = 89.99, P<0.001$], 75% [$F\ (16, 160) = 131.63, P<0.001$] and 50% [$F\ (16, 160) = 81.90, P<0.001$], see Fig. 2 for post-hoc comparisons. As intended, in the Control condition FBF did not change with application or release of sham compression at any exercise intensity. By design, in the hypoperfusion condition brachial artery compression rapidly decreased FBF by ~60% in all exercise intensities and this reduction was maintained until compression release. Upon brachial artery compression release, FBF rapidly increased to temporarily exceed FBF in Control in all exercise intensities before returning to levels similar to Control – though FBF remained elevated compared to Control at the 75% intensity. Within the hypoperfusion condition there was a time by intensity interaction effect [$F\ (32, 288) = 3.755, P<0.001$] such that upon brachial artery compression release, the overshoot of FBF was greater in the 50% and 75% intensities compared to 90%. By 315 and 375-sec, FBF remained elevated in the 75% intensity compared to the 50% and 90% intensities, respectively (see Fig. 2 for post hoc comparisons).

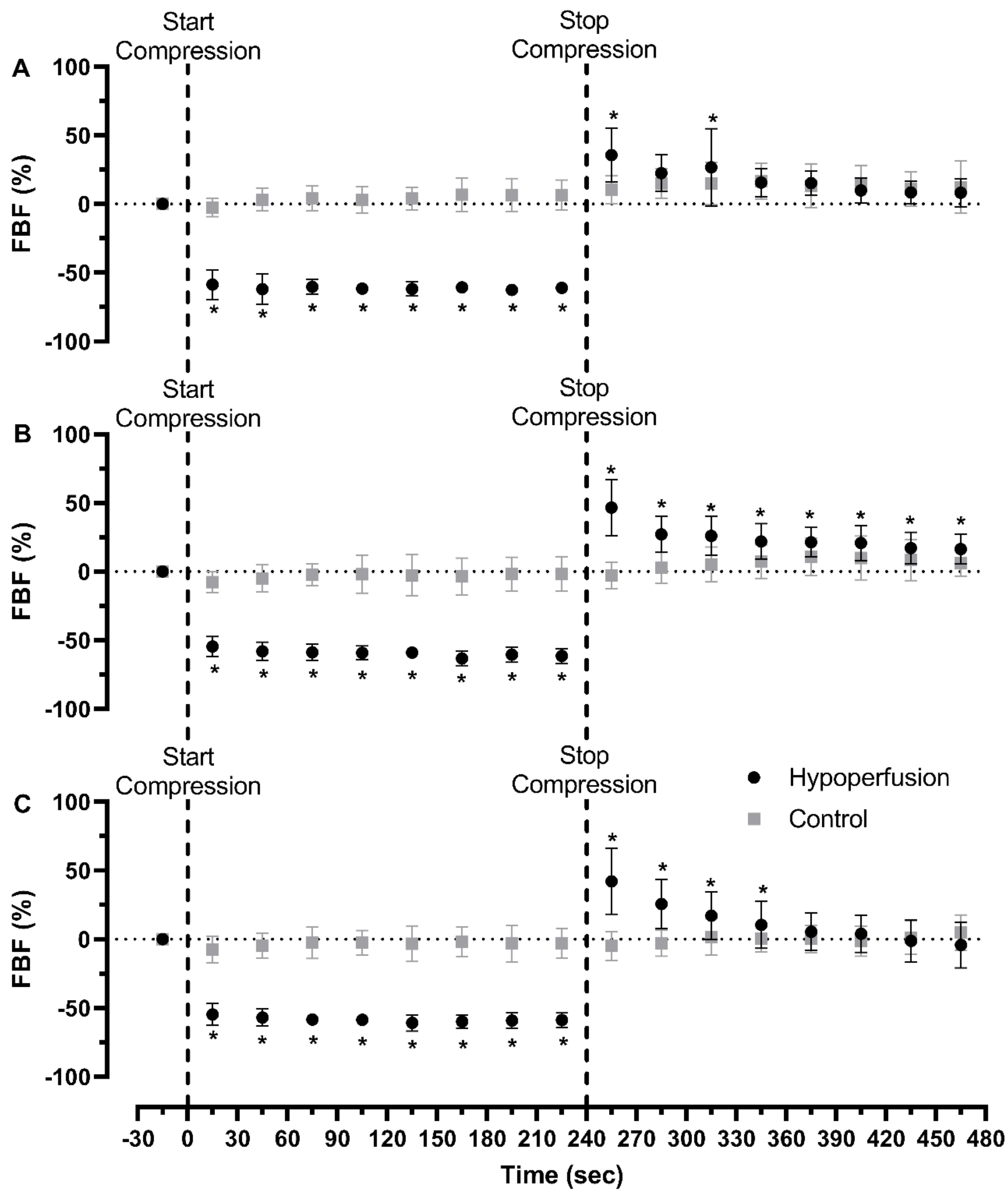

Figure 3-2. Forearm blood flow (FBF) plotted over time as a percent change from steady state (i.e., mean time = -15-sec) and compared between conditions (Hypoperfusion and Control) at 90% (panel: A), 75% (panel: B) and 50% (panel: C) critical impulse. Compression or sham compression began at 0-sec and ended at 240-sec. *Significantly different from Control within time and intensity.

3.6.4 What was the effect of manual compression on exercising forearm muscle oxygenation?

Oxy[haem]: There was a time by condition interaction at 90% [*$F(16, 176) = 21.88$, $P<0.001$]*, 75% *[$F(16, 144) = 5.98$, $P<0.001$]* and 50% *[$F(16, 176) = 10.29$, $P<0.001$]*, see Fig. 3 for post-hoc comparisons. As intended, in the Control condition oxy[haem] did not change with application or release of sham compression at any exercise intensity. Upon brachial artery compression, oxy[haem] rapidly (within 30-sec) decreased in all exercise intensities and this reduction was maintained until compression release. Upon brachial artery compression release oxy[haem] rapidly returned to Control levels and remained at those levels for the remainder of the exercise. There was a time by intensity interaction within the Hypoperfusion condition [*$F(32, 256) = 2.17$, $P<0.001$]*, though, post-hoc tests revealed no statistically significant differences between intensities within time (post-hoc results not reported).

Deoxy[haem]: There was a time by condition interaction at 90% [*$F(16, 176) = 20.13$, $P<0.001$]*, 75% *[$F(16, 144) = 14.36$, $P<0.001$]* and 50% *[$F(16, 176) = 26.47$, $P<0.001$]*, see Fig.4 and for post-hoc comparisons. As intended, in the Control condition deoxy[haem] did not change with application or release of sham compression at any exercise intensity. Upon brachial artery compression, deoxy[haem] increased within 30-sec at 90 and 50% intensities deoxy[haem], whereas deoxy[haem] increased within 60-sec in the 75% intensity. At all intensities, deoxy[haem] remained decreased throughout brachial artery compression. Upon brachial artery compression release deoxy[haem] rapidly returned to Control levels and remained at those levels for the remainder of the exercise. Within the hypoperfusion condition there was a main effect of time *[$F(16, 112) = 20.845$, $P<0.001$]* (main effects not displayed in figures) but there was no time by intensity interaction [*$F(32, 224) = 0.870$, $P=0.677$]*.

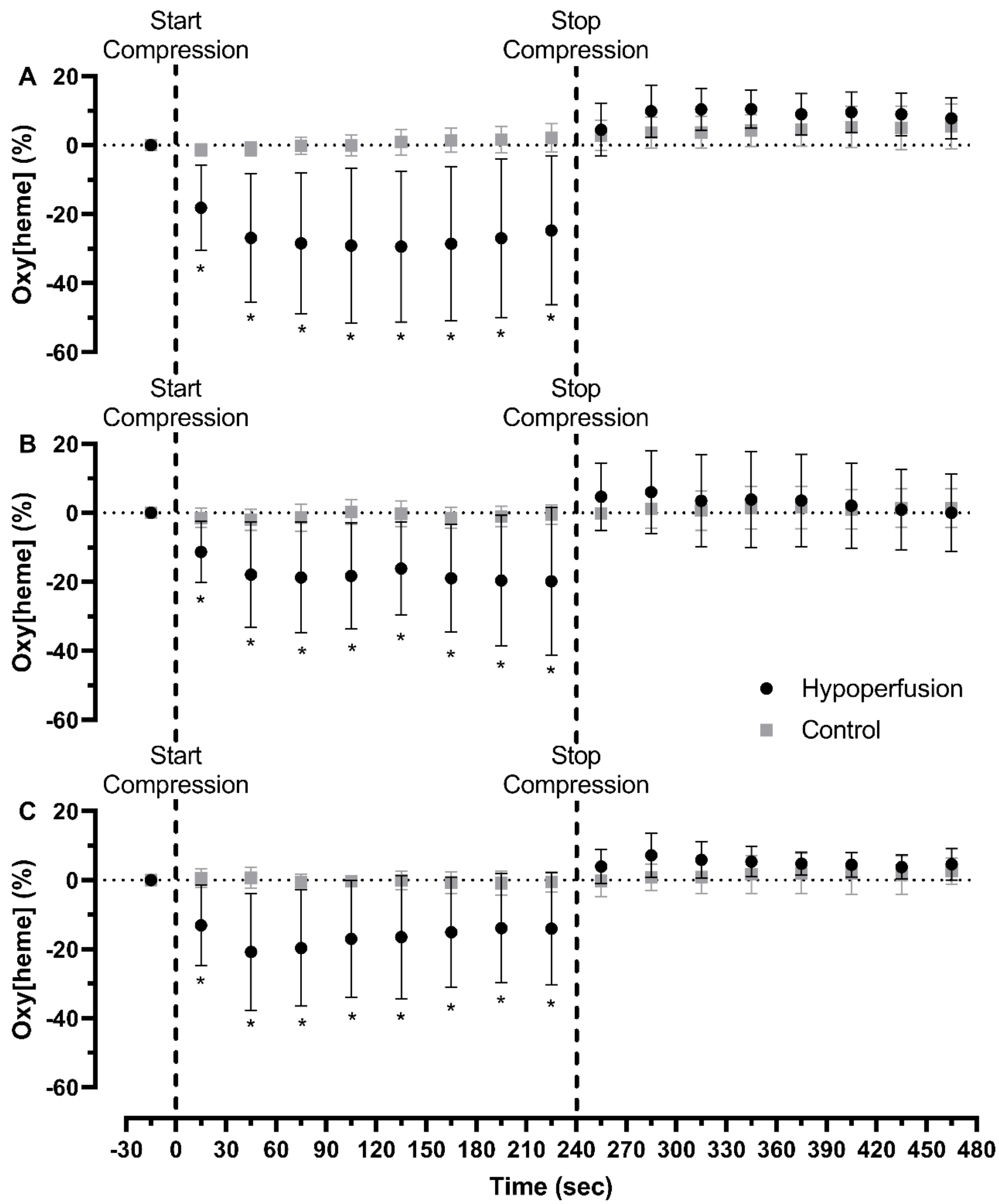

Figure 3-3. Oxy[haem] plotted over time as a percent change from steady state (i.e., mean time = -15-sec) and compared between conditions (Hypoperfusion and Control) at 90% (panel: A), 75% (panel: B) and 50% (panel: C) critical impulse. Compression or sham compression began at 0-sec and ended at 240-sec. *Significantly different from Control within time and intensity.

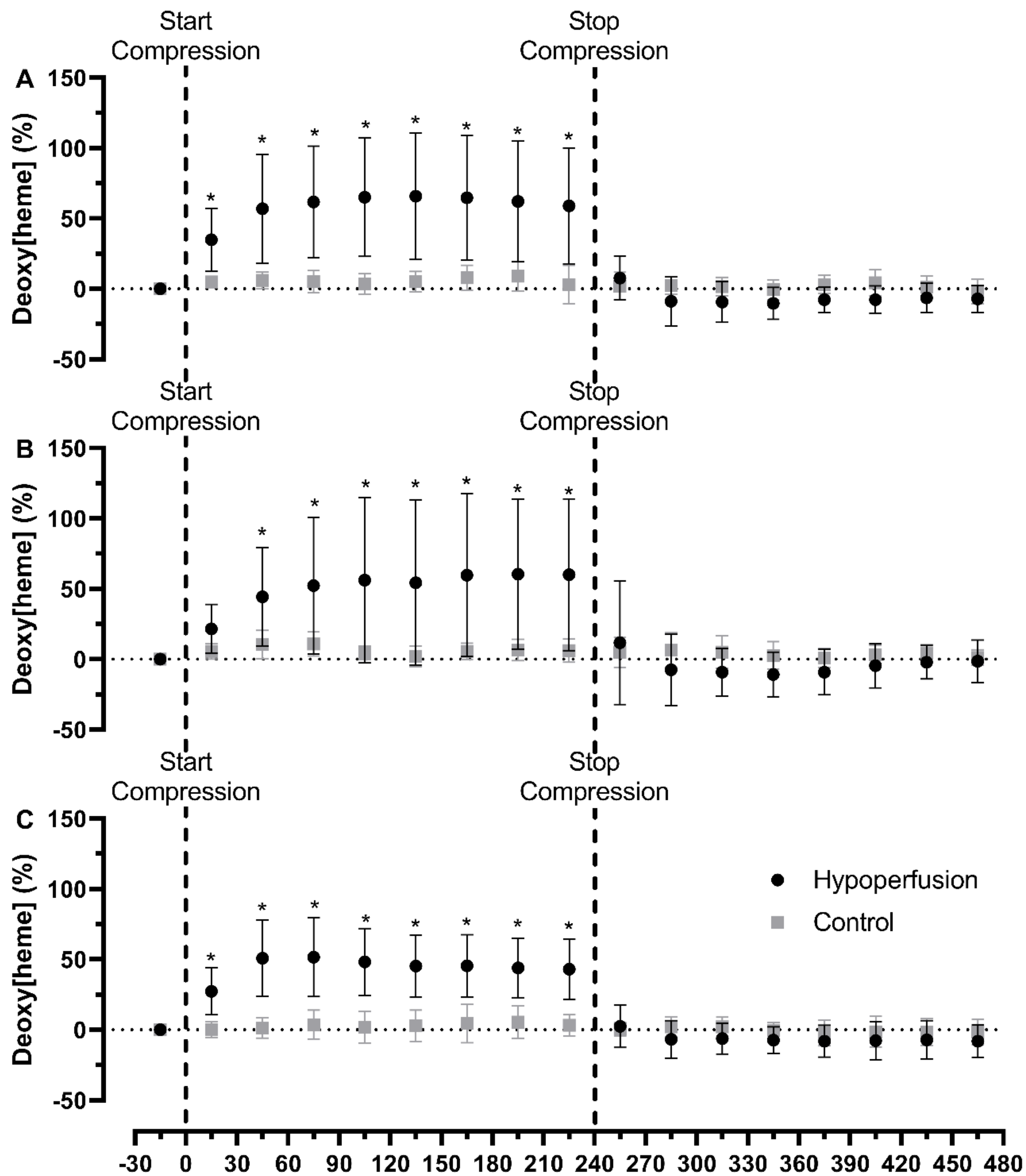

Figure 3-4. Deoxy[haem] plotted over time as a percent change from steady state (i.e., mean time = -15-sec) and compared between conditions (Hypoperfusion and Control) at 90% (panel: A), 75% (panel: B) and 50% (panel: C) critical impulse. Compression or sham compression began at 0-sec and ended at 240-sec. *Significantly different from Control within time and intensity.

3.6.5 Did muscle force output at a given muscle activation follow changes in muscle oxygenation and was this change different between intensities within the Hypoperfusion condition?

There was a time by condition interaction at 90% [*$F(16, 176) = 3.22$, $P<0.001$*] and 75% *[$F(16, 160) = 5.27$, $P<0.001$]* but not at 50% *[$F(16, 160) = 0.87$, $P=0.599$]*, see Fig. 5 for post-hoc comparisons. See Fig. 6 for a representation of raw handgrip force output, EMG RMS and MBV data pre to post brachial artery compression. In the Control condition, Force/EMG did not change with application or release of sham compression at any exercise intensity. Upon brachial artery compression, force/EMG began decreasing in the 75 and 90% conditions, becoming significantly different from Control after 120-sec and 150-sec respectively. Upon brachial artery compression release, force/EMG increased and was no longer different from Control levels within 30-sec (i.e., time = 270-sec) at 90% and after 90-sec (i.e., time = 330-sec) at 75% intensities. There was a time by intensity interaction within the hypoperfusion condition *[$F(32, 288) = 2.69$, $P<0.001$]*, see Fig. 7 for post-hoc comparisons. Post-hoc tests revealed only a statistically significant difference between the 90% and 50% intensity at time 165, 195 and 225-sec. Therefore, the force/EMG relationship changed similarly between the 75 and 90% intensities. Because no differences were detected between the 90 and 75% intensities – to achieve greater power in detecting when muscle force output at a given muscle activation changes under hypoperfusion conditions – we grouped the 90% and 75% intensities and re-analyzed the force/EMG over time between conditions. This analysis revealed a time by condition interaction *[$F(16,352) = 7.314$, $P<0.001$]* where force/EMG was reduced by 120-sec and remained reduced throughout compression. Upon brachial artery compression release, force/EMG was no longer different from control after 90-sec (i.e., time = 330-sec.

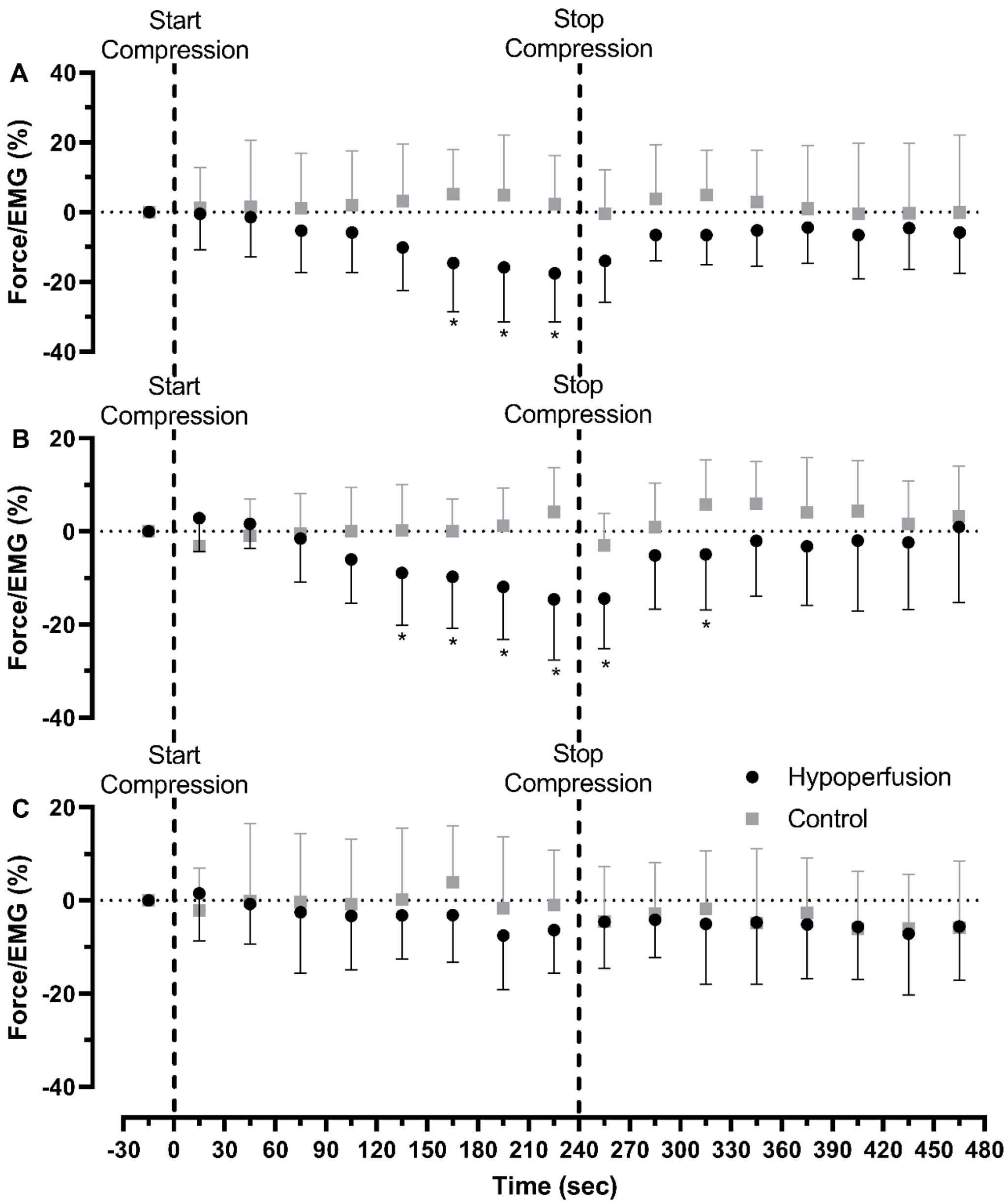

Figure 3-5. Force at a given electromyography (force/EMG) plotted over time as a percent change from steady state (i.e., mean time = -15-sec) and compared between conditions (Hypoperfusion and Control) at 90% (panel: A), 75% (panel: B) and 50% (panel: C) critical impulse. Compression or sham compression began at 0-sec and ended at 240-sec. *Significantly different from Control within time and intensity.

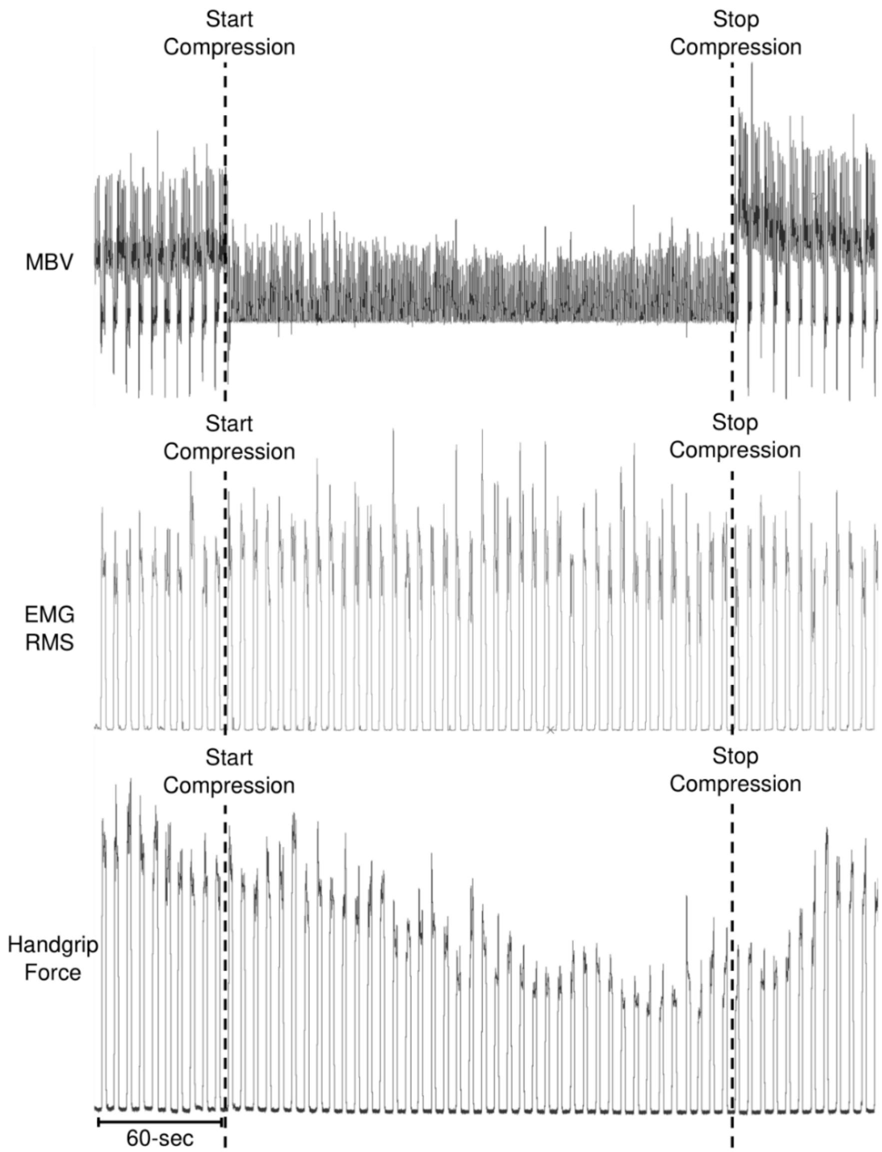

Figure 3-6. Individual response demonstrating the decrease in handgrip force at a given electromyography root mean square (EMG RMS) upon brachial artery compression-evoked hypoperfusion via a 50% reduction in forearm blood flow [represented by mean blood velocity (MBV)] and the rapid restoration of handgrip force when oxygen delivery was restored. Top: MBV. Middle: EMG RMS. Bottom: hand grip force output.

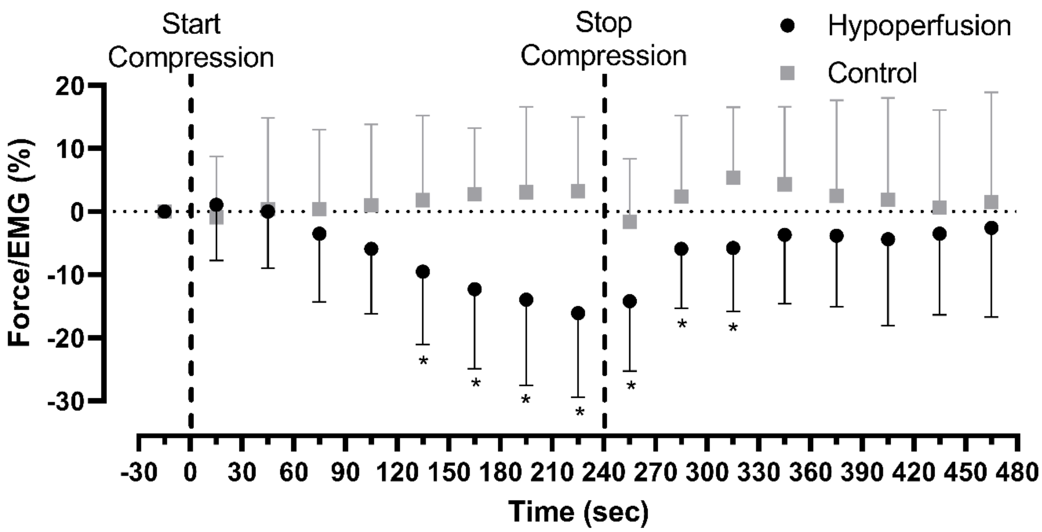

Figure 3-7. Force at a given electromyography (force/EMG) of 90% and 75% intensity groups pooled and plotted over time as a percent change from steady state (i.e., mean time = -15-sec) compared between conditions (Hypoperfusion and Control). Compression or sham compression began at 0-sec and ended at 240-sec. *Significantly different from Control within time and intensity.

3.7 Discussion

Compromise to skeletal muscle force production is a critical determinant of tolerance to exercise (Staiano et al., 2018) and therefore, can dramatically affect quality of life. Understanding mechanisms contributing to skeletal muscle force production compromise helps to identify potential interventions aimed at improving individual exercise tolerance. In this study we tested the hypotheses that force of contraction during maintained voluntary activation in humans rapidly conforms to muscle oxygen delivery, and that this oxygen conforming of force is exercise intensity dependent. The key findings from the present report were as follows: Force of contraction at a given muscle activation (force/EMG) rapidly followed changes in forearm muscle oxygen delivery only at the 90% and 75% critical impulse intensities. We interpret the above findings to support the existence of an oxygen conforming response in voluntary human exercise that – at this level of altered muscle oxygen delivery and therefore oxygenation – exists only at higher intensities.

3.7.1 Characteristics of oxygen conforming of force at constant voluntary muscle activation – response to reduced muscle oxygenation

To date the oxygen conforming response of human skeletal muscle force production has only been characterized in electrically stimulated models. First, with the clever use of arm position mediated perfusion pressure reduction, and therefore presumably reduced oxygen delivery, Fitzpatrick *et al.* (1996) were the first to show oxygen conforming of force produced at a given electrical stimulation in the adductor pollicis muscle of humans. Upon a reduction in perfusion pressure, adductor pollicis force at a given electrical stimulation rapidly decreased (within 120-sec) and returned to normal levels (within 60-sec) upon restoration of perfusion pressure. By adjusting the work rate, these authors were also the first to demonstrate the exercise intensity dependence for this oxygen conforming response – adductor pollicis force production conformed more to a reduction in perfusion pressure at higher work rates (Fitzpatrick et al., 1996). Seventeen years later, Luu and Fitzpatrick (2013) followed up on this work, this time using leg position mediated perfusion reduction (and again presumed reduced oxygen delivery) to demonstrate the oxygen conforming of force produced at a given electrical stimulation in the tibialis anterior muscle of humans. Upon a reduction in perfusion pressure, tibialis anterior force at a given electrical stimulation rapidly decreased (within 120-sec) and returned to normal levels (within 60-sec) upon restoration of perfusion pressure.

There are however key differences between electrically stimulated vs. voluntary activated muscle contractions. Electrical stimulation 1) violates the Henneman size principle of recruitment (Barss et al., 2018; Bergquist et al., 2012; Henneman, 1985), 2) does not reflect physiological motor unit firing frequencies (Lou et al., 2017) and 3) causes synchronous rather than asynchronous motor unit recruitment (Lou et al., 2017). This synchronous rather than asynchronous recruitment of motor units is of great import because in voluntary activation of muscle, rotation of motor unit recruitment could occur in the face of reduced oxygen delivery (Bawa & Murnaghan, 2009; Bawa et al., 2006). By rotating activated motor units – potentially reducing oxygen demand of a given motor unit – it is conceivable that force at a maintained voluntary activation could be maintained when total limb oxygen delivery is reduced. Thus, it cannot be assumed that oxygen conforming of skeletal muscle force production observed in electrically stimulated muscle translates to voluntarily activated muscle contractions. Furthermore, although the findings of Fitzpatrick *et al.* (1996) indicated greater oxygen conforming with higher exercise intensity this was not statistically tested, and oxygen delivery compromise was not measured. Therefore, greater oxygen conforming at higher exercise intensity may have been due to greater relative oxygen delivery compromise. Our study addressed these limitations by 1) having participants (both male and female) voluntarily maintain a constant level of forearm muscle activation at 2) three different exercise intensities while

3) creating the same relative reduction in oxygen delivery across exercise intensities and measuring both forearm blood flow and muscle oxygenation.

Upon commencing brachial artery compression to reduce forearm blood flow by ~60% of steady state values (see Fig. 2), muscle oxy[haem] decreased and muscle deoxy[haem] increased rapidly (within 30 to 60-sec) and remained in this state during compression at all exercise intensities (see Fig. 3 and 4). By design, there was no change in the Control condition with sham compression. Thus, the Control condition provided a time and compression discomfort control for the primary outcome variable, force/EMG. Despite the rapid and similar relative decrease in muscle oxygenation at all intensities, a statistically significant compromise to force/EMG was only evident at the 90% and 75% critical impulse exercise intensities. A potential explanation for this could be as follows. Oxygen conforming of force production, and therefore ATP demand, with a reduction in cell oxygen tension seems to occur because of a decrease in aerobic ATP production – preventing cellular disturbance (Hogan et al., 1996). The lack of force downregulation at the 50% critical impulse exercise intensity may mean that, at that rate of aerobic ATP production, the compromise to cell oxygen tension did not affect aerobic ATP production and therefore force downregulation was not required. Further studies, in which oxygen consumption is measured, are required to test this hypothesis.

Although not evident at 50% critical impulse, the force/EMG compromise was evident after 150-sec at 90% critical impulse and after 120-sec at 75% critical impulse (see Fig. 5), though when 90% and 75% intensities were grouped, force/EMG compromise was evident after 120-sec. These combined data are consistent with the work completed in the electrically stimulated human adductor pollicis (Fitzpatrick et al., 1996) and tibialis anterior (Luu & Fitzpatrick, 2013) muscles, which took 120-sec to see force decrease at a given electrical stimulation. At 75 and 90% critical impulse, we clearly show the first important key characteristic of the oxygen conforming response

– voluntary force of contraction at a given muscle activation rapidly downregulates in the face of reduced oxygen delivery.

3.7.2 Characteristics of oxygen conforming of force at constant voluntary muscle activation – force recovery with restoration of muscle oxygenation.

When brachial artery compression was released at 240-sec, muscle oxygenation was rapidly (within 30-sec) restored to match the Control condition (see Fig. 3 and 4). Although delayed compared to the rapid reversal of muscle blood flow and oxygenation, force/EMG was rapidly restored within 30-sec of reperfusion at 90% critical impulse and after 90-sec of reperfusion at 75% critical impulse (see Fig. 5). When data from the 75 and 90% critical impulse trials were combined, force/EMG was restored to Control levels after 90-sec of reperfusion. Interestingly, upon reperfusion a hyperaemia is observed (see Fig. 2) – indicating an increase in vascular conductance (i.e., vasodilation). This vasodilation could have a couple mediators. First, it may be possible that during hypoperfusion there was cellular disturbance. It is feasible that any cellular disturbance contributed to this vasodilation (Hess et al., 2009) – resulting in the hyperaemia seen upon reperfusion. However, as described below, if there were cellular disturbance, we would expect cellular disturbance mediated fatigue to contribute to a sustained (i.e., several minutes) compromise in force/EMG upon reperfusion. The compromise to force/EMG is however not sustained upon reperfusion. Therefore, although we cannot rule out cellular disturbance as a contributor to the force/EMG response observed, the rapid restoration of force/EMG would suggest it is likely a minor player. The second and more likely explanation for the hyperaemia upon reperfusion is release of ATP by haemoglobin during hypoperfusion (Dietrich et al., 2000; Ellsworth et al., 1995). Under conditions of ischemia there is an increase in oxygen dissociation from haemoglobin – compensating for some of the decrease in oxygen delivery. This increase in oxygen dissociation from haemoglobin also causes ATP release (Dietrich et al., 2000; Ellsworth et al., 1995). This ATP release under hypoperfusion conditions is likely to cause the vasodilation mediated hyperaemia seen in this study. Therefore, despite the minor delay in force/EMG restoration – compared to forearm blood flow and muscle oxygenation – our findings are consistent with the electrically stimulated exercise models where force at a given electrical stimulation was restored within 60-sec (Fitzpatrick et al., 1996; Luu & Fitzpatrick, 2013) and we extend them to show, for the first time, the existence of an oxygen conforming response in voluntary human exercise.

This rapid and complete recovery of force upon oxygen restoration is the second important key characteristic of the oxygen conforming response and is in marked contrast to the slow recovery of force depression associated with cellular disturbance-mediated fatigue. Under conditions of maintained force of contraction, if the intensity is high enough, there is an increase in cellular disturbance-mediated fatigue. Under these circumstances an increase in inorganic phosphate (P_i) can result in an increase in calcium (Ca^{2+}) + P_i precipitate in the sarcoplasmic reticulum, ultimately reducing the amount of free Ca^{2+} release from the sarcoplasmic reticulum – impairing excitation contraction coupling (Westerblad & Allen, 1996; Westerblad et al., 1993). Fatiguing levels of P_i and H^+ have also been shown to decrease the Ca^{2+} sensitivity of myofilaments (Debold, 2016). Specifically, decreased pH (i.e., acidosis) results in decreased affinity of Ca^{2+} for binding to troponin C, thereby reducing Ca^{2+} binding and therefore thin filament activation (Parsons et al., 1997). Further to the effects of P_i + Ca^{2+} precipitate, fatiguing levels of P_i are thought to decrease the level of thin filament activation by reducing the number of strongly bound actin-myosin heads (Debold et al., 2006). Together, an increase in H^+ and P_i, as well as a decrease in [Ca^{2+}], associated with fatiguing exercise, results in the majority of force depression seen during exercise (Debold, 2016).

Under these conditions of cellular disturbance-mediated force depression, recovery of force takes much longer to recover than force depression seen in the oxygen conforming designs where we would expect no cellular disturbance – as evidenced by the stable levels of lactate and PCr during electrically stimulated exercise with a gradual reduction in oxygen delivery (Hogan et al., 1996). For example, in the work of Romer *et al.* (2006), quadriceps twitch force remains compromised at varying levels of stimulus frequency for more than 70-min post fatiguing exercise. Another example, this time looking at fatiguing rhythmic handgrip exercise, results in a sustained compromise of force for more than 35-min post fatiguing exercise (Pitcher & Miles, 1997). Importantly, for cellular disturbance-mediated force depression to recover following fatiguing exercise, the fatiguing exercise must be discontinued (Amann et al., 2006; Katayama et al., 2007; McKeown et al., 2021; Pitcher & Miles, 1997; Romer & Dempsey, 2006; Romer et al., 2006; Ruggiero et al., 2020; Szubski et al., 2007; Wright et al., 1999). This is as opposed to the oxygen conforming response which sees force of contraction rapidly (within 60-sec) recover following changes in oxygen delivery while exercise is ongoing in electrically stimulated muscle (Fitzpatrick et al., 1996; Luu & Fitzpatrick, 2013). Our findings have now demonstrated that this is also the case in voluntarily activated muscle.

This summary of differences between cellular disturbance mediated fatigue and oxygen conforming mediated contribution to force depression highlights a clear knowledge gap in our understanding of oxygen's role in force depression. Importantly, no study has been completed to assess the mechanism(s) involved in determining the conforming response of skeletal muscle force production at a given motor drive upon a decrease in convective oxygen delivery, and the subsequent rapid and complete recovery of force production with restoration of oxygen delivery. Like cellular disturbance-mediated fatigue, this force/EMG-conforming-to-oxygen-delivery-response has the potential to greatly impair the relationship between force and muscle activation. Therefore, like cellular disturbance-mediated fatigue, our work demonstrates that understanding mechanisms of oxygen conforming warrants equal attention.

3.7.3 Potential mechanisms of the oxygen conforming response

Luu & Fitzpatrick (2013) proposed that the reversible modulation of force output by perfusion pressure is the result of ionic shifts partly dependent on the level of potassium ion clearance – thereby implicating blood flow as a determinant for the change in force output at a given muscle activation and not oxygen delivery per se. Important work from Hogan and colleagues oppose this interpretation. First, Hogan *et al.* (1996) demonstrated that force at a given muscle activation follows changes in oxygen delivery – this is regardless of whether the decrease in oxygen delivery is due to changes in muscle blood flow or arterial oxygen content. Second, Hogan *et al.* (1999) demonstrated that the rapid recovery of force/EMG was dependent on oxygen delivery and not blood flow. Hogan *et al.* (1996) then proposed an alternative explanation for the depression of force upon a decrease in oxygen delivery, in which the decrease in force production may be the result of an oxygen-mediated decrease in calcium release from the sarcoplasmic reticulum – no study, that we are aware of, has followed up and tested this hypothesis. Alternatively, calcium sensitivity of skinned smooth (Soloviev & Basilyuk, 1993) and striated muscle (Brotto et al., 2000) contractile apparatus is decreased with reduced oxygen tension.

Finally, multicellular organism free energy consumption is ultimately constrained by the rate of free energy provision having to match the rate of free energy consumption in a manner that allows removal of the waste products of free energy provision. Oxidative metabolism is the only means for more than very low rates of sustainable free energy provision to occur because its by-products of CO_2 and H_2O can be removed at substantial rates. Therefore, a thermodynamic basis for mechanisms that "conform" the rate of free energy consumption (force production and the related ion pump and contractile protein metabolic reactions) to effects of altered oxygenation on aerobic free energy provision (ATP synthesis) requires consideration. Nevertheless, at present, no experimental data has been generated that identifies the mechanism(s) of this force/EMG-conforming-to-oxygen-delivery-response and mechanism identification was beyond the scope of the current study.

3.7.4 Methodological considerations

There are methodological considerations that warrant discussion. First, this study did not assess the metabolic state of the exercising muscle during oxygen conforming conditions, therefore, we cannot confirm metabolic stability throughout oxygen conforming changes of force. However, if there were cellular disturbance-mediated fatigue, recovery of force would have been much slower (Pitcher & Miles, 1997; Romer et al., 2006) – yet we observed the rapid recovery of force upon recovery of muscle oxygenation that is consistent with oxygen conforming (Fitzpatrick et al., 1996; Luu & Fitzpatrick, 2013). Nevertheless, it is important for future work to confirm a stable cell environment during oxygen conforming changes to force in voluntary exercise in humans. This knowledge gap reflects the third and final important key characteristic of the oxygen conforming response – the cellular environment will remain stable during oxygen conforming changes in force at a given muscle activation.

Second, handgrip exercise involves several muscles – primarily the flexor digitorum profundus (FDP) and superficialis (FDS) muscles – and we only measured muscle activation in the FDS. Our ability to detect EMG signals in the FDP is challenged by superficial muscles (e.g., pronator teres, flexor carpi radialis, and palmaris longus) when using surface EMG electrodes. Accordingly, the FDS was chosen for its accessibility for measurement of simultaneous muscle activation and oxygenation. The FDS acted as a proxy for forearm muscle activation during handgrip exercise. Therefore, it must be acknowledged that a change in FDP muscle activation relative to FDS activation with altered oxygen delivery could conceivably result in altered forearm force during maintained FDS EMG that is not reflecting oxygen conforming. However, this would require selective reduction in activation of the FDP and its force over time with reduced oxygenation and subsequent rapid restoration of FDP activation with restoration of oxygenation. Considering our results are consistent with previous oxygen conforming work in electrically stimulated muscle, and that all forearm muscle experienced the same perfusion manipulation, such unique alteration in one vs. another muscle group corresponding to perfusion changes seems highly unlikely. Therefore, we interpret our findings to represent force conforming to oxygen delivery.

Important strengths of the present design must also be highlighted. First, although the maintenance of a consistent voluntary muscle activation target is difficult and therefore there is contraction to contraction variability, we were able to create a model that allowed participants to achieve a targeted voluntary muscle activation with little variation over time at the group level (see Fig. 6) – the mean EMG RMS data fluctuated by no more than ± 3% (data not shown). Second, we were able to control muscle oxygen delivery to ensure the same relative reduction in muscle blood flow and subsequent muscle oxygenation across exercise intensities. This allowed assessment of an exercise intensity dependence at the same relative compromise to muscle oxygenation. Third, we documented changes in force over time to gain insight into the temporal adjustment of force at a targeted voluntary muscle activation. The use of this model is therefore supported for future oxygen conforming work.

3.8 Conclusion

This study has demonstrated – for the first time in voluntarily exercising humans – the existence of two of the three key characteristics of the oxygen conforming response. First, voluntary force of contraction at a given muscle activation rapidly conforms to oxygen delivery. Second, voluntary force of contraction at a given muscle activation rapidly and completely recovers following restoration of oxygen delivery. The third characteristic – that the cellular environment will remain stable during oxygen conforming changes in force at a given muscle activation – remains to be tested and confirmed in voluntary human exercise. Importantly, this study advances understanding of oxygen conforming of force production in voluntary exercise by demonstrating that it is exercise intensity dependent.

In conclusion, although much is understood about cellular disturbance-mediated fatigue, the mechanisms of “oxygen conforming” remain unknown. Like cellular disturbance-mediated fatigue resulting from maintained exercising muscle force production under conditions of reduced oxygen delivery, the oxygen conforming response has important implications for exercise tolerance. Therefore, the mechanisms responsible for this oxygen conforming response require investigation.

Chapter 4 - The ‘normal’ adjustment of oxygen delivery to small muscle mass exercise is not optimized for muscle contractile function

Chapter 4 is published as:

Drouin PJ, Liu T, Lew LA, McGarity-Shipley E & Tschakovsky ME. The 'normal' adjustment of oxygen delivery to small muscle mass exercise is not optimized for muscle contractile function. J Physiol 601, 783-799, 2023.

4.1 Key points

- Oxygen delivery is viewed as tightly coupled to demand in exercise below critical power because increasing oxygen delivery does not increase the rate of oxygen uptake.
- Whether the “normal” adjustment of oxygen delivery in small muscle mass exercise below critical power is optimal for excitation-contraction coupling is not known.
- Here we show in humans that increasing oxygen delivery above “normal” improves excitation-contraction coupling.
- These results suggest that, in the heavy exercise intensity domain, the “normal” matching of oxygen delivery to metabolic demand is not optimal for muscle excitation-contraction coupling.
- Therefore, the nature of vasoregulation in exercising muscle is such that it does not support optimal perfusion for excitation-contraction coupling.

4.2 Abstract

Oxygen delivery is viewed as tightly coupled to demand in exercise below critical power because increasing oxygen delivery does not increase VO_2. However, whether the "normal" adjustment of oxygen delivery to small muscle mass exercise in the heavy intensity domain is optimal for excitation-contraction coupling is currently unknown. In 20 participants (10 female), a remote skeletal muscle (i.e., tibialis anterior) metaboreflex was (Hyperperfusion condition) or was not (control condition) activated for 4-min during both force of contraction (experimental model 1) and muscle activation targeted (experimental model 2) rhythmic forearm handgrip exercise. Analysis was completed on the combined data from both experimental models. After 30-sec of remote skeletal muscle metaboreflex activation, mean arterial blood pressure, forearm blood flow, and muscle oxygenation were increased and remained increased until metaboreflex discontinuation. While oxygen delivery was elevated, the muscle activation to force of contraction ratio was improved. Upon metaboreflex discontinuation, forearm oxygen delivery and the muscle activation and force of contraction ratio was rapidly (within 30-sec) returned to control levels. These findings demonstrate that (a) the metaboreflex was effective at increasing forearm muscle oxygen delivery and oxygenation, (b) the muscle activation to force of contraction ratio was improved with increased oxygen delivery, and (c) in the heavy exercise intensity domain, the normal matching of oxygen delivery to metabolic demand is not optimal for muscle excitation-contraction coupling. These results suggest that the nature of vasoregulation in exercising muscle is such that it does not support optimal perfusion for excitation-contraction coupling.

4.3 Introduction

The current dogma surrounding oxygen delivery:demand matching suggests that oxygen delivery is tightly matched to oxygen demand. This is supported by studies where (a) oxygen delivery increases linearly with oxygen demand (Radegran, 1997; Richardson et al., 1995) and (b) there is a counteracting vasoconstriction when arterial oxygen content is increased – thereby maintaining oxygen delivery (Gonzalez-Alonso et al., 2002; Gonzalez-Alonso et al., 2001). Importantly, recent evidence suggests that elevated sympathetic restraint in exercising forearm muscles in altitude acclimatized individuals is there to prevent "excess" vasodilation and oxygen delivery relative to demand (i.e., rate of oxygen consumption (VO_2)) – inferring that there is no benefit to increased perfusion beyond that achieved with the normal vasoregulatory response to exercise (Hansen et al., 2022).

In a recent review, Nyberg and Jones (2022) frame adequate oxygen delivery demand matching as follows: if delivery is adequate to support VO_2, then increasing oxygen delivery will not increase VO_2. This interpretation appears to hold up at intensities below critical power (Pawelczyk et al., 1992). However, this perspective does not consider that it is possible to maintain VO_2 with reduced oxygen delivery via increased redox and phosphorylation potentials (Erecinska & Wilson, 1982; Haseler et al., 1998; Hogan, Arthur, et al., 1992; Hogan et al., 1998; Hogan et al., 1996; Wilson & Erecinska, 1985; Wilson et al., 1979). The caveat to this response is that the increased metabolic disturbance at the same VO_2 compromises force at a given muscle activation (Fulco et al., 1996; Hogan, Arthur, et al., 1992; Hogan, Richardson, et al., 1999). Therefore, although VO_2 is maintained at a decreased oxygen delivery, inferring adequate oxygen delivery according to the criteria presented by Nyberg and Jones (2022), this oxygen delivery is not optimal for muscle contractile function.

Whether the "normal" adjustment of oxygen delivery (i.e., blood flow) in small muscle mass exercise below critical power is optimal for muscle performance requirements is not known.

To test the hypothesis that the “normal” adjustment of oxygen delivery is optimal for muscle performance we used remote skeletal muscle metaboreflex activation to increase arterial blood pressure and thereby increase exercising forearm muscle perfusion (Tschakovsky & Hughson, 1999). As a measure of exercising muscle excitation contraction coupling performance (force for a given muscle activation) we quantified the ratio of forearm muscle electromyography (EMG) relative to contraction force during constant rhythmic forearm handgrip exercise (Drouin et al., 2022; Drouin et al., 2019) at 90% of critical power. We speculated that if the normal adjustment in exercising forearm muscle oxygen delivery was not optimal, we would observe an improvement in muscle force relative to EMG during metaboreflex mediated hyperperfusion. Importantly, given the potential for hyperperfusion non-responders to the metaboreflex protocol (Perrey et al., 2001), data from these participants would allow for distinction between a generalized effect of the metaboreflex on the muscle activation to force of contraction relationship vs. an effect specific to exercising forearm hyperperfusion.

4.4 Methods

4.4.1 Participants and ethical approval

Twenty healthy participants (10 female) were recruited for this study (see Table 1 in Results). All experimental procedures were reviewed and approved by the Queen’s University Health Sciences and Affiliated Teaching Hospitals Research Ethics Board (6005158 PHE-036-02) and conformed to the standards set by the Declaration of Helsinki except for registration in a data base. Informed written consent of voluntary participation was obtained from all participants prior to participation in the study.

4.4.2 Experimental design and conditions

This study was a within-participant design in which participants completed 5-7 handgrip exercise tests over three testing days. Participants were asked to abstain from food 4 h before, caffeine and alcohol 12 h before and strenuous upper body exercise for 24 h before each testing day.

4.4.2.1 Exercise modality

Forearm exercise consisting of rhythmic isometric forearm handgrip contractions at a contraction:relaxation frequency of 2-sec:2-sec. Participants lay supine with their right and left arms at heart level. Handgrip exercise was always completed with the participant’s right hand.

4.4.2.2 Screening and critical power.

Participants were screened to make sure that (a) they could tolerate the discomfort associated with the metaboreflex protocol, (b) they could properly coordinate handgrip exercise and dorsiflexion exercise and (c) they have a metaboreflex response (i.e., increase in mean arterial blood pressure).

Participants then completed a 600-sec handgrip critical power test per that designed by Kellawan and Tschakovsky (2014). The force of contractions over the final 30-sec of this critical power test were averaged to provide a value for critical power. From this critical power value, 90% critical power was calculated as the workload for all subsequent exercise sessions.

4.4.2.3 Force of contraction maintenance with and without hyperperfusion.

To create conditions reflecting typical exercise – where force of contraction is maintained and skeletal muscle fatigue is evident – participants completed rhythmic handgrip exercise targeting 90% critical power handgrip force. To test the effect of metaboreflex-mediated hyperperfusion on the amount of muscle activation required to maintain force of contraction during fatiguing exercise, the metaboreflex was (Hyperperfusion condition) or was not (Control condition) stimulated in the participants lower legs at 240-sec of exercise for 240-sec (see below for metaboreflex procedure). The control protocol was run first to ensure participants could effectively target the desired force of contraction prior to adding concomitant dorsiflexion exercise. This was followed by 2-3 hyperperfusion tests (number of tests was dependent on how well the participant tolerated the metaboreflex protocol). Repeated trials of the Hyperperfusion condition were completed to reduce variability of the response to improve detection of an effect if one exists. A 10-min break was provided between trials completed on the same day to ensure resting mean blood velocity was restored prior to commencing another trial.

4.4.2.4 Muscle activation maintenance with and without hyperperfusion.

To create conditions where cellular disturbance is attenuated, participants completed rhythmic handgrip exercise targeting muscle activity to produce contractions at 90% critical power. To identify this target activation, as per Drouin et al. (2022) ten 2-sec contractions at 90% critical power were completed with 30-sec of rest between contractions. The average muscle activity of the ten handgrip contractions required to achieve 90% critical power was used as the muscle activation maintenance target. By maintaining a target muscle activation instead of force of contraction, we are creating a condition where force of contraction is allowed to adjust to alterations in oxygen delivery. To test the effect of metaboreflex-mediated hyperperfusion on the amount of force produced for a given muscle activation during fatiguing exercise, the metaboreflex was (Hyperperfusion condition) or was not (Control condition) stimulated in the participants lower legs at the 240-sec of exercise for 240-sec. The control protocol was run first to ensure participants could effectively target the desired muscle activation prior to adding concomitant dorsiflexion exercise. This was followed by 2-3 hyperperfusion tests (number of tests was dependent on how well the participant tolerated the metaboreflex protocol). Repeated trials of the Hyperperfusion condition were completed to reduce variability of the response to improve detection of an effect if one exists. A 10-min break was provided between trials completed on the same day to ensure resting mean blood velocity was restored prior to commencing another trial.

4.4.2.5 Metaboreflex protocol (hyperperfusion condition).

Prior to the onset of exercise, the dorsiflexion weight system was secured to the participant's feet and the weight was supported until dorsiflexion onset. Thirty seconds prior to the metaboreflex onset, a research assistant began manually inflating the blood pressure cuffs around the participants thighs directly proximal to the knee. By 240-sec of exercise, the blood pressure cuffs were inflated to between 200 and 220 mmHg and kept there throughout the metaboreflex procedure. At 240-sec exercise, the weights (10lbs each), secured to the participants feet, were dropped and the participant began rhythmic dorsiflexion exercise (2-sec contraction : 2-sec relaxation) with both feet –

dorsiflexion exercise continued for 120-sec. After 120-sec of dorsiflexion exercise, the weights were removed and the participant discontinued dorsiflexion exercise. The blood pressure cuffs remained inflated for another 120-sec. At 240-sec of cuff inflation, the cuffs were deflated and handgrip exercise continued for another 240-sec. See schematic of the experimental protocol in Fig. 1 (see Appendix C for more details).

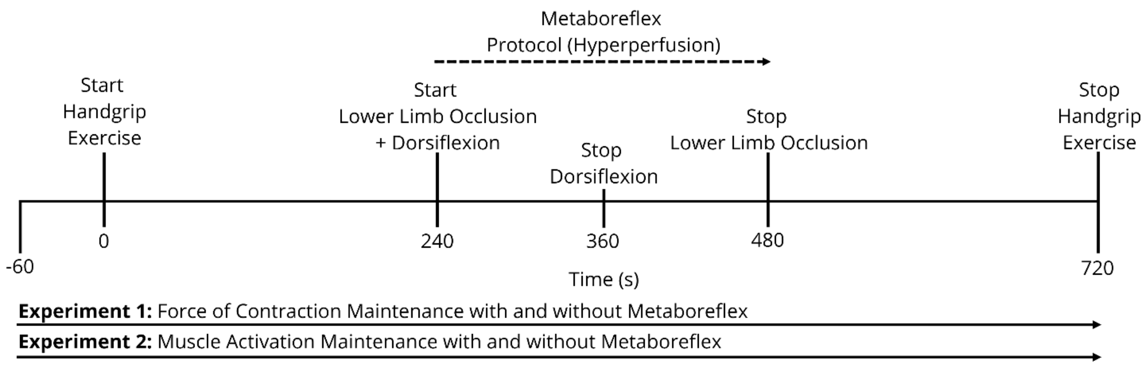

Figure 4-1. Summary of protocol. Rhythmic forearm handgrip exercise is completed for 720-sec. At 240-sec, bilateral dorsiflexion exercise begins with blood pressure cuffs inflated to suprasystolic levels (between 200-220 mmHg) just proximal to the knee – creating a metaboreflex. At 360-sec, dorsiflexion exercise is discontinued. At 480-sec, blood pressure cuffs are deflated.

4.4.2.6 Ischemic calibration of near infrared spectroscopy signals.

Calibration of near infrared spectroscopy signals were completed with an ischemic calibration protocol described elsewhere (Drouin et al., 2022) according to the guidelines set by Barstow (2019). Briefly, with the arm positioned horizontally, a blood pressure cuff was inflated to ~250 mmHg for 5-min or until a plateau in NIRS signals was achieved. The cuff was then deflated and the participant was asked to keep still for another 2-min or until NIRS signals had peaked.

4.4.3 Instrumentation and data acquisition

4.4.3.1 Mean arterial blood pressure.

A finger photoplethysmograph (Finometer MIDI; Finapres Medical Systems), placed on the participants left middle finger and kept at heart level, was used to measure mean arterial blood pressure.

4.4.3.2 Flexor digitorum superficialis muscle activation.

Flexor digitorum superficialis muscle activation was recorded via four mini wireless bipolar electrodes (Delsys, Natick, MA) placed according to guidelines reported elsewhere (Drouin et al., 2019) – using guidance from Bickerton et al. (1997). Muscle activity was wirelessly recorded via a Delsys Trigno Base (Delsys, Natick, MA) and then transmitted through a Trigno EMG 1-16 adapter (ADInstruments, Colorado Springs, CO) and PowerLab interface cable to be recorded in Labchart 7 software (ADInstruments, Colorado Springs, CO) at 2000 Hz/channel. In Labchart 7 software, the root mean square of each individual electromyography (EMG) signal was calculated in separate channels and then the average of all four sensors was calculated in another calculated channel. The average EMG root mean square signal was used as the target EMG signal for the muscle activation maintenance trials.

4.4.3.3 Flexor digitorum superficialis muscle oxygenation.

Flexor digitorum superficialis muscle oxygenation – change in oxygenated [haem] (oxy[haem]) and deoxygenated [haem] (deoxy[haem]) – was recorded via near infrared spectroscopy (NIRS, Oxymon MK III, Artinis Medical Systems, Netherlands) next to the EMG sensors placed on the forearm. The NIRS device used a single optical fiber operating at three wavelengths (874, 761, 803 nm), data was collected at 10 Hz, the interoptode distance was 25-mm with a constant differential pathlength factor of 3.59 (van der Zee et al., 1992), with participant-specific power and gain settings.

4.4.3.4 Handgrip force output.

Force of handgrip contraction was collected at 2000 Hz via a force transducer connected to a PowerLab/8_{SP}. The force transducer was calibrated by first measuring the voltage associated with known weights and creating a calibration curve. On each day, a two-point calibration was completed using this calibration curve.

4.4.3.5 Forearm blood flow.

Brachial artery mean blood velocity and vessel diameter were measured continuously during the 720-sec exercise tests. Brachial artery blood velocity was measured with a flat 4-MHz pulsed Doppler probe (model 500V 131 Transcranial Doppler; Multigon industries, Mt. Vernon, NY) attached to the skin over the brachial artery proximal to the antecubital fossa of the exercising forearm. Brachial artery blood velocity data were collected in volts by analog connection to a Powerlab/8_{SP} (ADInstruments, Colorado Springs, CO) and converted to cm/s in Labchart 7 software (ADInstruments, Colorado Springs, CO) using a previously created calibration curve – this calibration accounted for the insonation angle of the doppler ultrasound relative to the participants' brachial artery. Brachial artery diameter was measured with a linear echo ultrasound probe positioned over the brachial artery ~5cm proximal to the Doppler probe, operating at 13 MHz in 2D mode (Vivid I; GE Medical Systems, London, ON, Canada).

4.4.4 Data analysis

4.4.4.1 Mean arterial blood pressure.

Thirty second time bins were calculated for mean arterial blood pressure.

4.4.4.2 Flexor digitorum superficialis muscle activation and handgrip force output.

Flexor Digitorum Superficialis muscle activation and handgrip force was analyzed in Labchart 7 software using a manually created macro. To calculate the integral of handgrip force (units: N·s) and muscle activation (units: mV·s), the macro was designed to identify the onset and offset of each contraction (defined as the force channel passing above or below N = 9.81) and to calculate the associated integrals. These data were then exported to excel where the ratio of muscle activation to handgrip force (EMG/Force) was calculated and then 30-sec time bins were calculated for all measurements.

4.4.4.3 Flexor digitorum superficialis muscle oxygenation.

Ischemic calibration described previously helped us obtain an approximate 100% and 0% signal for both deoxy[haem] and oxy[haem]. During cuff inflation, 0% oxy[haem] and 100% deoxy[haem] signals were obtained. During hyperaemia following cuff deflation, 100% oxy[haem] and 0% deoxy[haem] signals were obtained. This approach has a reported excellent within-subject reproducibility (Ryan et al., 2012).

4.4.4.4 Forearm blood flow.

Thirty second time bins were calculated for brachial artery blood velocity. Brachial artery diameters were quantified with Measurements from Arterial Ultrasound Imaging (MAUI, Hedgehog

Medical) automated edge detection software and averaged over the same time as brachial artery blood velocity values. Forearm blood flow was calculated as MBV (cm/s) · 60 s/min · π · [brachial artery diameter (cm)/2]^2. Where MBV is mean blood velocity in cm/s.

4.4.4.5 General methods.

Following the above data analysis approaches, the two to three hyperperfusion trials completed on a single day were averaged to yield a single mean response for each experimental approach. In the present study we used two experimental models to assess the effect of remote muscle metaboreflex mediated forearm hyperperfusion on the voluntary forearm exercise EMG/Force ratio. Because both models measured EMG and Force, the EMG/Force relationship from both experimental models could be combined to achieve a large sample size to help detect a difference between hyperperfusion and control conditions – if one existed. Therefore, we combined data from both experimental models to increase our sample size – helping us detect a difference between conditions if one existed.

4.4.5 Statistical analysis

To test for differences in steady state values between conditions, paired t-tests were run on the steady state values for all variables. To assess the effectiveness of the metaboreflex protocol (i.e., Hyperperfusion condition) in creating a pressor reflex and increasing forearm blood flow, two-way (i.e., condition and time) repeated measures ANOVAs were run on forearm blood flow (FBF), mean arterial blood pressure (MAP) and forearm vascular conductance (FVC). To assess the effect of metaboreflex-mediated hyperperfusion over time on muscle oxygenation two-way repeated measures ANOVAs were run on oxy[haem] and deoxy[haem]. To assess the effect of metaboreflex-mediated hyperperfusion over time on force of contraction integral, muscle activation integral and the ratio between the two, two-way repeated measures ANOVAs were run. Statistical tests were first run on each experimental model separately. Similar to previous work where we combined data from 75 and 90% intensities to improve statistical power (Drouin et al., 2022), here we combined data from both force of contraction maintenance and muscle activation maintenance models, and ran statistical tests on these data – effectively doubling our sample size. Upon discovery of condition by time interactions, multiple comparisons were completed within time between conditions on measurements from metaboreflex onset to test end. Per Rothman (1990), to improve our ability to interpret time course data between conditions, when the null hypothesis for time by condition interactions were false, no mathematical corrections were made for multiple comparisons and we have reported the individual P values and confidence intervals for multiple comparisons. This approach requires that we acknowledge the possibility that, given $n = 16$ pairwise comparisons and $\alpha = 0.05$, there is a 56% chance of at least one statistically significant finding assuming all 16 of the null hypotheses are true (Rothman, 1990). Statistical tests were run using GraphPad Prism 9 software (GraphPad, San Diego, CA). Statistical significance was assumed at $P < 0.05$.

4.5 Results

Table 4-1. Age, anthropometric measures, force, critical power (CP) and percent maximal voluntary contraction (MVC).

Variable (unit)	Group Mean (n=20)
Age (years)	20.6 ± 3.72
Height (cm)	174 ± 7.71
Weight (Kg)	74.1 ± 12.0
Force of MVC (N)	332 ± 113
Force at CP (N)	121 ± 40.0
Force at 90% CP (N)	109 ± 36.0
%MVC at CP	36.8 ± 6.64
%MVC at 90% CP	33.1 ± 5.98

Values are mean ± SD

4.5.1 Participant's completion of protocols.

Of the 21 participants screened, one male could not tolerate the metaboreflex protocol, therefore the total sample size run through experimental testing was 20 (10 female) (see Table 1 for anthropometric data). As per previous work (Tschakovsky & Hughson, 1999), this study used the lower leg metaboreflex to increase mean arterial pressure and therefore forearm blood flow above normal steady state levels. However, given that there can be individual differences in the response to the metaboreflex procedure (Perrey et al., 2001), we expected that there could be counteracting vasoconstriction of the forearm with metaboreflex activation – resulting in no forearm blood flow increase. These individuals who did not have a forearm blood flow increase were excluded from statistical analysis of the effect of increased perfusion with metaboreflex activation. However, per our hypothesis, data from these participants provide important insight into the role of flow elevations on the muscle activation to force of contraction ratio. Their data is therefore plotted in Fig. 2. There was additional loss of participants for certain variables under certain conditions due to technical issues with measurement or execution of the exercise protocol, which decreased the n for certain comparisons (data not presented).

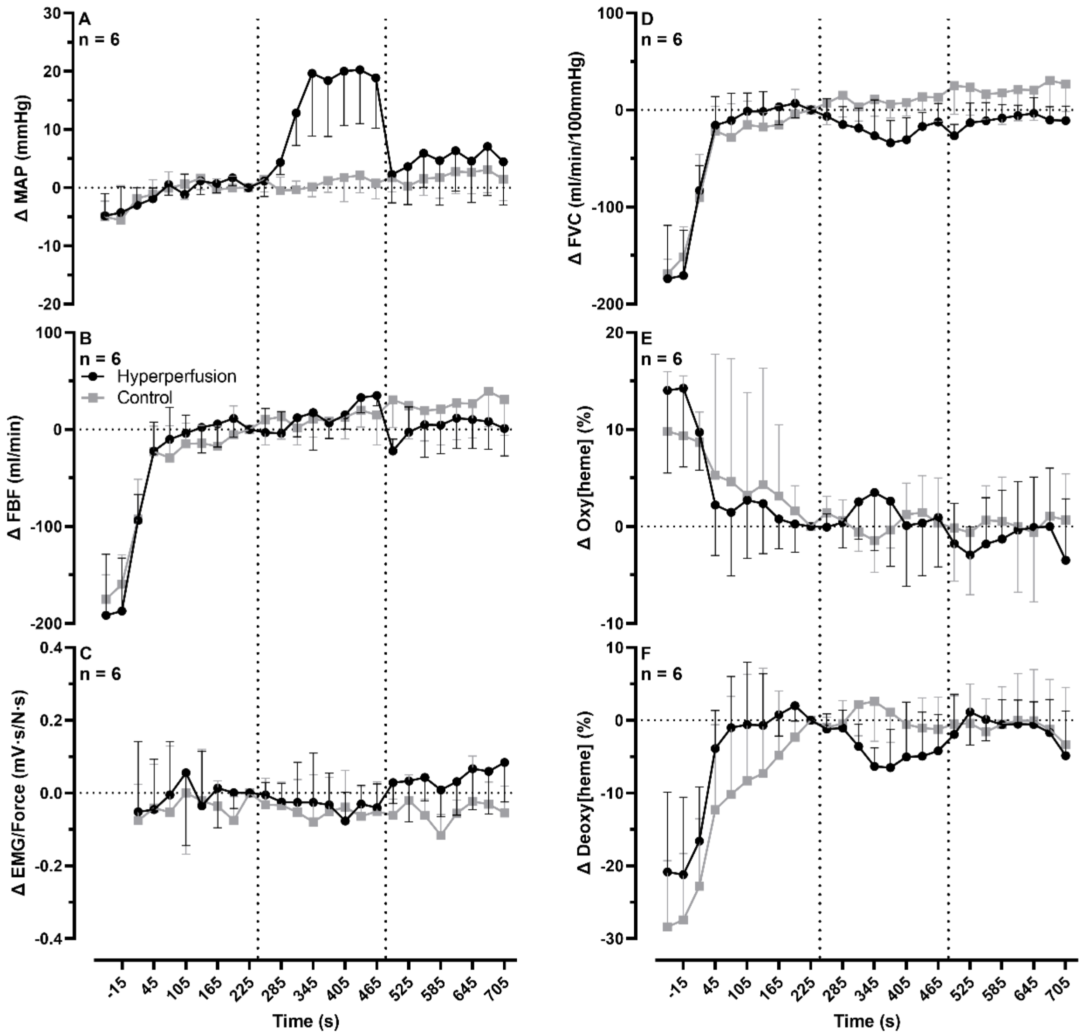

Figure 4-2. Data from participants excluded due to an absence of hyperperfusion upon metaboreflex activation. Data from force of contraction maintenance and muscle activation maintenance experiments combined for mean arterial blood pressure (MAP, panel A), forearm blood flow (FBF, panel B), EMG/Force (panel C), forearm vascular conductance (FVC, panel D), oxy[haem] (panel E) and deoxy[haem] (panel F) plotted over time as a delta from steady state values (time = 225-sec) and compared between conditions (Hyperperfusion and Control). The metaboreflex procedure began at time = 240-sec and ended at time = 480-sec. Dashed lines indicate period of metaboreflex activation. Data are mean ± SD.

4.5.2 Steady-state values.

4.5.2.1 Force of contraction maintenance.

Mean arterial blood pressure and FBF but not FVC measured at steady state were significantly higher in Hyperperfusion compared to Control. In line with higher steady state FBF, oxy[haem] was higher but deoxy[haem] was not different at steady state in Hyperperfusion compared to Control. There were no significant differences in steady state force integral, EMG integral and EMG/Force values between Hyperperfusion and Control conditions. Because of steady state differences, all values are presented as a delta from the steady state measures at time = 225-sec. See steady state values in Table 2.

Table 4-2. Steady state values (time = 225-sec), excluding non-responders, for forearm blood flow (FBF), mean arterial blood pressure (MAP), forearm vascular conductance (FVC), oxy[haem], deoxy[haem], force integral, electromyography (EMG) integral, and EMG per force (EMG/Force).

Variable (Units)	Force of Contraction Maintenance			Muscle Activation Maintenance		
	Hyper.	Control	P Value	Hyper.	Control	P Value
FBF (ml/min)	242 ± 106	216 ± 103	0.0320*	205 ± 115	202 ± 92.9	0.792
MAP (mmHg)	105 ± 8.95	99.3 ± 8.19	0.0037*	96.3 ± 7.98	90.8 ± 7.76	0.0003*
FVC (ml/min/100mmHg)	236 ± 110	218 ± 101	0.197	212 ± 113	223 ± 103	0.250
Oxy[haem] (%)	60.8 ± 11.4	47.5 ± 17.3	0.0068*	61.1 ± 15.6	52.6 ± 14.7	0.0918
Deoxy[haem] (%)	43.3 ± 15.1	48.8 ± 20.1	0.177	39.0 ± 13.8	52.6 ± 19.4	0.0013*
Force (N·s)	186 ± 68.0	183 ± 61.6	0.297	157 ± 52.5	167 ± 50.6	0.0619
EMG (mV·s)	267 ± 139	234 ± 128	0.0566	192 ± 74.3	203 ± 73.3	0.0427*
EMG/Force (mV·s/N·s)	1.41 ± 0.47	1.27 ± 0.51	0.090	1.28 ± 0.54	1.34 ± 0.60	0.517

Values are mean ± SD. *Significantly different between conditions, $P<0.05$. Hyper., Hyperperfusion.

4.5.2.2 Muscle activation maintenance.

Although mean arterial blood pressure was significantly higher in Hyperperfusion compared to Control at steady state, FBF and FVC were not. Steady state oxy[haem] was not different between conditions. Although FBF was not higher at steady state, deoxy[haem] was lower at steady state in Hyperperfusion compared to Control. There were no significant differences in baseline force integral and EMG/Force but EMG integral steady state values were lower in Hyperperfusion compared to Control. Because of steady state differences, all values are presented as a delta from the steady state measures at time = 225-sec. See steady state values in Table 2.

4.5.3 What was the effect of the metaboreflex procedure on MAP, FBF and FVC?

4.5.3.1 Force of contraction maintenance.

There was a time by condition interaction for MAP [$F(25,350) = 29.02$, $P<0.0001$], FBF [$F(25, 300) = 5.32$, $P<0.0001$] and FVC [$F(25, 300) = 3.00$, $P<0.0001$]. MAP elevated by 30-sec and reached maximal increase plateau of +19.9 mmHg by 180-sec. FBF was elevated by 60-sec, with timing of maximal increase plateau of +52.5 ml/min by 210-sec. There was evidence of temporary mild forearm vasoconstriction around 120-180-sec (see Fig. 3, panel A). Upon discontinuing metaboreflex activation, MAP returned to control levels within 30-sec. Upon discontinuing metaboreflex activation, FBF decreased below control levels for 60-sec where thereafter it returned to being not different from control levels. Upon discontinuing metaboreflex activation, FVC decreased for 90-sec in the Hyperperfusion condition, whereafter FVC returned to being not different from control levels. See Fig. 3 for post-hoc results and supplemental information Table 1.

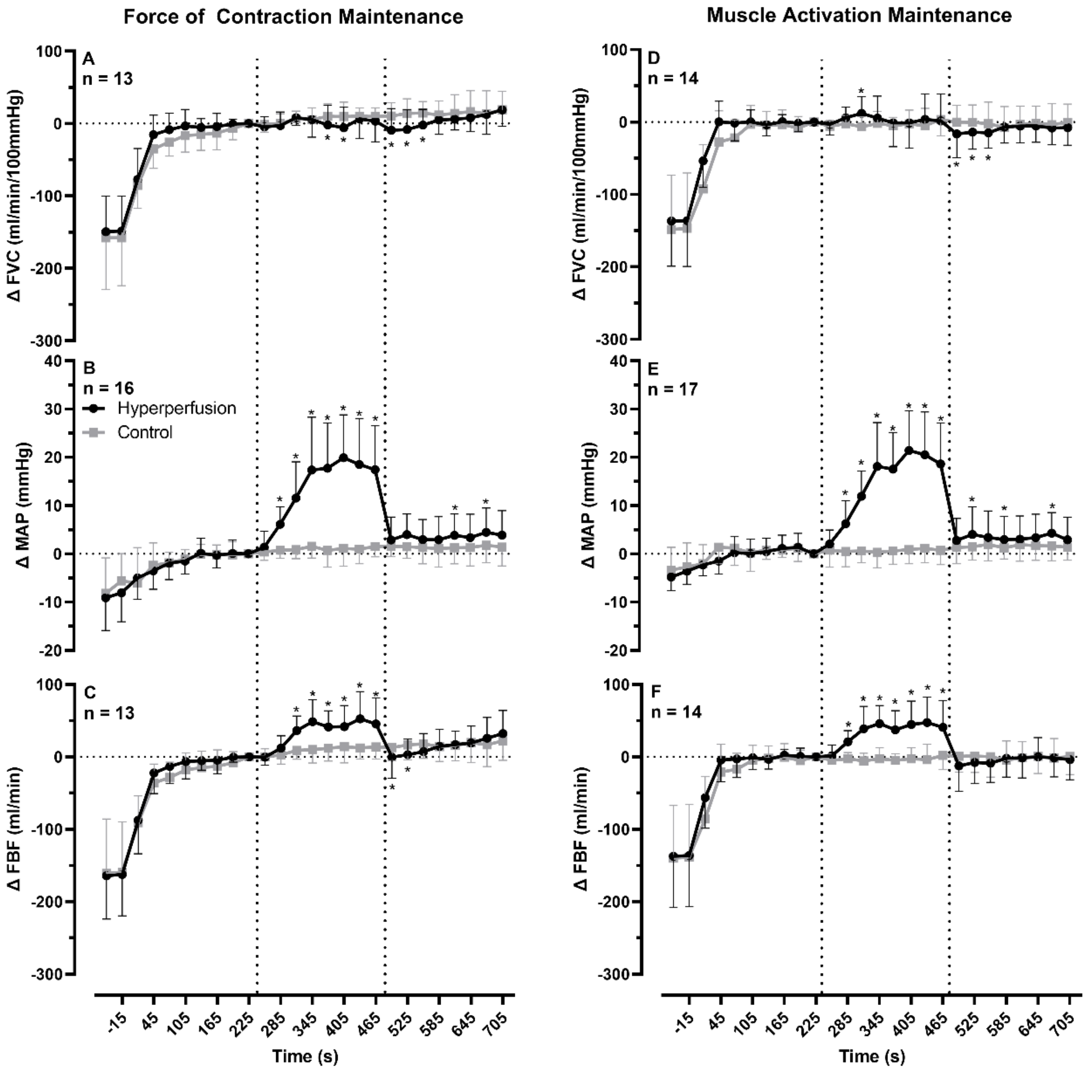

Figure 4-3. Forearm vascular conductance (FVC, panels A and D), mean arterial blood pressure (MAP, panels B and E) and forearm blood flow (FBF, panels C and F) plotted over time as a delta from steady state values (time = 225-sec) and compared between conditions (Hyperperfusion and Control) while either maintaining force of contraction (panels A-C) or muscle activation (panels D-F). The metaboreflex procedure began at time = 240-sec and ended at time = 480-sec. Dashed lines indicate period of metaboreflex activation. *Significantly different from control. Data are mean ± SD.

4.5.3.2 Muscle activation maintenance

There was a time by condition interaction for MAP [$F(25, 400) = 56.56$, $P<0.0001$], FBF [$F(25, 325) = 9.3$, $P<0.0001$] and FVC [$F(25, 325) = 3.08$, $P<0.0001$]. MAP elevated by 30-sec and reached maximal increase plateau of +21.4 mmHg by 180-sec. FBF was elevated by 60-sec, with timing of maximal increase plateau of +47.4 ml/min by 210-sec. There was evidence of temporary mild forearm vasoconstriction around 90-sec (see Fig. 3, panel D). Upon discontinuing metaboreflex activation, MAP and FBF returned to Control levels within 30-sec. There was evidence of vasoconstriction from 270-360-sec. See Fig. 3 for post-hoc results and supplemental information Table 3.

Table 4-3. Confidence interval of difference (CI of diff.) and P values for multiple comparisons of combined force of contraction and muscle activation maintenance data forearm blood flow (FBF), mean arterial blood pressure (MAP) data and forearm vascular conductance (FVC).

	FBF (ml/min) Hyper. – Con.		**MAP (mmHg) Hyper. – Con.**		**FVC (ml/min/100mmHg) Hyper. – Con.**	
Time (s)	**95% CI of diff.**	**P value**	**95% CI of diff.**	**P value**	**95% CI of diff.**	**P value**
255	-5.19 to 11.7	0.448	-0.351 to 2.67	0.132	-7.77 to 7.45	0.968
285	8.24 to 25.2	**0.0001**	4.06 to 7.08	**<0.0001**	-4.81 to 10.4	0.470
315	27.6 to 44.5	**<0.0001**	9.51 to 12.5	**<0.0001**	2.72 to 17.9	**0.0079**
345	35.3 to 52.2	**<0.0001**	15.4 to 18.4	**<0.0001**	-3.73 to 11.5	0.316
375	27.6 to 44.6	**<0.0001**	15.5 to 18.5	**<0.0001**	-11.2 to 3.98	0.349
405	29.5 to 46.4	**<0.0001**	18.2 to 21.2	**<0.0001**	-14.3 to 0.937	0.0855
435	37.4 to 54.3	**<0.0001**	17.0 to 20.0	**<0.0001**	-4.91 to 10.3	0.487
465	26.8 to 43.8	**<0.0001**	15.5 to 18.5	**<0.0001**	-11.5 to 3.71	0.315
495	-21.7 to -4.78	**0.0022**	-0.123 to 2.90	0.0717	-25.6 to -10.3	**<0.0001**
525	-19.5 to -2.57	**0.0108**	1.03 to 4.05	**0.0010**	-25.2 to -10.0	**<0.0001**
555	-18.3 to -1.41	**0.0224**	0.0315 to 3.05	**0.0454**	-22.3 to -7.06	**0.0002**
585	-6.80 to 10.1	0.700	0.273 to 3.29	**0.0207**	-10.6 to 4.62	0.441
615	-7.93 to 8.99	0.902	0.281 to 3.30	**0.0202**	-12.7 to 2.56	0.193
645	-9.07 to 7.85	0.888	0.333 to 3.35	**0.0169**	-13.6 to 1.66	0.125
675	-3.88 to 13.0	0.287	1.16 to 4.18	**0.0006**	-10.5 to 4.74	0.459
705	-5.89 to 11.0	0.550	0.474 to 3.49	**0.0101**	-11.4 to 3.78	0.323

Con., Control; Hyper., Hyperperfusion

4.5.3.3 Combined data from force of contraction maintenance and muscle activation maintenance.

There was a time by condition interaction for MAP [$F(25, 775) = 82.98$, $P<0.0001$], FBF [$F(25, 650) = 13.78$, $P<0.0001$] and FVC [$F(25, 650) = 5.22$, $P<0.0001$]. MAP elevated by 30-sec and reached maximal increase plateau of +20.7 mmHg by 180-sec. FBF was elevated by 60-sec, with timing of maximal increase plateau of +45.8 ml/min by 210-sec. There was evidence of temporary mild forearm vasoconstriction around 90-sec (see Fig. 6, panel D). Upon discontinuing metaboreflex activation, MAP returned to control levels within 30-sec, whereafter it increased and remained elevated for the remainder of the test. Upon discontinuing metaboreflex activation, FBF decreased below control levels for 90-sec where thereafter it returned to being not different from control levels. Upon discontinuing metaboreflex activation, there was evidence of vasoconstriction for 90-sec in the Hyperperfusion condition, whereafter FVC returned to being not different from control levels (see Fig. 6, panel D). See Fig. 6 for post-hoc results and Table 3 for confidence intervals and P values.

4.5.4 What was the effect of the metaboreflex procedure on oxy[haem] and deoxy[haem]?

4.5.4.1 Force of contraction maintenance.

There was a time by condition interaction for oxy[haem] [$F(25, 375) = 5.75$, $P<0.0001$] and deoxy[haem] [$F(25, 375) = 4.29$, $P<0.0001$]. After 60-sec of metaboreflex onset, oxy[haem] was higher and deoxy[haem] was lower in the Hyperperfusion condition compared to Control. Oxy[haem] remained higher and deoxy[haem] remained lower until the metaboreflex procedure was discontinued. Thereafter, both oxy- and deoxy-[haem] returned to control levels within 30-sec and remained there for the rest of the test. See Fig. 4 for post-hoc results and supplemental information Table 2.

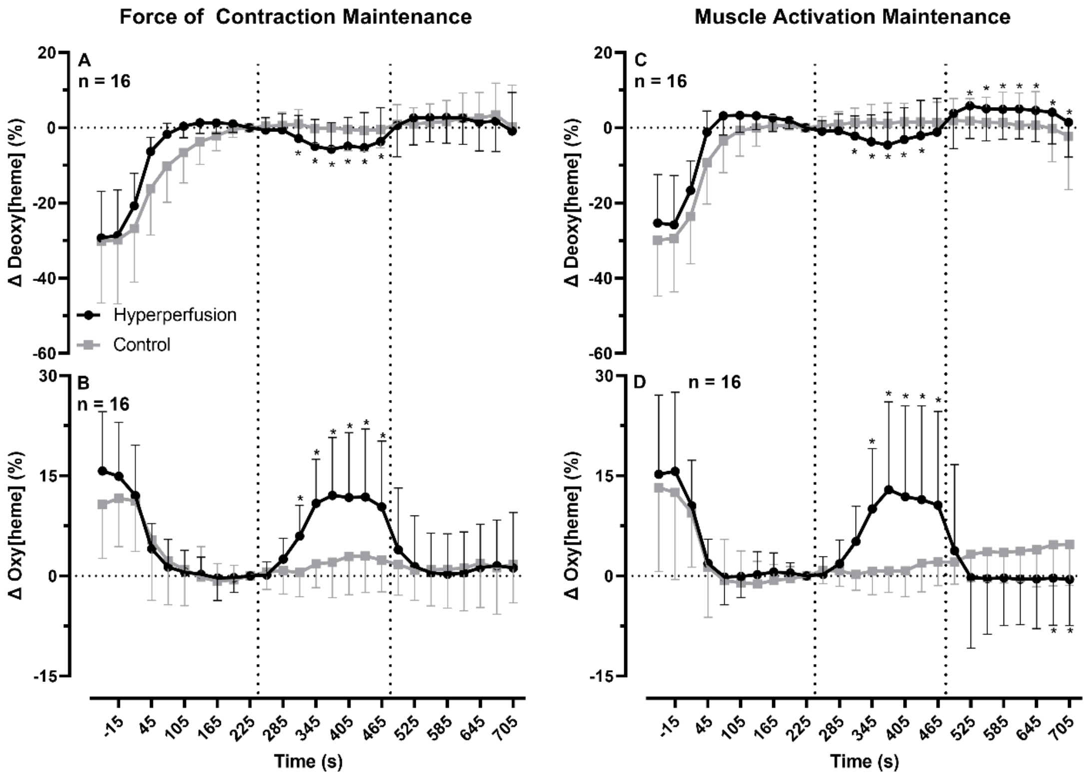

Figure 4-4. Deoxy[haem] (panels A and C) and oxy[haem] (panels B and D) plotted over time as a delta from time = 225-sec and compared between conditions (Hyperperfusion and Control) while either maintaining force of contraction (panels A-C) or muscle activation (panels D-F). The metaboreflex procedure began at time = 240-sec and ended at time = 480-sec. Dashed lines indicate period of metaboreflex activation. *Significantly different from Control within time. Data are mean ± SD.

4.5.4.2 Muscle activation maintenance.

There was a time by condition interaction for oxy[haem] [F(25, 375) = 6.26, P<0.0001] and deoxy[haem] [F(25, 375) = 4.64, P<0.0001]. After 90-sec of metaboreflex, oxy[haem] was higher, whereas after 60-sec deoxy[haem] was lower in the Hyperperfusion condition compared to Control. Oxy[haem] remained higher until metaboreflex discontinuation whereas deoxy[haem] remained lower until 30-sec before metaboreflex discontinuation. Within 30-sec of metaboreflex discontinuation, oxy[haem] returned to control levels. After metaboreflex discontinuation, deoxy[haem] was not different from control for 30-sec whereafter deoxy[haem] was higher in

Hyperperfusion compared to Control for the remainder of the test. By the final 60-sec of the test, oxy[haem] was elevated in the control condition compared to Hyperperfusion. See Fig. 4 for post-hoc results and supplemental information Table 4.

Table 4-4. Confidence interval of difference (CI of diff.) and P values for multiple comparisons of combined muscle activation per force of contraction (EMG/Force), oxy[haem] and deoxy[haem] data.

	Oxy[haem] (%) Hyper. – Con.		**Deoxy[haem] (%) Hyper. – Con.**		**EMG/Force (mV·s/N·s) Hyper. – Con.**	
Time (s)	**95% CI of diff.**	**P value**	**95% CI of diff.**	**P value**	**95% CI of diff.**	**P value**
255	-2.72 to 1.68	0.644	-3.28 to 0.836	0.244	-0.125 to -0.00832	**0.0253**
285	-0.796 to 3.60	0.211	-3.54 to 0.578	0.158	-0.136 to -0.0187	**0.0098**
315	2.99 to 7.39	**<0.0001**	-5.77 to -1.65	**0.0004**	-0.148 to -0.0306	**0.0029**
345	6.99 to 11.4	**<0.0001**	-7.05 to -2.93	**<0.0001**	-0.164 to -0.0471	**0.0004**
375	8.87 to 13.3	**<0.0001**	-7.79 to -3.67	**<0.0001**	-0.133 to -0.0158	**0.0129**
405	7.77 to 12.2	**<0.0001**	-6.65 to -2.53	**<0.0001**	-0.161 to -0.0438	**0.0006**
435	6.98 to 11.4	**<0.0001**	-6.19 to -2.07	**<0.0001**	-0.135 to -0.0184	**0.0101**
465	6.03 to 10.4	**<0.0001**	-4.96 to -0.837	**0.0059**	-0.116 to 0.000727	0.0529
495	-0.249 to 4.15	0.0821	-1.27 to 2.84	0.454	-0.0858 to 0.0313	0.360
525	-3.66 to 0.737	0.192	0.770 to 4.89	**0.0072**	-0.120 to -0.00308	**0.0391**
555	-4.42 to -0.0214	**0.0478**	0.445 to 4.56	**0.0172**	-0.0710 to 0.0461	0.677
585	-4.48 to -0.0780	**0.0424**	0.272 to 4.39	**0.0266**	-0.0937 to 0.0233	0.238
615	-4.68 to -0.284	**0.0270**	0.137 to 4.26	**0.0366**	-0.103 to 0.0140	0.136
645	-4.74 to -0.345	**0.0234**	-0.666 to 3.45	0.184	-0.0792 to 0.0379	0.488
675	-4.55 to -0.153	**0.0361**	-0.716 to 3.40	0.201	-0.0997 to 0.0173	0.167
705	-5.07 to -0.671	**0.0106**	-0.773 to 3.35	0.220	-0.0720 to 0.0451	0.651

Con., Control; Hyper., Hyperperfusion

4.5.4.3 Combined data from force of contraction maintenance and muscle activation maintenance.

There was a time by condition interaction for oxy[haem] [$F(25, 775) = 11.42$, $P<0.0001$] and deoxy[haem] [$F(25, 775) = 8.21$, $P<0.0001$]. After 60-sec of metaboreflex onset, oxy[haem] was higher and deoxy[haem] was lower in the Hyperperfusion condition compared to Control. Oxy[haem] remained higher and deoxy[haem] remained lower until the metaboreflex procedure was discontinued. Thereafter, both oxy- and deoxy-[haem] returned to control levels within 30-sec, whereafter oxy[haem] was lower for the remainder of the test. Deoxy[haem] was higher in Hyperperfusion between 525- and 615-sec. See Fig. 6 for post-hoc results and Table 4 for confidence intervals and P values.

4.5.5 What was the effect of the metaboreflex procedure on force, muscle activation and the relationship between the two?

4.5.5.1 Force of contraction maintenance.

There were no time by condition interactions for EMG [$F(23, 345) = 1.44$, $P = 0.0888$], EMG/Force [$F(23, 345) = 1.05$, $P = 0.3971$] or force [$F(23, 345) = 1.55$, $P = 0.0536$]. Despite the increase in FBF and oxy[haem] during metaboreflex activation – there was no significant improvement in the EMG/force relationship. A post-hoc effect size analysis revealed a small effect (Cohen's D = 0.2738) size during metaboreflex. See Fig. 5.

4.5.5.2 Muscle activation maintenance.

There were no time by condition interactions for EMG [$F(23, 368) = 1.32$, $P = 0.1481$], force [$F(23, 368) = 1.47$, $P = 0.0763$] and EMG/Force [$F(23, 368) = 0.93$, $P = 0.5545$]. As intended, EMG was not different between conditions over time, though – despite the increase in FBF and oxy[haem] during metaboreflex activation – there was no significant improvement in the EMG/force relationship. A post-hoc effect size analysis revealed a small effect (Cohen's D = 0.2191) during metaboreflex. See Fig. 5.

4.5.5.3 Combined data from force of contraction maintenance and muscle activation maintenance.

There was a time by condition interaction for EMG/Force [$F(23,736 = 1.55$, $P = 0.0476$]. In the Hyperperfusion condition, EMG/force was lower compared to control within 30-sec of metaboreflex activation and remained there until 30-sec before metaboreflex discontinuation. Within 30-sec of metaboreflex discontinuation, EMG/force returned to control levels where it then returned to being lower than the control condition for 30-sec. Thereafter, EMG/Force returned to being not different from control levels for the remainder of the test. See Fig. 6 for post-hoc results and Table 4 for confidence intervals and P values**.**

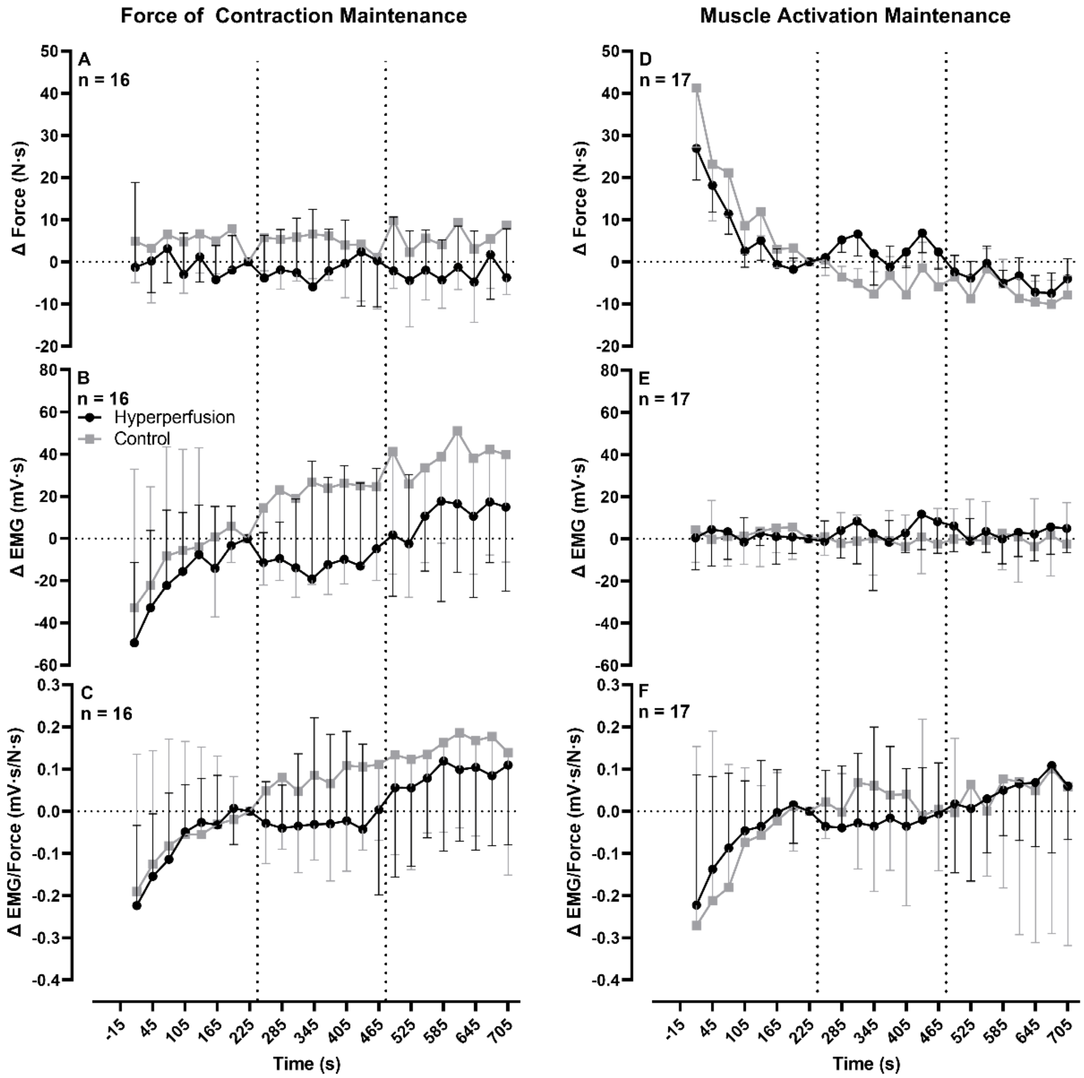

Figure 4-5. Force of contraction (panels A and D), forearm electromyography (EMG, panels B and E) and EMG/Force (panels C and F) plotted over time as a delta from steady state (time = 225-sec) values and compared between conditions (Hyperperfusion and Control) while either maintaining force of contraction (panels A-C) or muscle activation (panels D-F). The metaboreflex procedure began at time = 240-sec and ended at time = 480-sec. Dashed lines indicate period of metaboreflex activation. Data are mean ± SD.

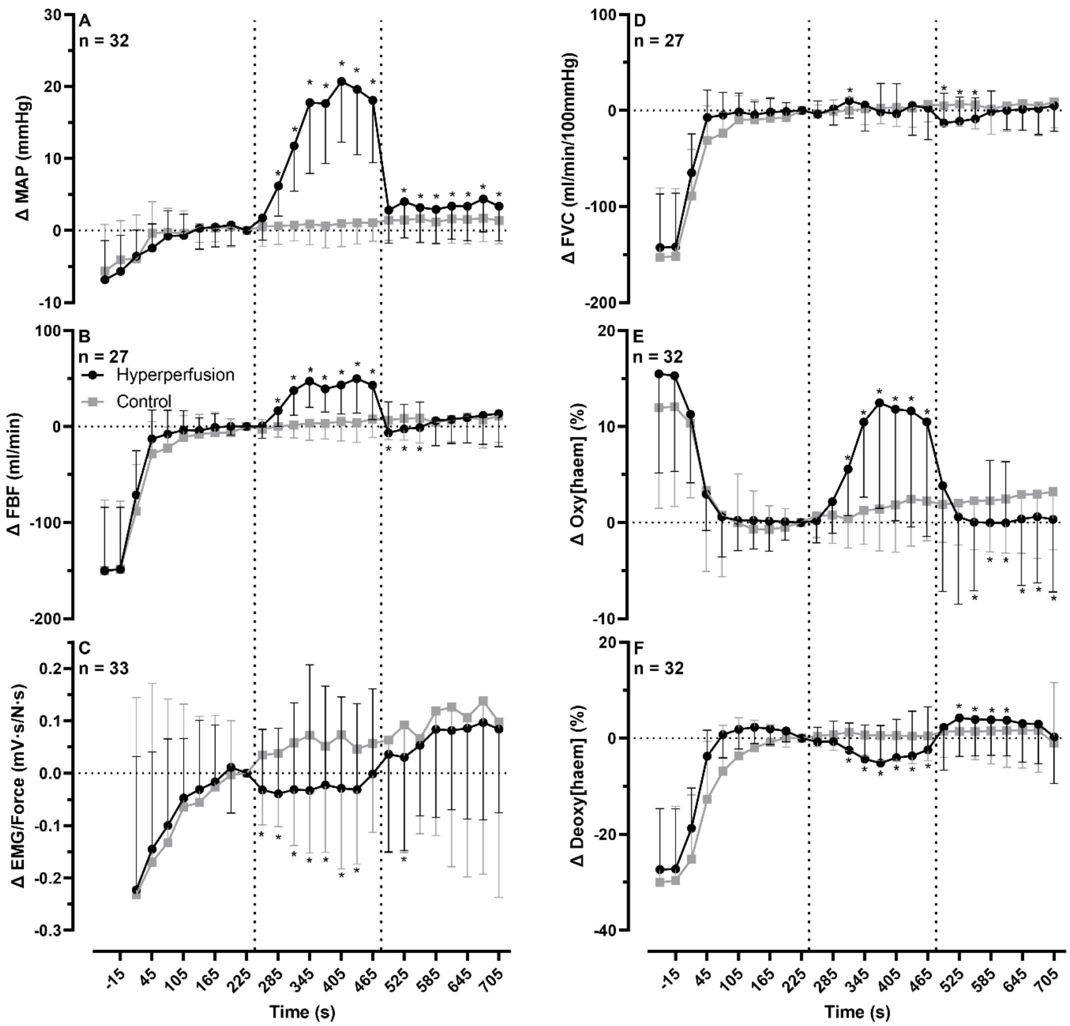

Figure 4-6. Data from force of contraction maintenance and muscle activation maintenance experiments combined for mean arterial blood pressure (MAP, panel A), forearm blood flow (FBF, panel B), EMG/Force (panel C), forearm vascular conductance (FVC, panel D), oxy[haem] (panel E), and deoxy[haem] (panel F) plotted over time as a delta from starting values and compared between conditions (Hyperperfusion and Control). The metaboreflex procedure began at time = 240-sec and ended at time = 480-sec. Dashed lines indicate period of metaboreflex activation. *Significantly different between conditions. Data are mean ± SD.

4.6 Discussion

Oxygen delivery demand matching is a key determinant of exercise tolerance (Amann et al., 2006; Bentley et al., 2017) and the current view is that oxygen delivery to a small exercising muscle mass is tightly matched to demand (Nyberg & Jones, 2022), because increased oxygen delivery does not increase VO_2. Given that VO_2 can generally be maintained even in the face of at least some decrease in oxygen delivery from normal, it may even be considered "in excess" for VO_2 maintenance. However, from a muscle contractility perspective of oxygen delivery adequacy, a decrease in oxygen delivery compromises the relationship between muscle activation and force of contraction – resulting in a rapidly reversible decrease in contraction force at the same muscle activation (Drouin et al., 2022) or a rapidly reversible increase in muscle activation at the same force of contraction (Drouin et al., 2019). This draws attention to an important distinction: an oxygen delivery:demand matching that is adequate for VO_2 maintenance does not mean it is optimal for muscle metabolic and contractile function. Whether the normal adjustment of oxygen delivery (i.e., blood flow) in small muscle mass exercise below critical power is matched optimally to muscle performance requirements was unclear. This study – using remote muscle metaboreflex activation – therefore tested the hypothesis that the "normal" adjustment of oxygen delivery is optimal for muscle performance.

The key findings from the present report are (a) that the metaboreflex – initiated in a remote muscle (i.e., tibialis anterior) – was effective at increasing forearm muscle oxygen delivery and oxygenation in most (see Fig. 6) but not all participants (see Fig. 2), (b) during the period of increased oxygen delivery, the muscle activation:force of contraction ratio was decreased (i.e., improved), and (c) upon cessation of metaboreflex activation and restoration of normal perfusion, improvement in excitation contraction coupling was lost (see Fig. 6). We interpret these key results to suggest that, in the heavy exercise intensity domain, below critical power, the nature of vasoregulation in voluntarily activated exercising muscle does not support optimal perfusion for excitation contraction coupling.

4.6.1 Remote muscle metaboreflex mediated hyperperfusion.

The metaboreflex activated in the leg can increase exercising forearm blood flow (Tschakovsky & Hughson, 1999), although some individuals demonstrate a counteracting forearm vasoconstriction such that blood flow does not change (Perrey et al., 2001). Here we show again that the metaboreflex initiated in the leg can be effective – by increasing mean arterial blood pressure – at increasing exercising forearm oxygen delivery in most (see Fig. 6) but not all (see Fig. 2) participants. Of the 20 participants recruited, five participants did not have an increase in forearm blood flow with metaboreflex activation in experimental model 1 and/or 2. Interestingly, only one participant was consistently a non-responder to the metaboreflex procedure. The other four participants did have an increase in blood flow during one of the two experimental models, and the lack of a blood flow response during muscle activation maintenance was not because of decreased contraction force (i.e., demand). These findings extend previous work by showing that there can be inter-day differences in a person's vasoregulatory response to metaboreflex activation – why this may be the case remains unknown.

Our findings also extend previous work by showing for the first time that this metaboreflex mediated hyperperfusion of the forearm also increases forearm muscle oxygenation (see Fig. 4 and 6). The metaboreflex activated in the bilateral tibialis anterior muscles achieves an increase in mean arterial pressure after 30-sec and remains elevated thereafter even upon dorsiflexion discontinuation (see Fig. 3 and 6). In participants with an increase in forearm blood flow, both forearm blood flow (see Fig. 3 and 6) and muscle oxygenation (see Fig. 4 and 6) followed increases in mean arterial blood pressure.

4.6.2 Small muscle mass oxygen delivery is suboptimal: the ergogenic effect of hyperperfusion on the muscle activation:contraction force ratio.

To date, adequate oxygen delivery demand matching has been described by Nyberg and Jones (2022) from the perspective of the "tipping point" hypothesis proposed by Poole et al. (2008). That is, if oxygen delivery exceeds demand, an increase or minor decrease in oxygen delivery will not change oxygen uptake (i.e., this is an oxygen delivery independent zone). Alternatively, if increased oxygen delivery increases oxygen uptake, then oxygen delivery is likely to be suboptimal (i.e., this is an oxygen delivery dependent zone). This perspective is supported by two key study designs. First, Gonzalez-Alonso et al. (2002); (Gonzalez-Alonso et al., 2001) demonstrated in humans that under hyperoxic conditions, leg vascular conductance decreases, thereby maintaining leg oxygen delivery at similar levels to normoxia. Therefore, the vasoregulatory response under hyperoxic conditions appears to be one that prevents "excess" oxygen delivery. Second, Hansen et al. (2022) demonstrated that, despite elevated sympathetic activation at altitude compared to sea level, oxygen delivery demand matching was not different. Though, upon removal of sympathetic restraint at altitude, there was a disproportionate increase in the oxygen delivery to oxygen uptake ratio – this was interpreted as indicating that sympathetic restraint at altitude is necessary to prevent "excess vasodilation".

This current perspective, however, does not consider the implication of reduced or increased oxygen delivery on muscle contractile function. First, to maintain force of contraction with reduced oxygen delivery, there must be a compensatory increase in muscle activation (Drouin et al., 2019; Fulco et al., 1996) – this results in increased metabolic disturbance (Fulco et al., 1996; Hogan, Richardson, et al., 1999). If muscle activation does not increase, force of contraction conforms to oxygen delivery (Drouin et al., 2022; Fitzpatrick et al., 1996; Luu & Fitzpatrick, 2013; Wright et al., 2000) – but cellular disturbance is prevented (Hogan et al., 1996). Whether force of contraction is maintained or not, there is a decrease in the contraction force to muscle activation ratio. Therefore, although oxygen uptake may be maintained with reduced oxygen delivery, there is a compromise to excitation-contraction coupling. Second, in electrically stimulated muscle contractions, with increased perfusion pressure, there is an increase in force production (Fitzpatrick et al., 1996; Luu & Fitzpatrick, 2013; Wright et al., 2000). This oxygen conforming of force production to oxygen delivery reflects a positive functional impact on skeletal muscle exercise performance.

Recently, in the context of force of contraction conforming to oxygen delivery, we demonstrated that compromise to the normal blood flow response in the exercising forearm did not compromise voluntary force of contraction at a given muscle activation at 50% of critical power (Drouin et al., 2022). These findings, at 50% critical power, are in line with the notion that the normal blood flow response appears to be optimal for excitation-contraction coupling. However, with decreased forearm blood flow, force of contraction was decreased at a given muscle activation at 75 and 90% critical power. These findings led us to question whether the normal oxygen delivery adjustment in the exercising forearm was beyond the contractile function "tipping point" (i.e., an increase in oxygen delivery does not improve the muscle activation to force of contraction ratio).

To assess whether normal oxygen delivery adjustment in the exercising forearm was optimal (i.e., beyond the "tipping point") for excitation-contraction coupling, we used a remote muscle metaboreflex to increase mean arterial blood pressure – the driving pressure for blood flow – during heavy intensity exercise (90% critical power). Here we see in most (see Fig. 6), but not all (see Fig. 2), that the remote metaboreflex was effective at increasing forearm blood flow and oxygenation above "normal" steady state levels. Importantly, we show for the first time in voluntary human exercise that, in the heavy intensity exercise domain, an increase in blood flow above "normal" can improve excitation-contraction coupling. That is, when forearm blood flow is elevated, there is a reduction in the muscle activation to force of contraction ratio (see Fig. 6). These findings demonstrate that like the oxygen delivery to oxygen uptake "tipping point" (Poole et al.,

2008) there is an oxygen delivery to excitation-contraction coupling "tipping point". In this small muscle mass exercise in the heavy intensity domain, the normal oxygen delivery and excitation-contraction coupling relationship was below this tipping point, whereby normal oxygen delivery was not optimal for excitation-contraction coupling. Ultimately, to understand the nature of oxygen delivery demand matching mechanisms, these findings demonstrate the necessity to consider the adequacy of oxygen delivery for optimal excitation-contraction coupling, and not only whether it is adequate to support a given VO_2.

4.6.3 Potential mechanisms of the improved forearm EMG/Force ratio with remote muscle metaboreflex mediated hyperperfusion.

Upon hyperperfusion the EMG/Force ratio was improved compared to control only until normal perfusion was restored. Such a response is consistent with an oxygen conforming response. Specifically, as per previous oxygen conforming work (Fitzpatrick et al., 1996; Luu & Fitzpatrick, 2013; Wright et al., 2000), we see a rapid and reversible improvement in the EMG/Force ratio upon hyperperfusion and then restoration thereafter (see Fig. 6). Although mean arterial blood pressure and forearm blood flow increased only after 30-sec of metaboreflex activation, the EMG/Force ratio was already improved within 30-sec (see Fig. 6). This immediate improvement in the EMG/Force relationship is not consistent with an oxygen delivery dependent response. Interestingly, in the work of Luu and Fitzpatrick (2013) we see a similar response. Although mean arterial blood pressure is not increased until 90-sec into handgrip exercise, force production of the tibialis anterior at a given electrical stimulation is already improved within 60-sec compared to the extrapolated exponential fit (Luu & Fitzpatrick, 2013). Therefore, it would appear at first glance that there is a rapid non-oxygen delivery dependent effect on the EMG/Force ratio. However, the observation that there was no EMG/Force ratio improvement in non-responder participants (see

Fig. 2) supports the interpretation that, following the first 30-sec of the metaboreflex procedure, hyperperfusion is the likely mechanism causing the improved EMG/Force ratio.

As predicted by the oxygen conforming response, at the same muscle activation, an increase in muscle oxygen delivery should cause an increase in force of contraction (Fitzpatrick et al., 1996; Luu & Fitzpatrick, 2013; Wright et al., 2000) without disturbance to the metabolic environment (Hogan et al., 1996). Alternatively, at the same force of contraction, an increase in muscle oxygen delivery should reduce the necessary muscle activation required. Whether maintaining force of contraction and measuring muscle activation or maintaining muscle activation and measuring force of contraction, an improvement in muscle contractility would be reflected in a decrease in the EMG/Force ratio. This is what we see when we combined data from the force of contraction maintenance and muscle activation maintenance experiments (see Fig. 6). As predicted by the oxygen conforming response, an increase in oxygen delivery (i.e., hyperperfusion) decreased the EMG/Force ratio compared to control. This improvement in EMG/Force with increased oxygen delivery supports the idea that normal steady state exercising muscle oxygen delivery is not optimal for excitation-contraction coupling.

4.6.4 Methodological considerations.

As highlighted in a recent review (Nyberg & Jones, 2022), VO_2 does not appear to be compromised in the "normal" oxygen delivery response below critical power. Therefore, we did not measure VO_2 as it was not necessary to test the hypothesis of an excitation-contraction coupling "tipping point". Second, the order of the single control test and the 2-3 hyperperfusion tests were not counterbalanced between participants. That is, the control test was always completed prior to the 2-3 hyperperfusion tests. This approach was taken to ensure that on testing days, participants could effectively target either the desired force of contraction or muscle activation prior to adding concomitant dorsiflexion exercise. This approach however invites the possibility of an order effect.

Importantly, data in Fig. 2 – from participants who did not have a forearm blood flow increase – helps to strengthen our interpretation that the improvement in the EMG/Force ratio is due to an increase in muscle oxygen delivery and not due to an order effect. In participants without a forearm blood flow increase with metaboreflex activation, the EMG/Force response displayed no observable difference between the control and hyperperfusion conditions. Furthermore, if the observed response were caused by an order effect, it would be unlikely to see a difference between hyperperfusion and control conditions only when the metaboreflex is active – yet this is precisely what we see. Therefore, we interpret these findings to support the interpretation that an increase in oxygen delivery caused an improvement in the muscle activation and force of contraction ratio – indicating suboptimal oxygen delivery for excitation-contraction coupling.

4.7 Conclusion

This study has demonstrated for the first time, in voluntary human exercise, that an increase in forearm oxygen delivery above "normal" steady state levels results in an improved muscle activation to force of contraction ratio – indicating improved forearm muscle contractile response to activation. We interpret these findings to suggest that "normal" steady state oxygen delivery is not optimal for excitation-contraction coupling in small muscle mass exercise in the heavy intensity domain assessed in this study. When considering the effectiveness of oxygen delivery:demand matching, adequacy of oxygen delivery from an excitation-contraction coupling perspective is necessary and can have important implications for understanding exercise intolerance.

4.8 Supplemental information

Table 4-5. Force of Contraction Maintenance: Confidence interval of difference (CI of diff.) and P values for multiple comparisons of forearm blood flow (FBF), mean arterial blood pressure (MAP) data and forearm vascular conductance (FVC).

	FBF (ml/min) Hyper. – Con.		**MAP (mmHg) Hyper. – Con.**		**FVC (ml/min/100mmHg) Hyper. – Con.**	
Time (s)	**95% CI of diff.**	**P value**	**95% CI of diff.**	**P value**	**95% CI of diff.**	**P value**
255	-12.263 to 11.853	0.9733	-1.5263 to 3.5407	0.4342	-14.338 to 7.9133	0.5697
285	-2.7314 to 21.385	0.1288	2.861 to 7.9285	**<0.0001**	-13.877 to 8.3744	0.6263
315	15.268 to 39.384	**<0.0001**	8.152 to 13.219	**<0.0001**	-9.4823 to 12.769	0.7711
345	26.432 to 50.548	**<0.0001**	13.280 to 18.347	**<0.0001**	-11.158 to 11.093	0.9954
375	17.368 to 41.484	**<0.0001**	14.464 to 19.531	**<0.0001**	-22.695 to -0.444	**0.0416**
405	15.726 to 39.842	**<0.0001**	16.248 to 21.315	**<0.0001**	-26.506 to -4.2542	**0.0070**
435	27.973 to 52.089	**<0.0001**	15.017 to 20.084	**<0.0001**	-14.777 to 7.4740	0.5182
465	19.605 to 43.721	**<0.0001**	13.412 to 18.479	**<0.0001**	-17.263 to 4.9885	0.2779
495	-25.261 to -1.1454	**0.0320**	-1.2049 to 3.862	0.3025	-30.888 to -8.636	**0.0006**
525	-25.525 to -1.4091	**0.0288**	-0.0346 to 5.032	0.0532	-33.233 to -10.981	**0.0001**
555	-22.797 to 1.3187	**0.0806**	-0.888 to 4.178	0.2020	-27.826 to -5.575	**0.0035**
585	-11.512 to 12.604	0.9290	-0.685 to 4.382	0.1519	-18.152 to 4.100	0.2144
615	-10.858 to 13.258	0.8446	0.0341 to 5.101	**0.0470**	-19.223 to 3.029	0.1528
645	-12.410 to 11.706	0.9541	-0.494 to 4.573	0.1141	-19.693 to 2.558	0.1305
675	-2.996 to 21.120	0.1399	0.138 to 5.206	**0.0388**	-12.093 to 10.159	0.8641
705	-1.917 to 22.199	0.0988	-0.050 to 5.017	0.0546	-11.178 to 11.074	0.9927

Con., Control; Hyper., Hyperperfusion

Table 4-6. Force of Contraction Maintenance: Confidence interval of difference (CI of diff.) and P values for multiple comparisons of oxy[haem] and deoxy[haem] data.

	Oxy[haem] (%) Hyper. – Con.		Deoxy[haem] (%) Hyper. – Con.	
Time (s)	**95% CI of diff.**	**P value**	**95% CI of diff.**	**P value**
255	-2.991 to 2.106	0.7326	-3.730 to 1.654	0.4483
285	-0.814 to 4.284	0.1813	-3.888 to 1.496	0.3822
315	2.913 to 8.011	**<0.0001**	-6.574 to -1.190	**0.0049**
345	6.524 to 11.623	**<0.0001**	-7.477 to -2.092	**0.0006**
375	7.450 to 12.548	**<0.0001**	-8.369 to -2.984	**<0.0001**
405	6.262 to 11.360	**<0.0001**	-7.163 to -1.779	**0.0012**
435	6.281 to 11.380	**<0.0001**	-7.316 to -1.932	**0.0008**
465	5.423 to 10.521	**<0.0001**	-5.860 to -0.475	**0.0213**
495	-0.358 to 4.740	**0.0917**	-3.032 to 2.352	0.8037
525	-1.996 to 3.102	0.6697	-1.109 to 4.276	0.2477
555	-2.980 to 2.118	0.7394	-1.321 to 4.063	0.3169
585	-3.292 to 1.806	0.5662	-1.628 to 3.756	0.4372
615	-3.281 to 1.817	0.5724	-2.668 to 2.716	0.9862
645	-3.235 to 1.863	0.5964	-3.790 to 1.594	0.4224
675	-2.242 to 2.856	0.8125	-4.319 to 1.065	0.2349
705	-3.072 to 2.026	0.6865	-3.781 to 1.604	0.4265

Con., Control; Hyper., Hyperperfusion

Table 4-7. Muscle Activation Maintenance: Confidence interval of difference (CI of diff.) and P values for multiple comparisons of forearm blood flow (FBF), mean arterial blood pressure (MAP) data and forearm vascular conductance (FVC).

	FBF (ml/min) Hyper. – Con.		MAP (mmHg) Hyper. – Con.		FVC (ml/min/100mmHg) Hyper. – Con.	
Time (s)	**95% CI of diff.**	**P value**	**95% CI of diff.**	**P value**	**95% CI of diff.**	**P value**
255	-5.410 to 18.392	0.2835	-0.522 to 3.109	0.1619	-7.918 to 13.283	0.6184
285	11.651 to 35.453	**0.0001**	3.906 to 7.537	**<0.0001**	-2.642 to 18.558	0.1404
315	32.315 to 56.117	**<0.0001**	9.492 to 13.124	**<0.0001**	7.801 to 29.002	**0.0007**
345	36.705 to 60.508	**<0.0001**	15.988 to 19.620	**<0.0001**	-3.081 to 18.120	0.1635
375	30.384 to 54.187	**<0.0001**	15.157 to 18.789	**<0.0001**	-6.865 to 14.336	0.4880
405	35.474 to 59.277	**<0.0001**	18.746 to 22.378	**<0.0001**	-9.190 to 12.011	0.7933
435	39.320 to 63.123	**<0.0001**	17.578 to 21.209	**<0.0001**	-2.009 to 19.192	0.1116
465	26.760 to 50.562	**<0.0001**	16.120 to 19.752	**<0.0001**	-12.415 to 8.786	0.7361
495	-25.177 to -1.375	**0.0290**	-0.376 to 3.255	0.1197	-26.887 to -5.686	**0.0028**
525	-20.660 to 3.143	0.1483	0.766 to 4.398	**0.0055**	-24.083 to -2.882	**0.0129**
555	-20.958 to 2.844	0.1351	-0.364 to 3.267	0.1167	-23.392 to -2.191	**0.0183**
585	-9.211 to 14.591	0.6564	-0.089 to 3.543	0.0622	-9.834 to 11.367	0.8868
615	-11.997 to 11.805	0.9874	-0.709 to 2.923	0.2310	-12.826 to 8.375	0.6793
645	-12.749 to 11.054	0.8885	-0.145 to 3.487	**0.0711**	-14.114 to 7.087	0.5142
675	-11.474 to 12.328	0.9437	0.848 to 4.479	**0.0042**	-15.234 to 5.967	0.3899
705	-16.354 to 7.4483	0.4616	-0.272 to 3.359	**0.0953**	-17.945 to 3.256	0.1734

Con., Control; Hyper., Hyperperfusion

Table 4-8. Muscle Activation Maintenance: Confidence interval of difference (CI of diff.) and P values for multiple comparisons of oxy[haem] and deoxy[haem] data.

	Oxy[haem] (%) Hyper. – Con.		**Deoxy[haem] (%) Hyper. – Con.**	
Time (s)	**95% CI of diff.**	**P value**	**95% CI of diff.**	**P value**
255	-4.900 to 3.788	0.8010	-4.533 to 1.718	0.3758
285	-3.590 to 5.099	0.7326	-4.892 to 1.360	0.2666
315	-0.329 to 8.359	0.0699	-6.665 to -0.414	**0.0266**
345	2.192 to 10.881	**0.0033**	-8.325 to -2.074	**0.0012**
375	3.431 to 12.120	**0.0005**	-8.908 to -2.657	**0.0003**
405	4.501 to 13.190	**<0.0001**	-7.832 to -1.582	**0.0033**
435	3.875 to 12.563	**0.0002**	-6.757 to -0.507	**0.0229**
465	3.668 to 12.357	**0.0003**	-5.750 to 0.501	0.0994
495	-0.660 to 8.028	0.0961	-1.214 to 5.036	0.2296
525	-4.670 to 4.018	0.8827	0.950 to 7.201	0.0108
555	-5.391 to 3.297	0.6354	0.513 to 6.764	0.0227
585	-5.122 to 3.566	0.7246	0.474 to 6.725	0.0242
615	-5.190 to 3.498	0.7015	1.244 to 7.495	0.0063
645	-5.269 to 3.420	0.6754	0.760 to 7.011	0.0150
675	-6.261 to 2.427	0.3856	1.188 to 7.439	0.0070
705	-6.490 to 2.199	0.3316	0.536 to 6.787	0.0219

Con., Control; Hyper., Hyperperfusion

Chapter 5 - An oxygen conforming response of muscle contraction force during maximal effort handgrip exercise

Chapter 5 is under review as:

P.J. Drouin, S.P.S. Mladen, S.P.A. Forbes, A.K. Zedic, S.P.B Inouye, E.N. Beaudette & M.E. Tschakovsky. Effect of altering oxygen delivery on excitation contraction-coupling during maximal effort forearm exercise: role of oxygen conforming response. JP-RP-2023-285215.

5.1 Key points

- At submaximal exercise intensities, when muscle excitation is targeted, muscle contraction force conforms to changes in oxygen delivery, preventing cellular disturbance.
- Maximal effort exercise is characterized by a rapid attainment of peak cellular disturbance, contributing to a near hyperbolic decline in muscle contraction force.
- It remained to be determined whether this oxygen conforming response of muscle contraction force occurs under conditions of maximal metabolic disturbance.
- Here we showed that – under conditions of maximal cellular disturbance established through maximal effort exercise – muscle contraction force follows changes in oxygen delivery.
- These findings demonstrate the important – cellular disturbance independent – role the oxygen conforming response of muscle contraction force can play in modifying exercise tolerance during maximal effort exercise.

5.2 Abstract

During muscle excitation targeted exercise muscle contraction force conforms to changes in muscle oxygen delivery, preventing cellular disturbance. It remained to be determined whether this oxygen conforming response of muscle contraction force occurs under conditions of maximal metabolic disturbance. Eleven participants (5 female) completed 840-sec maximal effort rhythmic forearm handgrip exercise under both a low (arm above heart level; LPP) and high (arm below heart level; HPP) perfusion pressure condition. In the LPP condition, the exercising arm was moved below heart at 360-sec to suddenly increase oxygen delivery to that of the HPP condition and moved back above heart to restore low oxygen delivery at 600-sec. During the first 360-sec, an ~18% lower oxygen delivery in LPP vs. HPP led to a greater decline in muscle contraction force. In the LPP condition, upon increasing oxygen delivery to match that of the HPP condition, muscle contraction force stabilized at what was ultimately critical force under HPP conditions. Importantly, muscle contraction force was not rapidly reversed, indicating that the initial decrease in muscle contraction force was not solely an oxygen conforming response of muscle contraction force. Rather, improved oxygen delivery appears to oppose ongoing negative cellular disturbance mediated fatigue. By 600-sec, cellular disturbance had contributed similarly to the muscle contraction force decline – a plateau was reached in both conditions. An instantaneous restoration of reduced oxygen delivery led to an immediate decrease in muscle contraction force – demonstrating the rapid oxygen conforming of muscle contraction force during maximal effort exercise.

5.3 Introduction

During muscle contraction force-targeted exercise, where ATP demand is maintained constant, a decrease in oxygen delivery necessitates (a) an increase in muscle excitation to maintain muscle contraction force (Drouin et al., 2019; Hobbs & McCloskey, 1987) and (b) an adjustment of redox and phosphorylation potentials to continue matching aerobic ATP supply to ATP demand (Erecinska & Wilson, 1982; Goulding et al., 2019; Haseler et al., 1998; Hogan, Arthur, et al., 1992; Hogan et al., 1998; Hogan et al., 1996; Korzeniewski, 2023; Wilson & Erecinska, 1985; Wilson et al., 1979). This increased disturbance of the cellular environment to maintain aerobic ATP supply in support of maintained muscle contraction force has a cost (Hogan, Nioka, et al., 1992). The accumulation of ADP, P_i and hydrogen ions (H^+) as part of the increased cellular disturbance contributes to the impairment of excitation-contraction coupling (Debold, 2016). Critically, the recovery of cellular disturbance mediated impairment of muscle excitation-contraction coupling necessitates that exercise be discontinued. Once exercise is discontinued, muscle excitation-contraction coupling remains impaired for some time (Pitcher & Miles, 1997; Romer et al., 2006).

Alternatively, when oxygen delivery is reduced under constant muscle excitation exercise conditions (electrical stimulation or targeted electromyography (EMG) in voluntary exercise), maintenance of the balance between ATP demand and supply is achieved through a reduction of muscle contraction force (i.e., ATP demand). Therefore, muscle contraction force “conforms” to a reduction in aerobic ATP production – protecting the cellular environment (Drouin et al., 2022; Fitzpatrick et al., 1996; Hobbs & McCloskey, 1987; Hogan, Kohin, et al., 1999; Hogan et al., 1996; Luu & Fitzpatrick, 2013). Upon a restoration of oxygen delivery, and the resulting increase in aerobic ATP production, muscle contraction force at a controlled muscle excitation is rapidly increased back to normal and this occurs while exercise is ongoing (Drouin et al., 2022; Fitzpatrick et al., 1996; Hobbs & McCloskey, 1987; Luu & Fitzpatrick, 2013). Critically, this rapid restoration of muscle contraction force is an oxygen delivery and not a blood flow mediated response (Hogan, Kohin, et al., 1999). Similarly to a decrease in oxygen delivery, a sudden increase in oxygen delivery (above normal levels), and therefore aerobic ATP production, results in an increase in muscle contraction force at a given muscle excitation (Drouin et al., 2023; Fitzpatrick et al., 1996; Luu & Fitzpatrick, 2013; Wright et al., 2000). Again, once muscle oxygen delivery is returned to normal levels, muscle contraction force (i.e., ATP demand) is rapidly reversed back to normal and this occurs while exercise is ongoing (Drouin et al., 2023; Fitzpatrick et al., 1996; Luu & Fitzpatrick, 2013; Wright et al., 2000). Therefore, this oxygen conforming response of muscle contraction force is defined as: the adjustment of muscle contraction force at a given muscle excitation to maintain the balance between aerobic ATP production and ATP consumption such that the cellular environment remains stable during oxygen delivery mediated changes in aerobic ATP production.

To date, this oxygen conforming response of muscle contraction force has been investigated at exercise intensities below critical power (Drouin et al., 2022; Drouin et al., 2019; Drouin et al., 2023; Fitzpatrick et al., 1996; Hobbs & McCloskey, 1987; Hogan, Kohin, et al., 1999; Luu & Fitzpatrick, 2013; Wright et al., 2000) where there is submaximal stabilization of the cellular environment (Black et al., 2017; Jones et al., 2008; Korzeniewski & Rossiter, 2020; Poole et al., 1988). At submaximal exercise intensities, with reduced oxygen delivery either (a) muscle excitation can increase to maintain muscle contraction force (resulting in cellular disturbance) or (b) muscle contraction force can decrease at a maintained muscle excitation (preventing cellular disturbance). However, with maximal effort exercise, maximal VO_2 (Fenuta et al., 2023; Goulding et al., 2020; Kellawan & Tschakovsky, 2014), oxidative ATP production (Broxterman et al., 2017) and cellular disturbance (i.e., Pi, pH and PCr) (Burnley et al., 2010; Korzeniewski & Rossiter, 2020) are rapidly reached. Considering this, if there is a decrease in oxygen delivery during maximal effort exercise, we would predict that there cannot be (a) a compensatory increase in muscle excitation to maintain muscle contraction force and (b) further disturbance of redox and phosphorylation potentials to support ATP production (Korzeniewski, 2023; Korzeniewski & Rossiter, 2020). Instead, the muscles only option should be to decrease ATP demand via muscle contraction force conforming to a reduction in oxygen delivery. Likewise, if there is an increase in oxygen delivery, muscle contraction force should be able to increase. This oxygen conforming response of muscle contraction force during maximal effort exercise remained to be demonstrated.

To test the hypothesis that – under conditions of maximal cellular disturbance established through maximal effort handgrip exercise – muscle contraction force would follow changes in oxygen delivery, we used arm position manipulations to alter forearm oxygen delivery. To assess the ability of muscle contraction force to conform to an increase in oxygen delivery, we first established conditions of low versus high oxygen delivery by having participants complete handgrip exercise with their arm starting either in an above *versus* below heart position, respectively. Then, we moved the exercising arm from the above to below heart position to suddenly increase oxygen delivery. Next, to assess the ability of muscle contraction force to conform to a decrease in oxygen delivery, we moved the exercising arm from the below back to above heart level – suddenly restoring low oxygen delivery conditions.

5.4 Methods

5.4.1 Participants and ethical approval.

Eleven healthy, non-smoking and forearm untrained, participants (5 female) were recruited for this study (see Table 1 in Results for anthropometric data). All experimental procedures were reviewed and approved by the Queen's University Health Sciences and Affiliated Teaching Hospitals Research Ethics Board (6005158 PHE-036-02) and conformed to the standards set by the Declaration of Helsinki except for registration in a data base. Informed written consent of voluntary participation was obtained from all participants prior to participation in the study.

5.4.2 Experimental design and conditions.

This study was a randomized within participant design in which participants completed seven handgrip exercise tests over seven testing days – 48-h minimum was given between sessions. Participants were asked to abstain from food 4-h before, caffeine and alcohol 12-h before and strenuous upper body exercise 24-h before each testing day.

5.4.2.1 Exercise modality.

Forearm exercise consisted of maximal voluntary rhythmic isometric forearm handgrip contractions at a contraction:relaxation frequency of 1-sec:2-sec. Participants lay supine with their left arm at heart level and their right arm on an armrest that could be rapidly raised or lowered with a pulley system – achieving ± ~20 cm change in mid-forearm height from heart level. Mid-forearm position was marked as the middle point of the four electromyography sensors placed on the forearm (see details below). Exercise was always completed with the participant's right hand but the starting position (i.e., above or below heart) of the exercise differed between conditions.

5.4.2.2 Screening and maximal effort exercise test practice.

Participants were screened to ensure that brachial artery blood velocity and diameter measurements could be made during exercise. Next, participants completed a 840-sec maximal effort exercise test – as described below – similar to that designed by Kellawan and Tschakovsky (2014). This first test acted as a practice trial prior to completing the six experimental testing days.

5.4.2.3 High perfusion pressure condition.

To create a condition of optimal exercising muscle perfusion pressure, and therefore, oxygen delivery, the participants right arm was lowered below heart for the duration of the 840-sec maximal effort exercise test – this was done on three of the six experimental testing sessions. See Fig. 1 for summary of the experimental protocol (see Appendix C for more details).

5.4.2.4 Low perfusion pressure condition.

To create a starting condition of sub-optimal exercising muscle perfusion pressure, and therefore, oxygen delivery, the participant's right arm was kept above heart for the first 360-sec of the 840-sec maximal effort exercise test. At 360-sec, to test the effect of rapid changes in oxygen delivery on muscle excitation-contraction coupling, the arm was lowered below heart for 240-sec – thereby increasing oxygen delivery to match that of the high perfusion pressure condition. At 600-sec, to test the effect of a rapid reversal of oxygen delivery on muscle excitation-contraction coupling, the arm was raised above heart and remained there until the end of the exercise test. This protocol was completed on three of the six experimental testing sessions. The starting order of the six experimental sessions was counter-balanced – always alternating between low and high perfusion pressure conditions between sessions. See Fig. 1 for summary of the experimental protocol (see Appendix C for more details).

5.4.2.5 Maximal effort exercise test.

On each of the six experimental testing days, participants completed an 840-sec maximal effort exercise test. This protocol followed the design of Kellawan and Tschakovsky (2014), with differences to test length – 840-sec instead of 600-sec – to accommodate the testing of rapid changes in perfusion pressure on excitation-contraction coupling during a maximal effort exercise test. Participants completed maximal forearm handgrip contractions at a contraction:relaxation frequency of 1-sec:2-sec for 840-sec. To minimize bias in when verbal encouragement was being provided, research assistants were asked to only provide verbal encouragement when the participants' contraction impulse dropped below the previous contraction impulse. Participants were able to see their contraction force profiles during the test to help motivate them to continuously try to beat their previous contraction impulse. Pilot testing demonstrated that critical force was not affected by whether the participants could or could not see their contraction impulse.

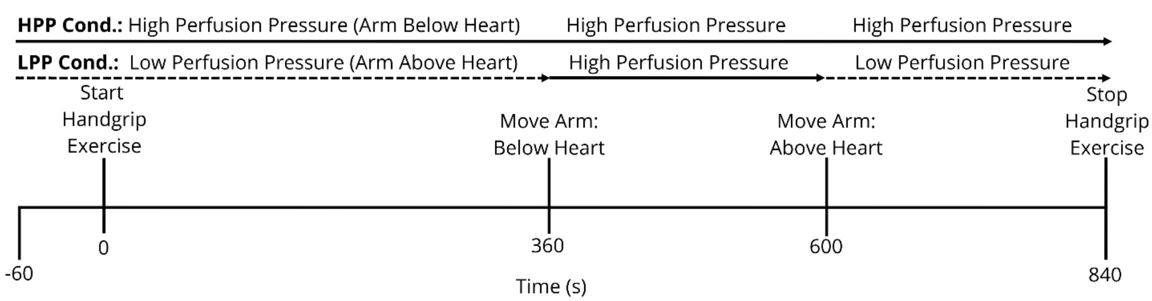

Figure 5-1. Summary of the experimental protocol. Maximal rhythmic forearm handgrip exercise is completed for 840-sec. In the High Perfusion Pressure Condition (HPP Cond.), participants complete the full exercise test with their exercising arm in the high perfusion pressure environment (i.e., below heart). In the Low Perfusion Pressure Condition (LPP Cond.), the exercising arm starts in a low perfusion pressure environment (i.e., above heart), moves to a high perfusion pressure environment at 360-sec for 240-sec and then returns to a low perfusion pressure environment at 600-sec until test end at 840-sec.

5.4.3 Instrumentation and data acquisition

5.4.3.1 Flexor digitorum superficialis muscle excitation.

Per methods previously described (Drouin et al., 2022; Drouin et al., 2019) with guidance from Bickerton et al. (1997), the four flexor digitorum superficialis muscle bellies were landmarked and four mini-wireless bipolar electrodes (Delsys, Natick, MA) were used to measure their muscle excitation continuously at a sampling rate of 2000-Hz in LabChart 7 software (ADInstruments, Colorado Springs, CO). The root mean square of each electromyography (EMG) channel was calculated and then averaged (in LabChart 7 software) to reflect forearm muscle EMG activity.

5.4.3.2 Handgrip force output.

Force of handgrip contraction was recorded continuously at 2000-Hz in LabChart 7 via a force transducer connected to a bridge amplifier to PowerLab/8_{SP} (ADInstruments, Colorado Springs, CO). The force transducer was calibrated by identifying the voltage output associated with known weights and creating a calibration curve. Prior to each test, the calibration curve was used to complete a two-point calibration of the force transducer.

5.4.3.3 Forearm blood flow.

Brachial artery blood velocity was measured with a flat 4-MHz pulsed Doppler probe (model 500V 131 Transcranial Doppler; Multigon Industries, Mt. Vernon, NY) attached to the skin proximal to the antecubital fossa of the right arm. Blood velocity data was recorded in volts via an analog connection to Powerlab/8_{SP} and converted to cm/s using a previously created calibration curve to account for the angle of Doppler signal insonation relative to the participants' brachial artery. Brachial artery diameter was recorded using a linear echo ultrasound probe ~5cm proximal to the

Doppler probe, operating at 13-MHz in 2D mode (Vivid I; GE Medical Systems, London, ON, Canada). Both velocity and diameter were recorded continuously.

5.4.4 Data analysis

5.4.4.1 Flexor digitorum superficialis muscle excitation and handgrip force output.

Flexor digitorum superficialis muscle excitation and handgrip force of contraction integrals were calculated in LabChart 7 software using a macro designed to identify the onset and offset of each contraction per that previously described (Drouin et al., 2023). These data were exported to excel where the first three contractions were averaged – per Hammer et al. (2020) – from which a delta was calculated for contraction force, muscle excitation and their ratio as these changed over time. Following this conversion to a delta, 30-sec time bins were calculated for contraction force (units: N·s), muscle excitation (units: mV·s) and their ratio (Force/EMG). Like previous work from our laboratory (Moynes et al., 2013), we used a mono-exponential fit to interpolate where contraction force values would have been in the low perfusion pressure condition if perfusion pressure had not been increased to match that of the high perfusion pressure condition. The mono-exponential fit was completed on all participants individually and then the group mean was plotted.

5.4.4.2 Flexor digitorum superficialis median power frequency.

Flexor digitorum superficialis median power frequency was calculated separately in LabChart 7 software for each of the four muscle bellies. In Excel the median power frequency from all four muscle bellies was averaged together to reflect the forearm muscle median power frequency. The first three contractions were averaged – per Hammer et al. (2020) – from which a delta was calculated for the median power frequency as it changed over time. Following this conversion to a delta, 30-sec time bins were calculated.

5.4.4.3 Forearm blood flow (FBF).

In LabChart 7 software, 30-sec averages of brachial artery mean blood velocity was calculated. Using Measurements from Arterial Ultrasound Imaging (MAUI, Hedgehog Medical) automated edge detection software, brachial artery diameter was calculated throughout the test and averaged into 30-sec time bins in Excel. Forearm blood flow was calculated as MBV (cm/s) · 60 s/min · π · [brachial artery diameter (cm)/2]^2. Where MBV is mean blood velocity in cm/s.

5.4.4.4 General methods.

Following the above analysis approaches, the three trials (i.e., triplicates) from each condition were averaged together to yield a single mean response for each participant and condition – thereby reducing variability in the observed response.

5.4.5 Statistical analysis

To test for differences in starting values – from which deltas were calculated – paired t-tests were run on the average of the first three contractions for contraction force, muscle excitation, Force/EMG and median power frequency. To statistically test our first hypothesis – that oxygen conforming can modify the progressive decline of muscle contraction force – comparisons only need to be made between conditions at the start of exercise (i.e., average time = 15-sec) and prior to oxygen delivery restoration at time 360-sec. To statistically test our second hypothesis – that oxygen conforming can rapidly shift the stabilized muscle contraction critical force – a comparison of changes in muscle contraction force over time is needed after time = 360-sec. Accordingly, for all variables, we ran two-way repeated measures ANOVAs on the 30-sec average measured at times 15-sec and 345-sec to test end. Upon discovery of condition by time interactions, multiple comparisons were completed within time between conditions. Post hoc assessment of time within condition was completed using one-way repeated measures ANOVAs. Upon discovery of a main effect of time, multiple comparisons were completed comparing values to measurement at time = 345-sec (i.e., the final measurement before arm position change). Statistical tests were run using GraphPad Prism 9 software (GraphPad, San Diego, CA). All pairwise comparisons were adjusted using the Sidak method. Statistical significance was assumed at $P < 0.05$.

5.5 Results

Table 5-1. Age, height and weight.

Variable (unit)	Group Mean (n=11)
Age (years)	20.7 ± 1.42
Height (cm)	171 ± 11.4
Weight (Kg)	67.7 ± 10.0

Values are mean ± SD.

5.5.1 Were there differences in the average of the first three contractions for muscle excitation integral, force integral, Force/EMG and median power frequency?

There were no differences in the average of the first three contractions between conditions for muscle contraction force ($t = 0.5998$, $P = 0.5620$), muscle excitation ($t = 0.6692$, $P = 0.5185$), Force/EMG ($t = 0.8415$, $P = 0.4197$) and median power frequency ($t = 1.129$, $P = 0.2852$). See Table 2 for group mean values.

Table 5-2. Average of first three contractions for electromyography (EMG) integral, force integral, Force/EMG and median power frequency.

Variable (Units)	Low Perfusion Pressure	High Perfusion Pressure
Force Integral (N·s)	253.8 ± 85.11	248.0 ± 75.59
EMG Integral (mV·s)	355.5 ± 132.7	371.8 ± 124.6
Force/EMG (N·s/mV·s)	0.6926 ± 0.1255	0.6703 ± 0.1281
Median Power Frequency (Hz)	92.11 ± 14.74	89.99 ± 12.43

Values are mean ± SD.

5.5.2 What was the effect of perfusion pressure on FBF?

There was a time by condition interaction for FBF [$F(19, 190) = 9.2843$, $P<0.0001$]. FBF was not different between conditions during baseline but FBF was significantly lower in the LPP condition within 30-sec of exercise onset and this difference remained until arm movement at time = 345-sec. At time = 345-sec, FBF was 402 ± 142 ml/min in the HPP compared to 331 ± 133 ml/min in the LPP condition – reflecting an ~18% difference in FBF between conditions. Upon arm movement from a low to high perfusion pressure environment, there is an immediate increase in FBF (Walker et al., 2007), and because of our 30-sec time bin approach, we observed FBF as being not different from the HPP condition within 30-sec of arm movement. FBF remained not different between conditions until the arm was moved back to the low perfusion pressure environment at 600-sec. Again, FBF would immediately decrease with arm movement back above heart (Walker et al., 2007). The 30-sec time bin meant that this effect was first quantified at 30-sec after arm movement back to the low perfusion pressure environment. FBF measured over the final 30-sec (time = 825-sec) of exercise was 391 ± 147ml/min in the HPP compared to 326 ± 118 ml/min in the LPP condition – reflecting a ~17% change between conditions. See Fig. 2 for pairwise comparisons and Table 3 for confidence intervals and P-values.

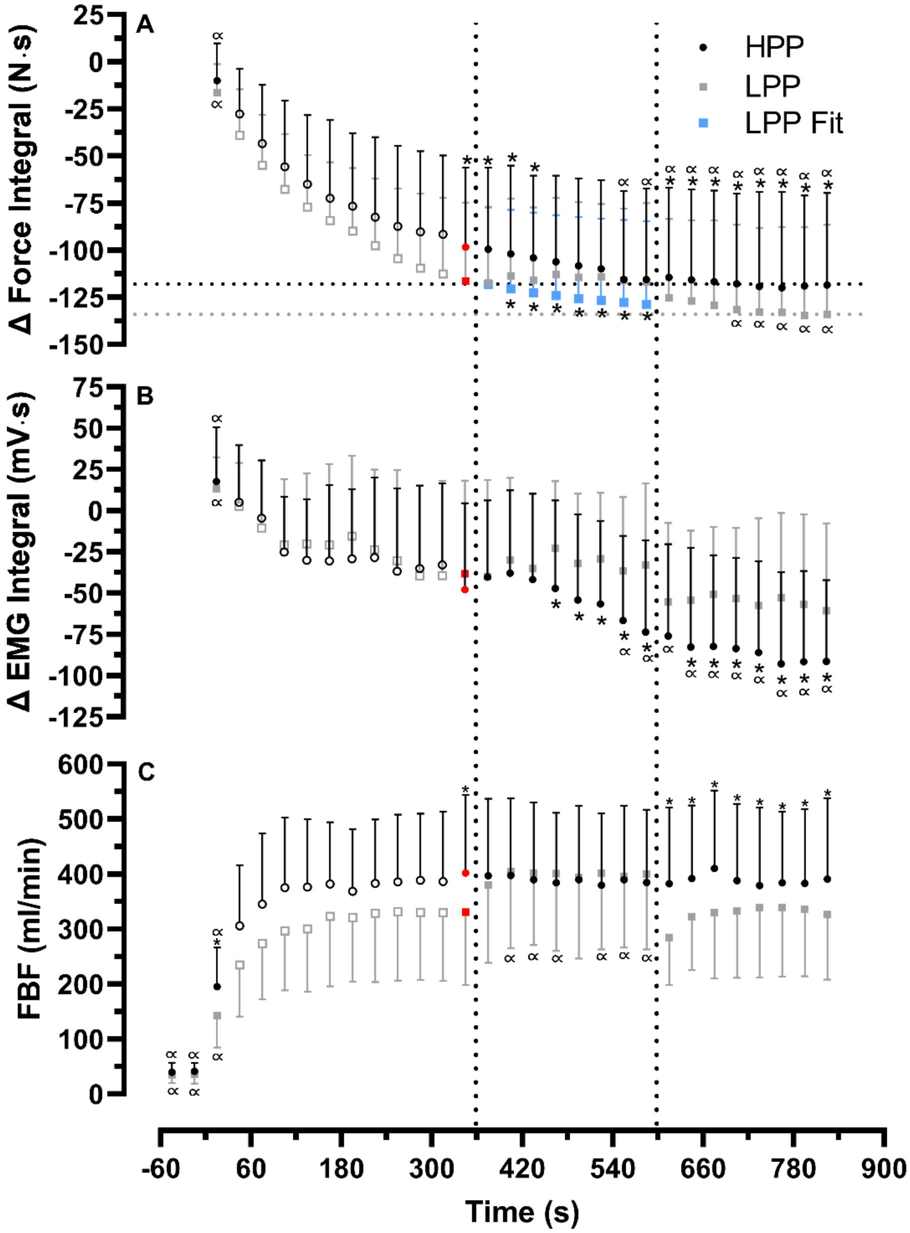

Figure 5-2. Muscle contraction force integral (panel A) and electromyography integral (Δ EMG, panel B) plotted over time as a delta from the average of the first three contractions and compared between Low Perfusion Pressure (LPP) and High Perfusion Pressure (HPP) conditions. Forearm blood flow (FBF, panel C) is plotted over time not as a delta. In the LPP condition, the exercising arm is moved from a low to high perfusion pressure environment at time = 360-sec (first dashed line) and from a high to low perfusion pressure environment at time = 600-sec (second dashed line). Statistics only run on filled data points. *Significantly different from LPP within time. $^{\alpha}$Significantly different from time = 345-sec (red data points) within condition. Data are mean ± SD.

Table 5-3. Confidence interval of difference (CI of diff.) and P values for multiple comparisons of muscle contraction force, muscle electromyography (EMG) and forearm blood flow (FBF).

	Force (N·s) HPP – LPP		**EMG (mV·s) HPP – LPP**		**FBF (ml/min) HPP – LPP**	
Time (s)	**95% CI of diff.**	**P value**	**95% CI of diff.**	**P value**	**95% CI of diff.**	**P value**
-45					-33.5 to 42.6	>0.9999
-15					-33.5 to 42.5	>0.9999
15	-3.07 to 15.7	0.5472	-17.6 to 26.2	>0.9999	15.1 to 91.1	**0.0006**
345	8.63 to 27.4	**<0.0001**	-31.5 to 12.3	0.9755	32.8 to 108	**<0.0001**
375	8.63 to 27.4	**<0.0001**	-22.1 to 21.6	>0.9999	-21.4 to 54.6	0.9825
405	2.40 to 21.2	**0.0036**	-29.8 to 13.9	0.9968	-45.2 to 30.8	>0.9999
435	2.50 to 21.3	**0.0032**	-28.6 to 15.1	0.9996	-49.6 to 26.4	0.9998
465	-2.59 to 16.2	0.4179	-46.3 to -2.50	**0.0164**	-54.6 to 21.4	0.9827
495	-3.16 to 15.6	0.5730	-44.1 to -0.342	**0.0432**	-41.7 to 34.3	>0.9999
525	-5.16 to 13.6	0.9682	-49.3 to -5.51	**0.0037**	-60.0 to 16.0	0.8047
555	-8.79 to 9.98	>0.9999	-51.9 to -8.13	**0.0009**	-43.8 to 32.2	>0.9999
585	-8.26 to 10.5	>0.9999	-62.6 to -18.8	**<0.0001**	-53.3 to 22.6	0.9929
615	1.54 to 20.3	**0.0098**	-42.5 to 1.22	0.0827	60.0 to 136	**<0.0001**
645	1.73 to 20.5	**0.0079**	-50.5 to -6.72	**0.0020**	31.3 to 107	**<0.0001**
675	3.14 to 21.9	**0.0015**	-53.6 to -9.85	**0.0004**	42.0 to 118	**<0.0001**
705	4.38 to 23.1	**0.0003**	-52.1 to -8.36	**0.0008**	17.4 to 93.4	**0.0003**
735	3.99 to 22.8	**0.0005**	-50.4 to -6.68	**0.0020**	2.40 to 78.4	**0.0270**
765	3.86 to 22.6	**0.0006**	-62.1 to -18.3	**<0.0001**	7.41 to 83.4	**0.0067**
795	6.22 to 25.0	**<0.0001**	-56.8 to -13.0	**<0.0001**	9.70 to 85.7	**0.0034**
825	6.26 to 25.0	**<0.0001**	-52.7 to -8.92	**0.0006**	26.8 to 102	**<0.0001**

HPP., High Perfusion Pressure ; LPP., Low Perfusion Pressure

5.5.3 What was the effect of suboptimal oxygen delivery during a maximal effort exercise test (time: 0-sec to 360-sec)?

5.5.3.1 Muscle contraction force.

There was a time by condition interaction for delta muscle contraction force integral [$F(17, 170) = 2.9075$, $P=0.0007$]. Muscle contraction force integral was not different between conditions over the first 30-sec of exercise, however, by 345-sec, muscle contraction force had decreased more in the LPP compared to HPP condition. At time = 345-sec, muscle contraction force had decreased by 98.4 ± 42.1 N·s in the HPP compared to 116 ± 41.6 N·s in the LPP condition – reflecting an ~18% difference in how much muscle contraction force decreased. One-way repeated measures ANOVAs revealed a main effect of time for LPP [$F(17, 170) = 59.13$] and HPP [$F(17, 170) = 65.32$] conditions. Compared to average time = 15-sec, muscle contraction force decreased under both conditions by time = 345-sec. See Fig. 2 for pairwise comparisons and Table 3 for confidence intervals and P-values.

5.5.3.2 Muscle excitation.

There was a time by condition interaction for delta EMG integral [$F(17, 170) = 3.3922$, $P<0.0001$]. Despite lower forearm blood flow in the LPP condition, delta EMG integral was not different between conditions at 30 and 345-sec into exercise. One-way repeated measures ANOVAs revealed a main effect of time for LPP [$F(17, 170) = 7.728$] and HPP [$F(17, 170) = 29.56$] conditions. Compared to average time = 15-sec, muscle excitation decreased under both conditions by time = 345-sec. See Fig. 2 for pairwise comparisons and Table 3 for confidence intervals and P-values.

5.5.3.3 Muscle contraction force per excitation.

There was a time by condition interaction for Force/EMG ratio [$F(17, 170) = 4.7687$, $P<0.0001$]. Because muscle contraction force integral dropped more in the LPP condition at the same EMG integral, the delta Force/EMG ratio was lower in the LPP compared to HPP condition. Force/EMG was not different between conditions over the first 30-sec of exercise, however, by 345-sec, Force/EMG force had decreased more in the LPP compared to HPP condition. One-way repeated measures ANOVAs revealed a main effect of time for LPP [$F(17, 170) = 29.68$] and HPP [$F(17, 170) = 18.33$] conditions. Compared to average time = 15-sec, Force/EMG decreased under both conditions by time = 345-sec. See Fig. 3 for pairwise comparisons and Table 4 for confidence intervals and P-values.

5.5.3.4 Median power frequency.

There was a time by condition interaction for delta median power frequency [$F(17, 170) = 3.1118$, $P<0.0001$]. Median power frequency was not different between conditions over the first 30-sec of exercise, however, by 345-sec, median power frequency force decreased more in the LPP compared to HPP condition. One-way repeated measures ANOVAs revealed a main effect of time for LPP [$F(17, 170) = 13.12$] and HPP [$F(17, 170) = 26.69$] conditions. Compared to average time = 15-sec, median power frequency decreased under both conditions by time = 345-sec. See Fig. 4 for pairwise comparisons and Table 4 for confidence intervals and P-values.

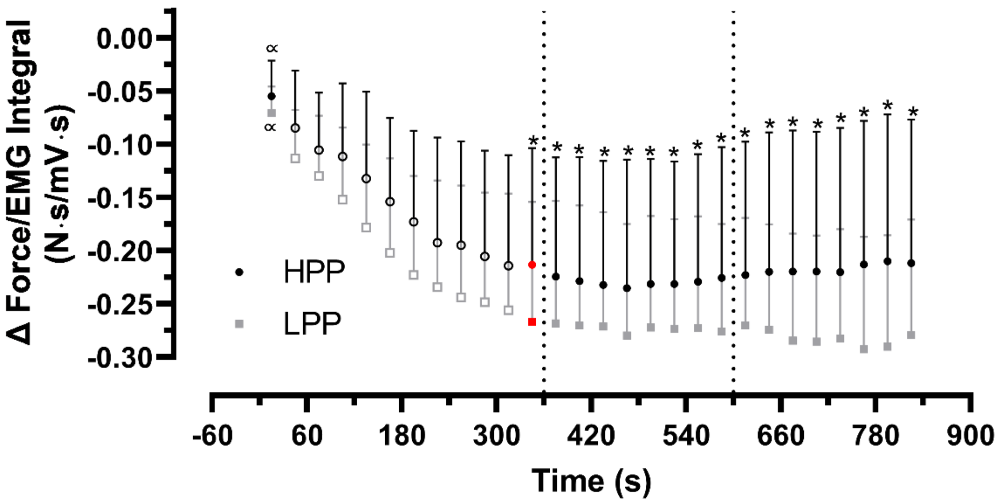

Figure 5-3. Muscle contraction force integral per electromyography (EMG) integral plotted over time as a delta from the average of the first three contractions and compared between Low Perfusion Pressure (LPP) and High Perfusion Pressure (HPP) conditions. In the LPP condition, the exercising arm is moved from a low to high perfusion pressure environment at time = 360-sec (first dashed line) and from a high to low perfusion pressure environment at time = 600-sec (second dashed line). Statistics only run on filled data points. *Significantly different from LPP within time. [α]Significantly different from time = 345-sec (red data points) within condition. Data are mean ± SD.

Table 5-4. Confidence interval of difference (CI of diff.) and P values for multiple comparisons of muscle contraction force per muscle electromyography (force/EMG) and median power frequency (MedPF).

	Force/EMG (N·s/ mV·s) HPP – LPP		**MedPF (Hz) HPP – LPP**		**Force (N·s) LPP fit – LPP**	
Time (s)	**95% CI of diff.**	**P value**	**95% CI of diff.**	**P value**	**95% CI of diff.**	**P value**
15	-0.00631 to 0.0380	0.4400	-0.14 to 4.49	0.0869	-9.28 to 3.46	0.9636
345	0.0314 to 0.0757	**<0.0001**	4.23 to 8.86	**<0.0001**	-5.67 to 7.06	>0.9999
375	0.0218 to 0.0662	**<0.0001**	4.17 to 8.80	**<0.0001**	-7.16 to 5.58	>0.9999
405	0.0196 to 0.0639	**<0.0001**	4.34 to 8.97	**<0.0001**	-13.3 to -0.597	**0.0202**
435	0.0170 to 0.0613	**<0.0001**	4.02 to 8.65	**<0.0001**	-13.0 to -0.242	**0.0349**
465	0.0223 to 0.0666	**<0.0001**	4.58 to 9.21	**<0.0001**	-17.6 to -4.83	**<0.0001**
495	0.0189 to 0.0632	**<0.0001**	4.03 to 8.66	**<0.0001**	-17.5 to -4.74	**<0.0001**
525	0.0202 to 0.0645	**<0.0001**	4.16 to 8.79	**<0.0001**	-19.0 to -6.25	**<0.0001**
555	0.0211 to 0.0654	**<0.0001**	3.71 to 8.34	**<0.0001**	-18.0 to -5.31	**<0.0001**
585	0.0282 to 0.0726	**<0.0001**	3.69 to 8.32	**<0.0001**	-18.3 to -5.61	**<0.0001**
615	0.0255 to 0.0698	**<0.0001**	1.48 to 6.11	**<0.0001**	-10.4 to 2.36	0.6615
645	0.0324 to 0.0767	**<0.0001**	2.71 to 7.33	**<0.0001**	-9.43 to 3.30	0.9422
675	0.0428 to 0.0871	**<0.0001**	4.87 to 9.50	**<0.0001**	-7.70 to 5.05	>0.9999
705	0.0440 to 0.0882	**<0.0001**	4.01 to 8.64	**<0.0001**	-5.80 to 6.94	>0.9999
735	0.0407 to 0.0850	**<0.0001**	3.30 to 7.93	**<0.0001**	-4.98 to 7.76	>0.9999
765	0.0578 to 0.102	**<0.0001**	5.46 to 10.1	**<0.0001**	-4.93 to 7.80	>0.9999
795	0.0584 to 0.103	**<0.0001**	5.40 to 10.0	**<0.0001**	-3.80 to 8.93	0.9895
825	0.0456 to 0.0900	**<0.0001**	4.55 to 9.18	**<0.0001**	-4.49 to 8.24	0.9998

HPP., High Perfusion Pressure ; LPP., Low Perfusion Pressure

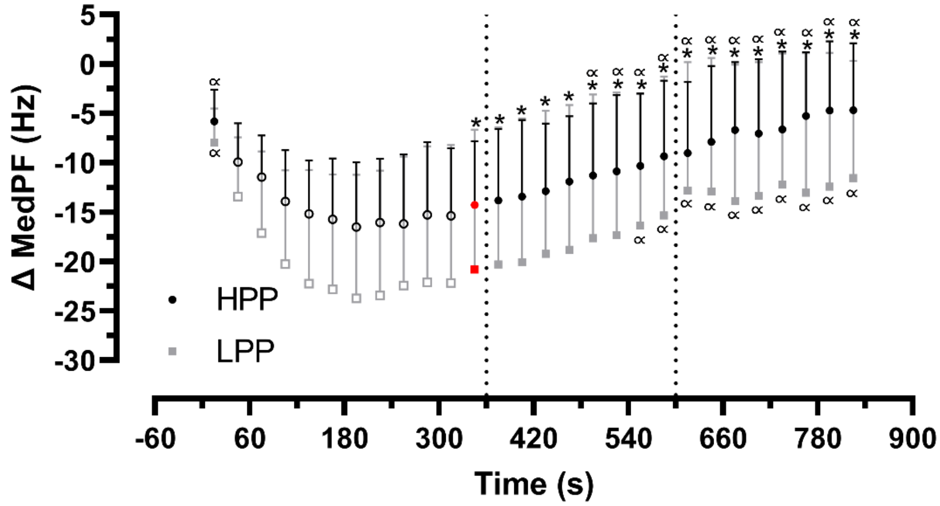

Figure 5-4. Median Power Frequency (MedPF) plotted over time as a delta from the average of the first three contractions and compared between Low Perfusion Pressure (LPP) and High Perfusion Pressure (HPP) conditions. In the LPP condition, the exercising arm is moved from a low to high perfusion pressure environment at time = 360-sec (first dashed line) and from a high to low perfusion pressure environment at time = 600-sec (second dashed line). Statistics only run on filled data points. *Significantly different from LPP within time. [α]Significantly different from time = 345-sec (red data points) within condition. Data are mean ± SD.

5.5.4 What was the effect of a rapid increase in oxygen delivery during a maximal effort exercise test (time 360-sec to 600-sec)?

5.5.4.1 Muscle contraction force.

Upon increasing oxygen delivery to match that of the HPP condition, further decrease in delta muscle contraction force integral was prevented in the LPP condition, whereas it continued to drop in the HPP condition. Therefore, in the LPP condition, after 90-sec of exposure to increased oxygen delivery (i.e., after time = 420-sec), delta muscle contraction force integral was not different between conditions. At time = 585-sec, contraction force had decreased by 115 ± 48.3 N·s in the HPP compared to 116 ± 41.6 N·s in the LPP condition. There was a time by condition interaction when comparing the LPP to HPP shift with the curve fit of the LPP condition had it continued [$F(17, 170) = 6.8247$, $P<0.0001$]. Within 60-sec of increasing oxygen delivery, the delta muscle contraction force integral is higher and remained there until time = 600-sec in the LPP condition compared to LPP fit. See Fig. 2 for pairwise comparisons and Table 3 and 4 for confidence intervals and P-values.

5.5.4.2 Muscle excitation.

Upon increasing oxygen delivery, further decrease in delta EMG integral was prevented in the LPP condition, whereas it continued to drop in the HPP condition. The delta EMG integral was therefore higher in the LPP compared to the HPP condition from time = 510 until arm movement at time = 600-sec. See Fig. 2 and Table 3 for confidence intervals and P-values.

5.5.4.3 Muscle contraction force per excitation.

There was no effect of increasing oxygen delivery on the delta Force/EMG ratio. The delta Force/EMG remained lower in the LPP compared to HPP condition. See Fig. 3 and Table 4 for confidence intervals and P-values.

5.5.4.4 Median power frequency.

There was no effect of increasing oxygen delivery on the median power frequency. The delta median power frequency remained lower in the LPP compared to HPP condition. See Fig. 4 and Table 4 for confidence intervals and P-values.

5.5.5 What was the effect of a rapid decrease in oxygen delivery during a maximal effort exercise test (time 600-sec to 840-sec (test end))?

5.5.5.1 Muscle contraction force.

Within 30-sec of decreasing oxygen delivery (back to suboptimal levels), delta muscle contraction force integral returned to being lower in the LPP compared to the HPP condition until test end. At time = 825-sec, muscle contraction force had decreased by 118 ± 48.7 N·s in the HPP compared to 134 ± 47.5 N·s in the LPP condition – reflecting a ~13% change in contraction force. See Fig. 2 for pairwise comparisons and Table 3 for confidence intervals and P-values.

5.5.5.2 Muscle excitation.

For 30-sec, within 30-sec of a decrease in oxygen delivery, delta EMG integral returned to being not different between conditions. Thereafter, delta EMG integral returned to being higher in the LPP condition compared to the HPP condition until test end. See Fig. 2 for pairwise comparisons and Table 3 for confidence intervals and P-values.

5.5.5.3 Muscle contraction force per excitation.

The decrease in oxygen delivery had no effect on the delta Force/EMG ratio. The delta Force/EMG ratio remained lower in the LPP compared to HPP condition. See Fig. 3 and Table 4 for confidence intervals and P-values.

5.5.5.4 Median power frequency.

The decrease in oxygen delivery had no effect on the median power frequency. The delta median power frequency remained lower in the LPP compared to HPP condition. See Fig. 4 and Table 4 for confidence intervals and P-values.

5.6 Discussion

The oxygen conforming response of muscle contraction force is defined as: the adjustment of muscle contraction force at a given muscle excitation to maintain the balance between aerobic ATP production and ATP consumption such that the cellular environment remains stable during oxygen delivery mediated changes in aerobic ATP production. This study tested the hypothesis that – under conditions of maximal cellular disturbance established through maximal effort handgrip exercise – muscle contraction force would follow changes in oxygen delivery.

The key findings were (a) during the first 360-sec of exercise, when oxygen delivery was lower (~18% lower in LPP at time = 345-sec), muscle contraction force was lower (~18% lower in LPP at time = 345-sec) – this occurred despite no differences in muscle excitation in the LPP compared to HPP condition (see Fig. 2). (b) Upon increasing oxygen delivery in the LPP condition to match that of the HPP condition (time 360 to 600-sec), muscle contraction force stabilized – but was not reversed – in the LPP condition whereas muscle contraction force continued to drop in the HPP condition – resulting in no difference in muscle contraction force between conditions from time = 420 to 600-sec (see Fig. 2). The stabilization of muscle contraction force occurred concurrently with maintained muscle excitation in the LPP condition, whereas muscle excitation in HPP condition continued to decline – this resulted in higher levels of muscle excitation in the LPP compared to HPP condition from time = 510 to 600-sec (see Fig. 2). (c) Upon a subsequent restoration of low oxygen delivery (~17% lower in LPP at time = 825-sec), muscle contraction force rapidly (within 30-sec) returned to being lower (~13% lower in LPP at time = 825-sec) in the LPP compared to HPP condition – this occurred despite a maintained higher muscle excitation in the LPP compared to the HPP condition (see Fig. 2). These key findings are consistent an oxygen conforming response of muscle contraction force during maximal effort exercise.

5.6.1 Perfusion pressure manipulation of forearm muscle oxygen delivery.

In the present study, we used arm position (above vs. below heart) to alter exercising muscle perfusion pressure (see Fig. 1 for summary of experimental protocol). With lower forearm arterial perfusion pressure (i.e., arm above heart) oxygen delivery was ~27% lower within 30-sec of exercise onset, reaching a ~13-18% lower oxygen delivery plateau during the first 360-sec of maximal effort exercise compared to the HPP condition (i.e., arm below heart; see Fig. 2). Upon arm movement from above to below heart, oxygen delivery rapidly increased along with perfusion pressure to match that of the HPP condition (see Fig. 2). A subsequent arm movement from below back to above heart led to a rapid decrease in oxygen delivery to ~14-17% lower compared to the HPP condition (see Fig. 2). Therefore, as intended, our perfusion pressure manipulation was effective at altering oxygen delivery to the exercising muscle during maximal effort rhythmic forearm handgrip exercise.

5.6.2 Forearm muscle contraction force at maximal effort is sensitive to oxygen delivery.

Muscle contraction force decreased more during the first 360-sec of maximal effort exercise in the low compared to high perfusion pressure condition, ending ~18% lower prior to perfusion pressure changes (i.e., time = 345-sec, see Fig. 2). This is consistent with 3-min all-out cycling critical power results compared between normoxic and hypoxic conditions (Simpson et al., 2015; Sousa et al., 2021). During all-out cycling exercise, power output decreased more in the hypoxic compared to normoxic condition, and this trend continued until a lower (~16-22%) plateau (i.e., critical power) was reached (within 180-sec) (Simpson et al., 2015; Sousa et al., 2021). Similarly, our data demonstrated that muscle excitation-contraction coupling above critical force – during a maximal effort rhythmic handgrip exercise test – is sensitive to local oxygen delivery. As opposed to the 3-min all out cycling exercise test used to identify critical power, a true plateau in muscle contraction force was not yet evident by 360-sec of maximal effort rhythmic handgrip exercise in our study. Therefore, critical force had not yet been achieved under either HPP or LPP conditions (see Fig. 2) – this reflects that, within a given oxygen delivery environment, peak cellular disturbance has not yet contributed maximally to the muscle contraction force decline.

The accelerated decline in muscle contraction force under LPP conditions is consistent with an increased rate of oxygen delivery mediated cellular disturbance (Korzeniewski & Rossiter, 2020; Korzeniewski, 2023). That is, to achieve high rates of ATP production during maximal effort exercise with reduced oxygen delivery, there must be an adjustment of redox and phosphorylation potentials to continue matching aerobic ATP supply to ATP demand (Wilson et al., 1979; Erecinska & Wilson, 1982; Wilson & Erecinska, 1985; Hogan et al., 1992a; Hogan et al., 1996; Haseler et al., 1998; Hogan et al., 1998; Goulding et al., 2019; Korzeniewski, 2023). Though this adjustment of redox and phosphorylation potentials helps maintain ATP production, there will be an associated faster accumulation of ADP, Pi and H+. Although we did not measure the metabolic environment, it is likely that part of the initial difference in contraction force between conditions was a peripherally acting Pi mediated excitation-contraction coupling impairment. In particular, it is possible that there was an increased Pi mediated (a) reduction of strongly bound actin-myosin heads (Parsons et al., 1997), (b) reduction in the affinity of calcium binding to troponin C on tropomyosin filaments (Debold, 2016) and (c) precipitation of calcium in the sarcoplasmic reticulum thereby reducing free calcium release per excitation (Westerblad et al., 1993; Westerblad & Allen, 1996; Dutka et al., 2005; Allen & Trajanovska, 2012). Although the mechanism of muscle contraction force compromise was likely of peripheral origin – as supported by the lack of muscle excitation difference between conditions – it is possible that an increased accumulation of Pi and H+ contributed to afferent feedback mediated central fatigue (Broxterman et al., 2015; Hammer et al., 2020; Hureau et al., 2022). Though central fatigue did not appear to act via a reduction in muscle excitation, it is possible that there was de-recruitment of larger more fatigable type II fibers – as evidenced by a decrease in the observed median power frequency (reflecting muscle conduction velocity; see Fig. 4) (Bilodeau et al., 2003; Methenitis et al., 2016). Critically, like in the work of Hammer et al. (2020), the initial low oxygen delivery resulted in an irreversible compromise of median power frequency.

In summary, by simultaneously measuring forearm blood flow, muscle contraction force and excitation during a maximal effort exercise test, our study demonstrates that an initial compromise to muscle oxygen delivery exacerbates the rate of muscle contraction force decline in small muscle mass exercise. Like the systemic effect of hypoxia on critical power, we have demonstrated that a relatively small decrease in local oxygen delivery (i.e., ~18%) can impair muscle excitation-contraction coupling above critical force during a maximal effort exercise test.

5.6.3 Maximal forearm muscle contraction force follows changes in oxygen delivery.

Following the first 360-sec of maximal effort exercise – to test the effect of a rapid increase in oxygen delivery (i.e., increased to match that of the high perfusion pressure condition) on muscle excitation-contraction coupling – the exercising arm was moved from a low to high perfusion pressure environment for 240-sec (time 360 to 600-sec). Measurements from time 360 to 600-sec are therefore made under the same local oxygen delivery conditions for HPP and LPP conditions. The instantaneous reversal of oxygen delivery led to an immediate stabilization of muscle contraction force under LPP conditions at critical force levels seen under HPP conditions (by 600-sec; see Fig. 2). Furthermore, compared to the low perfusion pressure curve fit, which interpolates the predicted force profile if low perfusion pressure had continued (see Fig. 2, blue open squares in panel A), muscle contraction force was higher within 60-sec in the LPP condition. Combined, these data demonstrate a rapid-acting benefit of increased oxygen delivery for muscle excitation-contraction coupling – this is consistent with findings below critical power (Drouin et al., 2023). Importantly, muscle contraction force was not rapidly restored (i.e., increased) to levels occurring in the HPP condition. We interpret this as indicating that, by 360-sec, cellular disturbance had not yet contributed equally to the decrease in muscle contraction force between perfusion pressure conditions. Therefore, non-oxygen conforming response of muscle contraction force differences remained between conditions.

Key to this interpretation is the differentiation between possible muscle contraction force mediated compromising mechanisms. The first mechanism of muscle contraction force compromise is cellular disturbance mediated. Above critical force – in the severe exercise intensity domain – a rapidly developed maximal cellular disturbance contributes (through central and peripheral mechanisms) to a near hyperbolic decline in muscle contraction force (Burnley et al., 2010; Vanhatalo et al., 2010; Black et al., 2017; Broxterman et al., 2017; Korzeniewski & Rossiter, 2020; Hureau et al., 2022). Reaching a plateau in muscle contraction force reflects (a) attainment of steady oxygen delivery demand matching (Kellawan & Tschakovsky, 2014) and (b) peak contributions of maximal cellular disturbance to the muscle contraction force decline (Korzeniewski & Rossiter, 2020). Under these conditions, so long as exercise persists and there are no other manipulations taking place, lost muscle contraction force capacity cannot be recovered. Therefore, this cellular disturbance-mediated muscle contraction force compromise is 'irreversible' while exercise is ongoing. The second mechanism of muscle contraction force compromise is the oxygen conforming response of muscle contraction force. As opposed to cellular disturbance-mediated muscle contraction force compromise, the oxygen conforming response of muscle contraction force is rapidly reversible and it can occur while exercise is ongoing (Fitzpatrick et al., 1996; Luu & Fitzpatrick, 2013; Drouin et al., 2022; Drouin et al., 2023).

Had the difference in muscle contraction force between conditions – prior to restoration of muscle oxygen delivery – been fully explained by an oxygen conforming response of muscle contraction force, we would have expected muscle contraction force to rapidly increase to levels seen in the HPP condition (Fitzpatrick et al., 1996; Luu & Fitzpatrick, 2013; Drouin et al., 2022) – rather a continued decrease in muscle contraction force was prevented. On the other hand, had the difference in muscle contraction force been fully explained by oxygen delivery-mediated differences in the magnitude of cellular disturbance, we would have expected a sustained compromise to muscle contraction force (Pitcher & Miles, 1997; Romer et al., 2006), yet, following restoration of oxygen delivery, muscle contraction force becomes not different between conditions. Therefore, we interpret these findings as supporting a positive oxygen conforming response of muscle contraction force working in opposition of a negative ongoing cellular disturbance-mediated effect, ultimately contributing to a net stabilization of muscle contraction force at HPP critical force levels.

Consistent with this interpretation is the continued decline in muscle contraction force under HPP conditions – this reflects continued cellular disturbance-mediated compromise to muscle contraction force under the same oxygen delivery conditions. This continued slow decline in muscle contraction force is consistent with the continued contribution of maximal Pi levels (i.e., maximal cellular disturbance) to the slower developing precipitation of calcium within the sarcoplasmic reticulum (Allen & Westerblad, 2001; Korzeniewski & Rossiter, 2020). Given that muscle excitation continues to decrease concomitantly with muscle contraction force, it is possible that there was feedback inhibition (i.e., central fatigue) – via group III/IV afferents – contributing to the continued muscle contraction force decline after 360-sec in the HPP condition (Burnley, 2009; Broxterman et al., 2017; Hammer et al., 2020). However, considering oxygen delivery was higher in the HPP compared to LPP condition, we would consider it unlikely that there would be more central fatigue under the HPP condition compared to the LPP condition. Importantly, despite the slower muscle contraction force decline under HPP conditions, the lack of a muscle contraction force difference between conditions by 600-sec suggests that maximal cellular disturbance has contributed similarly – albeit at different rates – to the muscle contraction force decline.

In summary, although an initial compromise to muscle oxygen delivery accelerated the rate of muscle contraction force decline, a rapid restoration of muscle oxygen delivery (to HPP levels) led to a rapid stabilization of muscle contraction force at critical force levels seen under HPP conditions. That muscle contraction force stabilized, rather than reversed, supports the interpretation that a positive oxygen conforming response of muscle contraction force was working in opposition of a negative ongoing cellular disturbance mediated effect.

5.6.4 Differentiating the contributions of cellular disturbance-mediated fatigue and oxygen conforming to the decline in muscle contraction force.

During a maximal effort exercise test, maximal VO2 (Kellawan & Tschakovsky, 2014; Goulding et al., 2020; Fenuta et al., 2023), oxidative ATP production (Broxterman et al., 2017) and cellular disturbance (i.e., Pi and PCr) (Burnley et al., 2010; Korzeniewski & Rossiter, 2020) are rapidly reached. Although their plateau occurs quickly, the attainment of a plateau in muscle contraction force occurs more slowly – reflecting a slower development of cellular disturbance-mediated muscle contraction force decline (Korzeniewski & Rossiter, 2020). Once a critical force plateau is achieved, during a maximal effort exercise test, maximal cellular disturbance cannot be further increased and therefore, the critical force plateau reflects the peak contribution of cellular disturbance to the decline in muscle contraction force (Korzeniewski & Rossiter, 2020). This perspective is supported by the observation that task failure will occur at a maximal level of cellular disturbance (i.e., maximal Pi or minimal PCr) (Hogan et al., 1999b; Burnley et al., 2010; Korzeniewski & Rossiter, 2020; Korzeniewski, 2023). Therefore, the decrease in muscle contraction force during maximal effort exercise reflects peak cellular disturbance contribution to ongoing task failure – muscle contraction force continues to decrease until a plateau is reached. Therefore, considering we have achieved peak levels of cellular disturbance-mediated muscle contraction force reduction – as evidenced by the plateau in contraction force prior to time 600-sec under HPP and LPP conditions – any subsequent concomitant change in muscle contraction force and oxygen delivery should solely reflect an oxygen conforming response of muscle contraction force.

In line with this perspective, a subsequent restoration of low oxygen delivery led to a rapid decrease in muscle contraction force. The decrease in muscle contraction force rapidly reached a new plateau, averaging ~12% lower (from time 690 to 840-sec) than the HPP condition. Importantly, this decreased muscle contraction force reflects the 'reversible' oxygen conforming response of muscle contraction force contribution to the decrease in muscle contraction force seen throughout the maximal effort exercise test. This interpretation is corroborated by how rapidly muscle contraction force conforms to changes in oxygen delivery. Within 30-sec of decreasing oxygen delivery, muscle contraction force returns to being lower in the LPP compared to HPP condition. These findings are consistent with previous electrical stimulation (Hobbs & McCloskey, 1987; Fitzpatrick et al., 1996; Luu & Fitzpatrick, 2013) and voluntary (Drouin et al., 2022) exercise studies where we see muscle contraction force rapidly (within 120-sec) follow changes in oxygen delivery at a given muscle excitation. Therefore, over the final 150-sec of exercise, an average ~13% difference in oxygen delivery accounted for an average ~12% decrease in muscle contraction force.

In summary, by assessing the oxygen conforming response of muscle contraction force under conditions of maximal cellular disturbance, we have demonstrated that these rapid changes in muscle contraction force with changes in oxygen delivery are not occurring because of additional cellular disturbance. Therefore, independent of cellular disturbance, the oxygen conforming response of muscle contraction force occurs during maximal effort exercise.

5.6.5 Methodological considerations.

In this study we used arm position to create low (above heart) and high (below heart) perfusion pressure environments. Despite the isometric nature of the exercise, it is possible that that there could be differences in muscle fiber length between arm positions. Any change in muscle fiber length could feasibly alter contraction force independent of muscle excitation (Lloyd & Besier, 2003; Vigotsky et al., 2017). Importantly, in Table 2, we compare the average of the first three contractions between low and high perfusion pressure conditions – reflecting different starting arm positions. Here we see no difference in muscle contraction force between conditions. Therefore, if there were differences in muscle fiber length between arm positions, its contribution to the overall difference in contraction force between conditions was small. It must also be acknowledged that because of the randomness of amplitude cancelation (Farina et al., 2014), it is possible that any observed differences, or lack thereof, in our surface EMG signal could be the result of differences in amplitude cancelation. Therefore, interpretation of muscle excitation data should be considered cautiously. Despite possible limitations of our EMG measurements, a strength of our study design is that we have performed each experimental condition in triplicate. That is, we had each participant complete three trials of both the high perfusion pressure and low perfusion pressure conditions – we then averaged the three trials. By doing so, we have effectively reduced the variability of our response, and therefore, despite potential limitations of surface EMG measures, we have greater confidence that the observed response is in-fact an effect of changes in oxygen delivery and not some other limitation of surface EMG measurement.

5.7 Conclusion

This study has demonstrated for the first time, in voluntary human exercise, that muscle excitation-contraction coupling is sensitive to relatively small changes in local oxygen delivery during maximal effort exercise. First, we have demonstrated that muscle contraction force decreases to a greater extent in a low perfusion pressure condition but that upon restoration of high perfusion pressure, muscle contraction force stabilizes at critical force levels seen under a high perfusion pressure condition. This is consistent with the ability of oxygen delivery to modify the progressive decline of muscle contraction force during maximal effort exercise. Second, we have demonstrated that – once peak cellular disturbance has contributed maximally to the muscle contraction force decline (i.e., a critical force plateau has been achieved) – muscle contraction force rapidly conforms to changes in oxygen delivery. This supports a role of an oxygen conforming response of muscle contraction force in modifying muscle contraction force during maximal effort exercise. Combined, these findings demonstrate the important – cellular disturbance independent – role an oxygen conforming response of muscle contraction force can play in modifying exercise tolerance during maximal effort exercise.

Chapter 6

General Discussion

6.1 Integrated summary and contributions of the thesis work to the field of study

We can all appreciate that as we exercise hard and/or long enough, the same exercise begins to feel more difficult. This happens because exercise related metabolites (the byproduct of metabolic reactions) contribute to an impairment of excitation-contraction coupling (i.e., skeletal muscle fatigue). As our skeletal muscles fatigue, we need to increase the electrical activity sent from our brain to the muscle to support the ongoing task. With electromyography, the amount of electrical activity can be measured in the muscle (referred to as muscle excitation). During fatiguing exercise, the benefit of increasing muscle excitation is that we can continue performing the task, however, the consequence is that we have continued build-up of fatigue inducing metabolites and via corollary discharge we sense the increased amount of muscle excitation as an increase in perceived effort (de Morree et al., 2012; Drouin et al., 2019). Unfortunately, the only way to reverse skeletal muscle fatigue is to stop exercising (Pitcher & Miles, 1997; Romer et al., 2006).

Like the increase in muscle fatigue, a decrease in oxygen delivery can also impair the relationship between muscle excitation and contraction force. In voluntarily exercised muscle, when exercising muscle perfusion pressure or blood flow is reduced, muscle excitation needs to increase to maintain muscle contraction force (Drouin et al., 2019; Hobbs & McCloskey, 1987). What's interesting about this phenomenon, and what distinguishes it from muscle fatigue, is that when we restore normal oxygen delivery, muscle excitation per contraction force is rapidly reversed back to normal levels (Drouin et al., 2019). Although work from our laboratory demonstrated, for the first time, the existence of an oxygen conforming response in voluntary human exercise (Drouin et al., 2019), it did not replicate the muscle contraction force conforming to oxygen delivery response evident in electrically stimulated exercise models. Critically, at a maintained muscle contraction force with reduced oxygen delivery, we would expect an increased metabolic disturbance mediated muscle fatigue – this is exactly what we saw during the first bout of reduced oxygen delivery (Drouin et al., 2019). Upon recovery of normal oxygen delivery, muscle excitation was not restored to normal levels – this is consistent with skeletal muscle fatigue (Drouin et al., 2019). This metabolic disturbance is not characteristic of typical oxygen conforming work completed in electrically stimulated models where muscle excitation – rather than muscle contraction force – is controlled. Because of this critical difference between muscle contraction force and muscle excitation maintenance exercise, a muscle contraction force conforming to oxygen delivery response had yet to be demonstrated during voluntary exercise.

Accordingly, in Chapter 3, we developed a model enabling participants to target a given level of muscle excitation during voluntary rhythmic handgrip contractions. While participants voluntarily exercised at a target muscle excitation, we used manual brachial artery compression to reduce forearm blood flow by ~50%. Upon a decrease in forearm blood flow (and muscle oxygenation), muscle contraction force per excitation decreased at 90 and 75 but not 50% critical force exercise intensities. At 90 and 75% critical force intensities, a restoration of forearm blood flow led to a rapid recovery of muscle contraction force. This work in voluntarily exercised muscle added to the field of study by demonstrating for the first time the existence of two of the three key oxygen conforming response characteristics during voluntary human exercise: (1) muscle contraction force conforms to decreased muscle blood flow and (2) muscle contraction force is rapidly recovered following blood flow restoration. Additionally, we demonstrated, for the first time, that the oxygen conforming response is exercise intensity dependent – occurring only at or above 75% critical force. Critically, these findings highlight the distinct (from skeletal muscle fatigue) – and underappreciated – role oxygen delivery can play in altering exercise tolerance.

As opposed to decreasing oxygen delivery, which can reversibly impair muscle excitation-contraction coupling, it remained to be determined if an increase in oxygen delivery above 'normal' levels could improve excitation-contraction coupling. Accordingly, in Chapter 4 we designed an experimental model that would allow us to increase forearm oxygen delivery above 'normal' levels. We took advantage of group III/IV afferent feedback to stimulate a pressor reflex, thereby increasing arterial blood pressure – the driving pressure for blood flow. In participants experiencing an increase in forearm blood flow, the muscle excitation to contraction force ratio was rapidly decreased (i.e., improved) compared to their time control. Interestingly, upon reversal of oxygen delivery back to normal levels, the muscle excitation to contraction force ratio rapidly returned to being not different from control levels. This study therefore demonstrated, for the first time, in voluntary human exercise that an increase in oxygen delivery above 'normal' levels can reversibly improve muscle excitation-contraction coupling. Critically, these findings highlight the need for a shift in the current dogma; that oxygen delivery is tightly matched to demand. Future oxygen delivery demand matching work should therefore consider the adequacy of oxygen delivery for optimal excitation-contraction coupling, and not only whether it is adequate to support a given VO_2.

As opposed to exercise intensities below critical force – where there is a rapid submaximal stabilization of the metabolic environment – during maximal effort exercise there is a rapid attainment of maximal cellular disturbance. Bearing in mind the considerably different metabolic environments, it remained to be determined whether oxygen conforming could (a) modify the progressive decline of muscle contraction force and (b) rapidly shift the stabilized muscle contraction critical force. Here, we used arm position to alter forearm perfusion pressure. In an arm above heart condition (i.e., low perfusion pressure) muscle contraction force decreased more compared to an arm below heart condition (i.e., high perfusion pressure). Upon moving the arm from above to below heart level, muscle contraction force rapidly stabilized at what would be critical force under high perfusion pressure conditions. Importantly, as opposed to our hypothesis, the rapid reversal of oxygen delivery did not cause a rapid restoration of muscle contraction force – this is not consistent with the sole contribution of an oxygen conforming response. Instead, considering the continued muscle contraction force decline under high perfusion pressure conditions, the stabilization of muscle contraction force in the low perfusion pressure condition is consistent with a positive oxygen conforming response acting in opposition of the negative ongoing cellular disturbance mediated fatigue. When the arm was moved back above heart level (i.e., back to a low perfusion pressure environment), muscle contraction force rapidly (within 30-sec) decreased with reduced oxygen delivery. The rapidity of the compromise to muscle contraction force is consistent with an oxygen conforming response. This study has demonstrated for the first time, in voluntary human exercise, that muscle excitation-contraction coupling is sensitive to relatively small – physiologically relevant – changes in local oxygen delivery during maximal effort exercise. Critically, these findings highlight the distinct contribution of cellular mediated disturbance and oxygen conforming to maximal muscle contraction force – once again highlighting the distinct and underappreciated role oxygen delivery can play in altering exercise tolerance.

6.2 Strengths of thesis work

A general strength of Chapters 3-5 is the method of flexor digitorum superficialis landmarking for electromyography electrode and near infrared spectroscopy optode positioning. Unlike SENIAM (Surface ElectroMyoGraphy for the Non-Invasive Assessment of Muscles) (Hermens et al., 2000) guided placement of electromyography sensors for tibialis anterior muscle excitation measurement, the forearm does not have well established guidelines. Although previous studies have used manual palpation to locate the flexor digitorum superficialis (Broxterman et al., 2014; Hammer et al., 2020), this method does not provide consistent landmarking for repeated measurements. Accordingly, rather than using palpation to locate the flexor digitorum superficialis muscle bellies, we used guidance from dissected cadavers to locate the four flexor digitorum superficialis muscle bellies (Bickerton et al., 1997; Henzel et al., 2010; Munin et al., 2004). We then recorded the muscle excitation from each muscle belly individually and took the average of their excitation to reflect forearm muscle excitation. As opposed to a single EMG sensor, this method theoretically provides a better representation of forearm muscle excitation.

A second general strength of Chapters 3-5 is the concomitant measurement of muscle excitation, contraction force and most critically, forearm blood flow – a measurement often missing from electrically stimulated oxygen conforming work. This strength is highlighted by previous observations that a change in arm position (Bentley et al., 2014; Bentley et al., 2017) or pressor reflex mediated increase in blood pressure (Perrey et al., 2001) may not cause the intended change in forearm blood flow. Therefore, measurement of blood flow is critical to confirming oxygen delivery is in fact changing with the chosen methodology. A third general strength of Chapters 3-5, critical to demonstrating an oxygen conforming response, is the documented changes in muscle contraction force per excitation over time. Unlike previous voluntary human oxygen conforming work (Drouin et al., 2019; Hobbs & McCloskey, 1987), this approach gives us insight into the temporal adjustment of the oxygen conforming response during voluntary exercise.

Next, key strengths of Chapters 3 and 4 are the innovative methods used to assess the oxygen conforming response in vivo. A primary limitation of previous oxygen conforming work stems from the violation of key characteristics of voluntarily exercised muscle when muscle is electrically stimulated. A key strength of our experimental design in Chapter 3 was therefore the development of a model that would permit participants to achieve targeted voluntary muscle excitation. This model was used again in Chapter 4. A secondary limitation of previous electrically stimulated exercise designs originates from the use of arm position changes to alter exercising muscle perfusion pressure. Although previous work has attempted to control muscle length between positions, it is not possible to completely discount the potential for limb position differences to contribute to the observed muscle contraction force response. Therefore, in Chapter 3, we used manual brachial artery compression – a model similar to that previously developed in our laboratory (Pyke et al., 2004) – to control forearm blood flow. This approach is preferable to the typical limb position change models because (a) limb position is controlled thereby ensuring changes in excitation-contraction coupling are not due to limb position changes independent of blood flow, (b) unlike measuring blood flow during arm position transitions, blood flow measurements are more easily made under brachial artery compression conditions, and (c) unlike limb position change models, where compensatory vasodilation may occur (Bentley et al., 2014; Bentley et al., 2017), we could control and therefore achieve the same relative compromise to muscle blood flow and oxygenation across exercise intensities. Brachial artery compression therefore permitted the assessment of exercise intensity dependence of an oxygen conforming response at the same relative compromise to oxygen delivery. This dissertation work therefore supports the use of this novel manual brachial artery compression method in future investigations. Next, in Chapter 4, to again overcome some of the limitations of arm position change, we used a remote skeletal muscle metaboreflex to create a pressor reflex to increase forearm blood flow. This method helped us achieve the same benefits as highlighted by points (a) and (b) of brachial artery compression.

In Chapter 5, as opposed to previous critical force estimate work, which used the multiple constant load work rate method of critical force identification (Broxterman et al., 2014), we used a maximal effort exercise test. The benefit to using a maximal effort exercise test is that we can assess the effect of changes in oxygen delivery on maximal contraction force while exercise is ongoing – this permitted the identification of oxygen conforming contribution to maximal contraction force.

6.3 Limitations of thesis work

Handgrip exercise involves several different muscles; the flexor digitorum superficialis and profundus as well as stabilizing forearm extensor muscles. Measurement of the flexor digitorum profundus is complicated by superficial muscles and forearm extensor muscles do not contribute to handgrip force output. Therefore, as is commonplace in physiological research, the flexor digitorum superficialis was used as a proxy for forearm muscle excitation during handgrip exercise. Because of this, we must acknowledge that a change in flexor digitorum profundus muscle excitation relative to flexor digitorum superficialis excitation with altered oxygen delivery could conceivably result in altered contraction force during maintained flexor digitorum superficialis excitation that is not reflecting oxygen conforming. However, this would require selective reduction in excitation of the flexor digitorum profundus and its force over time with reduced oxygenation and subsequent rapid restoration of flexor digitorum profundus activation with restoration of oxygenation. Given that the entire forearm is experiencing the same oxygen delivery compromise, such a selective alteration of muscle excitation would be very unlikely.

A general limitation of Chapters 3-5 is the absence of a measurement of the metabolic environment. Therefore, we cannot confirm the third key oxygen conforming characteristic; that changes in muscle contraction force relative to muscle excitation were occurring without metabolic disturbance. In Chapter 4, a key limitation was the lack of power to assess separately the effect of an increase in oxygen delivery above 'normal' levels on (a) muscle contraction force per maintained muscle excitation and (b) muscle excitation per maintained muscle contraction force. To improve our power to detect a difference between hyperperfusion and control conditions, if one existed, we combined data from both the aforementioned methodological designs – this proved to be effective. A second limitation of Chapter 4 is the absence of counterbalancing of control and experimental conditions between participants. This approach was taken to ensure participants could effectively target muscle excitation or contraction force prior to adding concomitant dorsiflexion exercise – though, this invites an order effect. That muscle excitation per contraction force was only improved when blood flow was increased supports an O_2 conforming and not an order effect.

In Chapter 5, arm position changes could have contributed to muscle fiber length differences between arm positions – this could feasibly contribute to altered muscle contraction force independent of muscle excitation (Lloyd & Besier, 2003; Vigotsky et al., 2017). We observed no difference in the average of the first three contractions when comparing between arm positions. Therefore, if there were muscle fiber length differences, their contribution to the overall difference in muscle contraction force between conditions was small.

6.4 Directions for future research and Conclusion

Although this dissertation has focused on performance fatigability, future work should examine the ability of an oxygen conforming response to affect perceived fatigability – a key determinant of exercise tolerance. To effectively assess perceived fatigability, I recommend using a large muscle mass model, like the quadriceps, where I demonstrated in pilot testing that femoral artery compression could be effective at reducing leg blood flow. Critically, the third key characteristic of the oxygen conforming response – that muscle contraction force conforms to oxygen delivery to protect the metabolic environment – has yet to be replicated in a human model (Hogan et al., 1996). Therefore, future work should be directed at developing methodologies that would permit the assessment of this key characteristic in humans. Finally, this dissertation examined the oxygen conforming response in healthy university aged persons, therefore, future work should assess whether/how the oxygen conforming response affects exercise tolerance in age and disease.

In conclusion, this dissertation has developed and utilized novel methodologies to, for the first time, demonstrate that during voluntary human exercise the oxygen conforming response (a) exists, (b) is exercise intensity dependent, (c) can reversibly improve excitation-contraction coupling, (d) can modify the progressive decline of muscle contraction force, and (e) can rapidly shift the stabilized maximal muscle contraction critical force. These key findings highlight the underappreciated cellular disturbance independent role oxygen delivery can play in modifying exercise tolerance. This dissertation is only beginning to shed light on a phenomenon that – like skeletal muscle fatigue – deserves continued attention. Critically, this dissertation – highlighting the existence of an oxygen conforming response in voluntary human exercise – has set the stage for important future work into understanding (a) what its mechanisms are, (b) whether it exists and how it might affect exercise in age and disease, and (c) whether it can feasibly be improved with interventions.

References

Allen, D. G., & Trajanovska, S. (2012). The multiple roles of phosphate in muscle fatigue. *Front Physiol, 3*, 463. https://doi.org/10.3389/fphys.2012.00463

Amann, M., Eldridge, M. W., Lovering, A. T., Stickland, M. K., Pegelow, D. F., & Dempsey, J. A. (2006, Sep 15). Arterial oxygenation influences central motor output and exercise performance via effects on peripheral locomotor muscle fatigue in humans. *J Physiol, 575*(Pt 3), 937-952. https://doi.org/10.1113/jphysiol.2006.113936

Amann, M., Romer, L. M., Subudhi, A. W., Pegelow, D. F., & Dempsey, J. A. (2007, May 15). Severity of arterial hypoxaemia affects the relative contributions of peripheral muscle fatigue to exercise performance in healthy humans. *J Physiol, 581*(Pt 1), 389-403. https://doi.org/10.1113/jphysiol.2007.129700

Barclay, J. K., Boulianne, C. M., Wilson, B. A., & Tiffin, S. J. (1979, Nov). Interaction of hyperoxia and blood flow during fatigue of canine skeletal muscle in situ. *J Appl Physiol Respir Environ Exerc Physiol, 47*(5), 1018-1024. https://doi.org/10.1152/jappl.1979.47.5.1018

Barss, T. S., Ainsley, E. N., Claveria-Gonzalez, F. C., Luu, M. J., Miller, D. J., Wiest, M. J., & Collins, D. F. (2018, Apr). Utilizing Physiological Principles of Motor Unit Recruitment to Reduce Fatigability of Electrically-Evoked Contractions: A Narrative Review. *Arch Phys Med Rehabil, 99*(4), 779-791. https://doi.org/10.1016/j.apmr.2017.08.478

Barstow, T. J. (2019, May 1). Understanding near infrared spectroscopy and its application to skeletal muscle research. *J Appl Physiol (1985), 126*(5), 1360-1376. https://doi.org/10.1152/japplphysiol.00166.2018

Bawa, P., & Murnaghan, C. (2009, Oct). Motor unit rotation in a variety of human muscles. *J Neurophysiol, 102*(4), 2265-2272. https://doi.org/10.1152/jn.00278.2009

Bawa, P., Pang, M. Y., Olesen, K. A., & Calancie, B. (2006, Sep). Rotation of motoneurons during prolonged isometric contractions in humans. *J Neurophysiol, 96*(3), 1135-1140. https://doi.org/10.1152/jn.01063.2005

Beall, C. M. (2014). Adaptation to High Altitude: Phenotypes and Genotypes. *Annual Review of Anthropology, 43*(1), 251-272. https://doi.org/10.1146/annurev-anthro-102313-030000

Bellemare, F., Woods, J. J., Johansson, R., & Bigland-Ritchie, B. (1983, Dec). Motor-unit discharge rates in maximal voluntary contractions of three human muscles. *J Neurophysiol*, *50*(6), 1380-1392. https://doi.org/10.1152/jn.1983.50.6.1380

Bentley, R. F., Kellawan, J. M., Moynes, J. S., Poitras, V. J., Walsh, J. J., & Tschakovsky, M. E. (2014, Aug 15). Individual susceptibility to hypoperfusion and reductions in exercise performance when perfusion pressure is reduced: evidence for vasodilator phenotypes. *J Appl Physiol (1985)*, *117*(4), 392-405. https://doi.org/10.1152/japplphysiol.01155.2013

Bentley, R. F., Walsh, J. J., Drouin, P. J., Velickovic, A., Kitner, S. J., Fenuta, A. M., & Tschakovsky, M. E. (2017, Sep 1). Dietary nitrate restores compensatory vasodilation and exercise capacity in response to a compromise in oxygen delivery in the noncompensator phenotype. *J Appl Physiol (1985)*, *123*(3), 594-605. https://doi.org/10.1152/japplphysiol.00953.2016

Bergquist, A. J., Wiest, M. J., & Collins, D. F. (2012, Jul). Motor unit recruitment when neuromuscular electrical stimulation is applied over a nerve trunk compared with a muscle belly: quadriceps femoris. *J Appl Physiol (1985)*, *113*(1), 78-89. https://doi.org/10.1152/japplphysiol.00074.2011

Betik, A. C., & Hepple, R. T. (2008, Feb). Determinants of VO2 max decline with aging: an integrated perspective. *Appl Physiol Nutr Metab*, *33*(1), 130-140. https://doi.org/10.1139/H07-174

Bickerton, L. E., Agur, A. M. R., & Ashby, P. (1997). Flexor digitorum superficialis: Locations of individual muscle bellies for botulinum toxin injections. *Muscle & Nerve*, *20*(8), 1041-1043. https://doi.org/10.1002/(sici)1097-4598(199708)20:8<1041::Aid-mus18>3.0.Co;2-y

Black, M. I., Jones, A. M., Blackwell, J. R., Bailey, S. J., Wylie, L. J., McDonagh, S. T., Thompson, C., Kelly, J., Sumners, P., Mileva, K. N., Bowtell, J. L., & Vanhatalo, A. (2017, Mar 1). Muscle metabolic and neuromuscular determinants of fatigue during cycling in different exercise intensity domains. *J Appl Physiol (1985)*, *122*(3), 446-459. https://doi.org/10.1152/japplphysiol.00942.2016

Brotto, M. A., Andreatta-van Leyen, S., Nosek, C. M., Brotto, L. S., & Nosek, T. M. (2000, Sep). Hypoxia and fatigue-induced modification of function and proteins in intact and skinned murine diaphragm muscle. *Pflugers Arch*, *440*(5), 727-734. https://doi.org/10.1007/s004240000327

Broxterman, R. M., Ade, C. J., Wilcox, S. L., Schlup, S. J., Craig, J. C., & Barstow, T. J. (2014, Feb 1). Influence of duty cycle on the power-duration relationship:

observations and potential mechanisms. *Respir Physiol Neurobiol*, *192*, 102-111. https://doi.org/10.1016/j.resp.2013.11.010

Broxterman, R. M., Craig, J. C., Smith, J. R., Wilcox, S. L., Jia, C., Warren, S., & Barstow, T. J. (2015, Sep 1). Influence of blood flow occlusion on the development of peripheral and central fatigue during small muscle mass handgrip exercise. *J Physiol*, *593*(17), 4043-4054. https://doi.org/10.1113/JP270424

Broxterman, R. M., Layec, G., Hureau, T. J., Amann, M., & Richardson, R. S. (2017, May 1). Skeletal muscle bioenergetics during all-out exercise: mechanistic insight into the oxygen uptake slow component and neuromuscular fatigue. *J Appl Physiol (1985)*, *122*(5), 1208-1217. https://doi.org/10.1152/japplphysiol.01093.2016

Burnley, M. (2009, Mar). Estimation of critical torque using intermittent isometric maximal voluntary contractions of the quadriceps in humans. *J Appl Physiol (1985)*, *106*(3), 975-983. https://doi.org/10.1152/japplphysiol.91474.2008

Burnley, M., Vanhatalo, A., Fulford, J., & Jones, A. M. (2010, Jul). Similar metabolic perturbations during all-out and constant force exhaustive exercise in humans: a (31)P magnetic resonance spectroscopy study. *Exp Physiol*, *95*(7), 798-807. https://doi.org/10.1113/expphysiol.2010.052688

Burnley, M., Vanhatalo, A., & Jones, A. M. (2012, Jul). Distinct profiles of neuromuscular fatigue during muscle contractions below and above the critical torque in humans. *J Appl Physiol (1985)*, *113*(2), 215-223. https://doi.org/10.1152/japplphysiol.00022.2012

Carson, R. G., Riek, S., & Shahbazpour, N. (2002, Mar 15). Central and peripheral mediation of human force sensation following eccentric or concentric contractions. *J Physiol*, *539*(Pt 3), 913-925. https://doi.org/10.1113/jphysiol.2001.013385

Cohen, C. C. H., Popovic, M. A., Klooster, J., Weil, M. T., Mobius, W., Nave, K. A., & Kole, M. H. P. (2020, Jan 23). Saltatory Conduction along Myelinated Axons Involves a Periaxonal Nanocircuit. *Cell*, *180*(2), 311-322 e315. https://doi.org/10.1016/j.cell.2019.11.039

Crewe, H., Tucker, R., & Noakes, T. D. (2008, Jul). The rate of increase in rating of perceived exertion predicts the duration of exercise to fatigue at a fixed power output in different environmental conditions. *Eur J Appl Physiol*, *103*(5), 569-577. https://doi.org/10.1007/s00421-008-0741-7

Dalton, B. H., Harwood, B., Davidson, A. W., & Rice, C. L. (2009, Dec). Triceps surae contractile properties and firing rates in the soleus of young and old men. *J Appl*

Physiol (1985), *107*(6), 1781-1788. https://doi.org/10.1152/japplphysiol.00464.2009

de Morree, H. M., Klein, C., & Marcora, S. M. (2012, Sep). Perception of effort reflects central motor command during movement execution. *Psychophysiology*, *49*(9), 1242-1253. https://doi.org/10.1111/j.1469-8986.2012.01399.x

Dean, E. (1997, Feb). Oxygen transport deficits in systemic disease and implications for physical therapy. *Phys Ther*, *77*(2), 187-202. https://doi.org/10.1093/ptj/77.2.187

Debold, E. P. (2016, Oct). Decreased Myofilament Calcium Sensitivity Plays a Significant Role in Muscle Fatigue. *Exerc Sport Sci Rev*, *44*(4), 144-149. https://doi.org/10.1249/JES.0000000000000089

Debold, E. P., Romatowski, J., & Fitts, R. H. (2006, Apr). The depressive effect of Pi on the force-pCa relationship in skinned single muscle fibers is temperature dependent. *Am J Physiol Cell Physiol*, *290*(4), C1041-1050. https://doi.org/10.1152/ajpcell.00342.2005

Dietrich, H. H., Ellsworth, M. L., Sprague, R. S., & Dacey, R. G., Jr. (2000, Apr). Red blood cell regulation of microvascular tone through adenosine triphosphate. *Am J Physiol Heart Circ Physiol*, *278*(4), H1294-1298. https://doi.org/10.1152/ajpheart.2000.278.4.H1294

Drouin, P. J., Forbes, S. P. A., Liu, T., Lew, L. A., McGarity-Shipley, E., & Tschakovsky, M. E. (2022, Nov). Muscle contraction force conforms to muscle oxygenation during constant-activation voluntary forearm exercise. *Exp Physiol*, *107*(11), 1360-1374. https://doi.org/10.1113/EP090576

Drouin, P. J., Kohoko, Z. I. N., Mew, O. K., Lynn, M. J. T., Fenuta, A. M., & Tschakovsky, M. E. (2019, Jul 1). Fatigue-independent alterations in muscle activation and effort perception during forearm exercise: role of local oxygen delivery. *J Appl Physiol (1985)*, *127*(1), 111-121. https://doi.org/10.1152/japplphysiol.00122.2019

Drouin, P. J., Liu, T., Lew, L. A., McGarity-Shipley, E., & Tschakovsky, M. E. (2023, Feb). The 'normal' adjustment of oxygen delivery to small muscle mass exercise is not optimized for muscle contractile function. *J Physiol*, *601*(4), 783-799. https://doi.org/10.1113/JP283933

Dutka, T. L., Cole, L., & Lamb, G. D. (2005, Dec). Calcium phosphate precipitation in the sarcoplasmic reticulum reduces action potential-mediated Ca2+ release in mammalian skeletal muscle. *Am J Physiol Cell Physiol*, *289*(6), C1502-1512. https://doi.org/10.1152/ajpcell.00273.2005

Egana, M., Ryan, K., Warmington, S. A., & Green, S. (2010, Mar). Effect of body tilt angle on fatigue and EMG activities in lower limbs during cycling. *Eur J Appl Physiol*, *108*(4), 649-656. https://doi.org/10.1007/s00421-009-1254-8

Ellsworth, M. L., Forrester, T., Ellis, C. G., & Dietrich, H. H. (1995, Dec). The erythrocyte as a regulator of vascular tone. *American Journal of Physiology-Heart and Circulatory Physiology*, *269*(6), H2155-H2161. https://doi.org/DOI 10.1152/ajpheart.1995.269.6.H2155

Erecinska, M., & Wilson, D. F. (1982). Regulation of cellular energy metabolism. *J Membr Biol*, *70*(1), 1-14. https://doi.org/10.1007/BF01871584

Eston, R., Faulkner, J., St Clair Gibson, A., Noakes, T., & Parfitt, G. (2007, Sep). The effect of antecedent fatiguing activity on the relationship between perceived exertion and physiological activity during a constant load exercise task. *Psychophysiology*, *44*(5), 779-786. https://doi.org/10.1111/j.1469-8986.2007.00558.x

Farina, D., Merletti, R., & Enoka, R. M. (2014, Dec 1). The extraction of neural strategies from the surface EMG: an update. *J Appl Physiol (1985)*, *117*(11), 1215-1230. https://doi.org/10.1152/japplphysiol.00162.2014

Fenuta, A. M., Drouin, P. J., Kohoko, Z. I. N., Lynn, M. J. T., & Tschakovsky, M. E. (2023, Apr 1). Does a single bout maximal effort forearm exercise test for determining critical impulse result in maximal oxygen delivery and consumption in men? A randomized crossover trial. *Appl Physiol Nutr Metab*, *48*(4), 293-306. https://doi.org/10.1139/apnm-2022-0317

Fitzpatrick, R., Taylor, J. L., & McCloskey, D. I. (1996). Effects of arterial perfusion pressure on force production in working human hand muscles. *J Physiol*, *495*(Pt 3), 885-891.

Fontaine, K. R. (2000, Oct). Physical activity improves mental health. *Phys Sportsmed*, *28*(10), 83-84. https://doi.org/10.3810/psm.2000.10.1256

Fulco, C. S., Lewis, S. F., Frykman, P. N., Boushel, R., Smith, S., Harman, E. A., Cymerman, A., & Pandolf, K. B. (1996, Nov). Muscle fatigue and exhaustion during dynamic leg exercise in normoxia and hypobaric hypoxia. *J Appl Physiol (1985)*, *81*(5), 1891-1900. https://doi.org/10.1152/jappl.1996.81.5.1891

Ganjeh, P., Meyer, T., Hagmayer, Y., Kuhnert, R., Ravens-Sieberer, U., von Steinbuechel, N., Rothenberger, A., & Becker, A. (2021, Feb 24). Physical Activity Improves Mental Health in Children and Adolescents Irrespective of the Diagnosis of

Attention Deficit Hyperactivity Disorder (ADHD)-A Multi-Wave Analysis Using Data from the KiGGS Study. *Int J Environ Res Public Health, 18*(5). https://doi.org/10.3390/ijerph18052207

Gonzalez-Alonso, J., Olsen, D. B., & Saltin, B. (2002, Nov 29). Erythrocyte and the regulation of human skeletal muscle blood flow and oxygen delivery: role of circulating ATP. *Circ Res, 91*(11), 1046-1055. https://doi.org/10.1161/01.res.0000044939.73286.e2

Gonzalez-Alonso, J., Richardson, R. S., & Saltin, B. (2001, Jan 15). Exercising skeletal muscle blood flow in humans responds to reduction in arterial oxyhaemoglobin, but not to altered free oxygen. *J Physiol, 530*(Pt 2), 331-341. https://doi.org/10.1111/j.1469-7793.2001.0331l.x

Goulding, R. P., Roche, D. M., & Marwood, S. (2019). Hyperoxia speeds pulmonary oxygen uptake kinetics and increases critical power during supine cycling. *Exp Physiol, 104*(7), 1061-1073.

Goulding, R. P., Roche, D. M., & Marwood, S. (2020, May). Effect of Hyperoxia on Critical Power and V O2 Kinetics during Upright Cycling. *Med Sci Sports Exerc, 52*(5), 1041-1049. https://doi.org/10.1249/MSS.0000000000002234

Hammer, S. M., Alexander, A. M., Didier, K. D., & Barstow, T. J. (2020, Jul 28). Influence of blood flow occlusion on muscular recruitment and fatigue during maximal-effort small muscle-mass exercise. *J Physiol*. https://doi.org/10.1113/JP279925

Hansen, A. B., Moralez, G., Amin, S. B., Hofstatter, F., Simpson, L. L., Gasho, C., Tymko, M. M., Ainslie, P. N., Lawley, J. S., & Hearon, C. M., Jr. (2022, Aug). Global REACH 2018: increased adrenergic restraint of blood flow preserves coupling of oxygen delivery and demand during exercise at high-altitude. *J Physiol, 600*(15), 3483-3495. https://doi.org/10.1113/JP282972

Hartline, D. K., & Colman, D. R. (2007, Jan 9). Rapid conduction and the evolution of giant axons and myelinated fibers. *Curr Biol, 17*(1), R29-35. https://doi.org/10.1016/j.cub.2006.11.042

Haseler, L. J., Richardson, R. S., Videen, J. S., & Hogan, M. C. (1998, Oct). Phosphocreatine hydrolysis during submaximal exercise: the effect of FIO2. *J Appl Physiol (1985), 85*(4), 1457-1463. https://doi.org/10.1152/jappl.1998.85.4.1457

Henneman, E. (1985, Mar). The size-principle: a deterministic output emerges from a set of probabilistic connections. *J Exp Biol, 115*, 105-112. https://www.ncbi.nlm.nih.gov/pubmed/3161974

Henneman, E., Somjen, G., & Carpenter, D. O. (1965, May). Functional Significance of Cell Size in Spinal Motoneurons. *J Neurophysiol*, *28*, 560-580. https://doi.org/10.1152/jn.1965.28.3.560

Henzel, M. K., Munin, M. C., Niyonkuru, C., Skidmore, E. R., Weber, D. J., & Zafonte, R. D. (2010, Jul). Comparison of surface and ultrasound localization to identify forearm flexor muscles for botulinum toxin injections. *PM R*, *2*(7), 642-646. https://doi.org/10.1016/j.pmrj.2010.05.002

Hermens, H. J., Freriks, B., Disselhorst-Klug, C., & Rau, G. (2000, Oct). Development of recommendations for SEMG sensors and sensor placement procedures. *J Electromyogr Kinesiol*, *10*(5), 361-374. https://doi.org/10.1016/s1050-6411(00)00027-4

Hess, C. N., Kou, R., Johnson, R. P., Li, G. K., & Michel, T. (2009, Nov 20). ADP signaling in vascular endothelial cells: ADP-dependent activation of the endothelial isoform of nitric-oxide synthase requires the expression but not the kinase activity of AMP-activated protein kinase. *J Biol Chem*, *284*(47), 32209-32224. https://doi.org/10.1074/jbc.M109.032656

Hill, D. W. (1993, Oct). The critical power concept. A review. *Sports Med*, *16*(4), 237-254. https://doi.org/10.2165/00007256-199316040-00003

Hirvonen, L., & Sonnenschein, R. R. (1962, Jan). Relation between blood flow and contraction force in active skeletal muscle. *Circ Res*, *10*, 94-104. https://doi.org/10.1161/01.res.10.1.94

Ho, F. K., Louie, L. H., Chow, C. B., Wong, W. H., & Ip, P. (2015, Apr 22). Physical activity improves mental health through resilience in Hong Kong Chinese adolescents. *BMC Pediatr*, *15*, 48. https://doi.org/10.1186/s12887-015-0365-0

Hobbs, S. F., & McCloskey, D. I. (1987). Effects of blood pressure on force production in cat and human muscle. *J Appl Physiol (1985)*, *63*(2), 834-839.

Hogan, M. C., Arthur, P. G., Bebout, D. E., Hochachka, P. W., & Wagner, P. D. (1992, Aug). Role of O2 in regulating tissue respiration in dog muscle working in situ. *J Appl Physiol (1985)*, *73*(2), 728-736. https://doi.org/10.1152/jappl.1992.73.2.728

Hogan, M. C., Cox, R. H., & Welch, H. G. (1983, Oct). Lactate accumulation during incremental exercise with varied inspired oxygen fractions. *J Appl Physiol Respir Environ Exerc Physiol*, *55*(4), 1134-1140. https://doi.org/10.1152/jappl.1983.55.4.1134

Hogan, M. C., Gladden, L. B., Grassi, B., Stary, C. M., & Samaja, M. (1998, Jun). Bioenergetics of contracting skeletal muscle after partial reduction of blood flow. *J Appl Physiol (1985)*, *84*(6), 1882-1888. https://doi.org/10.1152/jappl.1998.84.6.1882

Hogan, M. C., Kohin, S., Stary, C. M., & Hepple, R. T. (1999). Rapid force recovery in contracting skeletal muscle after brief ischemia is dependent on O2 availability. *J Appl Physiol (1985)*, *87*(6), 2225-2229.

Hogan, M. C., Kurdak, S. S., & Arthur, P. G. (1996). Effect of gradual reduction in O2 delivery on intracellular homeostasis in contracting skeletal muscle. *J Appl Physiol (1985)*, *80*(4), 1313-1321.

Hogan, M. C., Nioka, S., Brechue, W. F., & Chance, B. (1992, Oct). A 31P-NMR study of tissue respiration in working dog muscle during reduced O2 delivery conditions. *J Appl Physiol (1985)*, *73*(4), 1662-1670. https://doi.org/10.1152/jappl.1992.73.4.1662

Hogan, M. C., Richardson, R. S., & Haseler, L. J. (1999, Apr). Human muscle performance and PCr hydrolysis with varied inspired oxygen fractions: a 31P-MRS study. *J Appl Physiol (1985)*, *86*(4), 1367-1373. https://doi.org/10.1152/jappl.1999.86.4.1367

Hogg, R. C., Raggenbass, M., & Bertrand, D. (2003). Nicotinic acetylcholine receptors: from structure to brain function. *Rev Physiol Biochem Pharmacol*, *147*, 1-46. https://doi.org/10.1007/s10254-003-0005-1

Holodny, A. I., Gor, D. M., Watts, R., Gutin, P. H., & Ulug, A. M. (2005, Mar). Diffusion-tensor MR tractography of somatotopic organization of corticospinal tracts in the internal capsule: initial anatomic results in contradistinction to prior reports. *Radiology*, *234*(3), 649-653. https://doi.org/10.1148/radiol.2343032087

Hunter, S. K. (2018, Jul 2). Performance Fatigability: Mechanisms and Task Specificity. *Cold Spring Harb Perspect Med*, *8*(7). https://doi.org/10.1101/cshperspect.a029728

Jones, A. M., Vanhatalo, A., Burnley, M., Morton, R. H., & Poole, D. C. (2010, Oct). Critical power: implications for determination of V O2max and exercise tolerance. *Med Sci Sports Exerc*, *42*(10), 1876-1890. https://doi.org/10.1249/MSS.0b013e3181d9cf7f

Jones, A. M., Wilkerson, D. P., DiMenna, F., Fulford, J., & Poole, D. C. (2008, Feb). Muscle metabolic responses to exercise above and below the "critical power" assessed using 31P-MRS. *Am J Physiol Regul Integr Comp Physiol*, *294*(2), R585-593. https://doi.org/10.1152/ajpregu.00731.2007

Katayama, K., Amann, M., Pegelow, D. F., Jacques, A. J., & Dempsey, J. A. (2007, Mar). Effect of arterial oxygenation on quadriceps fatigability during isolated muscle exercise. *Am J Physiol Regul Integr Comp Physiol*, *292*(3), R1279-1286. https://doi.org/10.1152/ajpregu.00554.2006

Kellawan, J. M., & Tschakovsky, M. E. (2014). The single-bout forearm critical force test: a new method to establish forearm aerobic metabolic exercise intensity and capacity. *PLoS One*, *9*(4), e93481. https://doi.org/10.1371/journal.pone.0093481

Knapen, J., Vancampfort, D., Morien, Y., & Marchal, Y. (2015). Exercise therapy improves both mental and physical health in patients with major depression. *Disabil Rehabil*, *37*(16), 1490-1495. https://doi.org/10.3109/09638288.2014.972579

Korzeniewski, B. (2023, Jan). Sensitivity of $\dot{V}$O(2max), critical power and $\dot{V}$O(2) on-kinetics to O(2) concentration/delivery and other factors in skeletal muscle. *Respir Physiol Neurobiol*, *307*, 103977. https://doi.org/10.1016/j.resp.2022.103977

Korzeniewski, B., & Rossiter, H. B. (2020, Jul). Exceeding a "critical" muscle P(i): implications for VO2 and metabolite slow components, muscle fatigue and the power-duration relationship. *Eur J Appl Physiol*, *120*(7), 1609-1619. https://doi.org/10.1007/s00421-020-04388-4

Larkum, M. E., Launey, T., Dityatev, A., & Luscher, H. R. (1998, Aug). Integration of excitatory postsynaptic potentials in dendrites of motoneurons of rat spinal cord slice cultures. *J Neurophysiol*, *80*(2), 924-935. https://doi.org/10.1152/jn.1998.80.2.924

Lloyd, D. G., & Besier, T. F. (2003, Jun). An EMG-driven musculoskeletal model to estimate muscle forces and knee joint moments in vivo. *J Biomech*, *36*(6), 765-776. https://doi.org/10.1016/s0021-9290(03)00010-1

Lou, J. W., Bergquist, A. J., Aldayel, A., Czitron, J., & Collins, D. F. (2017, Feb). Interleaved neuromuscular electrical stimulation reduces muscle fatigue. *Muscle Nerve*, *55*(2), 179-189. https://doi.org/10.1002/mus.25224

Luu, B. L., & Fitzpatrick, R. C. (2013, Nov 1). Blood pressure and the contractility of a human leg muscle. *J Physiol*, *591*(21), 5401-5412. https://doi.org/10.1113/jphysiol.2013.261107

Magee, J. C., & Johnston, D. (1995, Apr 14). Synaptic activation of voltage-gated channels in the dendrites of hippocampal pyramidal neurons. *Science, 268*(5208), 301-304. https://doi.org/10.1126/science.7716525

McKeown, D. J., McNeil, C. J., Brotherton, E. J., Simmonds, M. J., & Kavanagh, J. J. (2021, Dec). Severe acute hypoxia impairs recovery of voluntary muscle activation after sustained submaximal elbow flexion. *J Physiol, 599*(24), 5379-5395. https://doi.org/10.1113/JP281897

Milner-Brown, H. S., Stein, R. B., & Yemm, R. (1973, Apr). The orderly recruitment of human motor units during voluntary isometric contractions. *J Physiol, 230*(2), 359-370. https://doi.org/10.1113/jphysiol.1973.sp010192

Mochida, S. (2019, May 6). Presynaptic Calcium Channels. *Int J Mol Sci, 20*(9). https://doi.org/10.3390/ijms20092217

Mougios, V. (2006). *Exercise Biochemistry*. Human Kinetics. https://books.google.ca/books?id=udCMDwAAQBAJ

Mougios, V. (2020). *Exercise Biochemistry* (Second Edition ed.). https://doi.org/10.5040/9781492595496

Moynes, J., Bentley, R. F., Bravo, M., Kellawan, J. M., & Tschakovsky, M. E. (2013). Persistence of functional sympatholysis post-exercise in human skeletal muscle. *Front Physiol, 4*, 131. https://doi.org/10.3389/fphys.2013.00131

Munin, M. C., Navalgund, B. K., Levitt, D. A., Breisinger, T. P., & Zafonte, R. D. (2004, Apr). Novel approach to the application of botulinum toxin to the flexor digitorum superficialis muscle in acquired brain injury. *Brain Inj, 18*(4), 403-407. https://doi.org/10.1080/02699050310001617334

Nakamura, F. Y., Okuno, N. M., Perandini, L. A., LF, S. C., Simoes, H. G., Cardoso, J. R., & Bishop, D. J. (2008, May). Critical power can be estimated from nonexhaustive tests based on rating of perceived exertion responses. *J Strength Cond Res, 22*(3), 937-943. https://doi.org/10.1519/JSC.0b013e31816a41fa

Nyberg, M., & Jones, A. M. (2022). Matching of O2 Utilization and O2 Delivery in Contracting Skeletal Muscle in Health, Aging, and Heart Failure. *Front Physiol, 13*, 898395. https://doi.org/10.3389/fphys.2022.898395

Olson, C. B., Carpenter, D. O., & Henneman, E. (1968, Dec). Orderly recruitment of muscle action potentials. *Arch Neurol, 19*(6), 591-597. https://doi.org/10.1001/archneur.1968.00480060061008

Parsons, B., Szczesna, D., Zhao, J., Van Slooten, G., Kerrick, W. G., Putkey, J. A., & Potter, J. D. (1997, Oct). The effect of pH on the Ca2+ affinity of the Ca2+ regulatory sites of skeletal and cardiac troponin C in skinned muscle fibres. *J Muscle Res Cell Motil, 18*(5), 599-609. https://doi.org/10.1023/a:1018623604365

Pawelczyk, J. A., Hanel, B., Pawelczyk, R. A., Warberg, J., & Secher, N. H. (1992, Nov). Leg vasoconstriction during dynamic exercise with reduced cardiac output. *J Appl Physiol (1985), 73*(5), 1838-1846. https://doi.org/10.1152/jappl.1992.73.5.1838

Perotto, A., & Delagi, E. F. (1994). *Anatomical guide for the electromyographer: the limbs and trunk* (r. ed., Ed.). Springfield, Ill., USA : Charles C. Thomas.

Perrey, S., Tschakovsky, M. E., & Hughson, R. L. (2001, Nov). Muscle chemoreflex elevates muscle blood flow and O2 uptake at exercise onset in nonischemic human forearm. *J Appl Physiol (1985), 91*(5), 2010-2016. https://doi.org/10.1152/jappl.2001.91.5.2010

Pitcher, J. B., & Miles, T. S. (1997, Jul). Influence of muscle blood flow on fatigue during intermittent human hand-grip exercise and recovery. *Clin Exp Pharmacol Physiol, 24*(7), 471-476. https://doi.org/10.1111/j.1440-1681.1997.tb01229.x

Pivovarov, A. S., Calahorro, F., & Walker, R. J. (2018, Nov 28). Na(+)/K(+)-pump and neurotransmitter membrane receptors. *Invert Neurosci, 19*(1), 1. https://doi.org/10.1007/s10158-018-0221-7

Poole, D. C., Barstow, T. J., McDonough, P., & Jones, A. M. (2008, Mar). Control of oxygen uptake during exercise. *Med Sci Sports Exerc, 40*(3), 462-474. https://doi.org/10.1249/MSS.0b013e31815ef29b

Poole, D. C., Burnley, M., Vanhatalo, A., Rossiter, H. B., & Jones, A. M. (2016, Nov). Critical Power: An Important Fatigue Threshold in Exercise Physiology. *Med Sci Sports Exerc, 48*(11), 2320-2334. https://doi.org/10.1249/MSS.0000000000000939

Poole, D. C., Ward, S. A., Gardner, G. W., & Whipp, B. J. (1988, Sep). Metabolic and respiratory profile of the upper limit for prolonged exercise in man. *Ergonomics, 31*(9), 1265-1279. https://doi.org/10.1080/00140138808966766

Proctor, D. N., Koch, D. W., Newcomer, S. C., Le, K. U., Smithmyer, S. L., & Leuenberger, U. A. (2004, Apr). Leg blood flow and VO2 during peak cycle exercise in younger and older women. *Med Sci Sports Exerc, 36*(4), 623-631. https://doi.org/10.1249/01.mss.0000121951.10417.b5

Proctor, D. N., Shen, P. H., Dietz, N. M., Eickhoff, T. J., Lawler, L. A., Ebersold, E. J., Loeffler, D. L., & Joyner, M. J. (1998, Jul). Reduced leg blood flow during dynamic exercise in older endurance-trained men. *J Appl Physiol (1985)*, *85*(1), 68-75. https://doi.org/10.1152/jappl.1998.85.1.68

Pyke, K. E., Dwyer, E. M., & Tschakovsky, M. E. (2004, Aug). Impact of controlling shear rate on flow-mediated dilation responses in the brachial artery of humans. *J Appl Physiol (1985)*, *97*(2), 499-508. https://doi.org/10.1152/japplphysiol.01245.2003

Radegran, G. (1997, Oct). Ultrasound Doppler estimates of femoral artery blood flow during dynamic knee extensor exercise in humans. *J Appl Physiol (1985)*, *83*(4), 1383-1388. https://doi.org/10.1152/jappl.1997.83.4.1383

Richardson, R. S., Kennedy, B., Knight, D. R., & Wagner, P. D. (1995, Nov). High muscle blood flows are not attenuated by recruitment of additional muscle mass. *Am J Physiol*, *269*(5 Pt 2), H1545-1552. https://doi.org/10.1152/ajpheart.1995.269.5.H1545

Romer, L. M., & Dempsey, J. A. (2006, Apr). Effects of exercise-induced arterial hypoxaemia on limb muscle fatigue and performance. *Clin Exp Pharmacol Physiol*, *33*(4), 391-394. https://doi.org/10.1111/j.1440-1681.2006.04361.x

Romer, L. M., Haverkamp, H. C., Lovering, A. T., Pegelow, D. F., & Dempsey, J. A. (2006, Feb). Effect of exercise-induced arterial hypoxemia on quadriceps muscle fatigue in healthy humans. *Am J Physiol Regul Integr Comp Physiol*, *290*(2), R365-375. https://doi.org/10.1152/ajpregu.00332.2005

Rothman, K. J. (1990). No Adjustments Are Needed for Multiple Comparisons. *Epidemiology*, *1*(1), 43-46.

Ruggiero, L., Hoiland, R. L., Hansen, A. B., Ainslie, P. N., & McNeil, C. J. (2020, Jan). High-Altitude Acclimatization Improves Recovery from Muscle Fatigue. *Med Sci Sports Exerc*, *52*(1), 161-169. https://doi.org/10.1249/MSS.0000000000002100

Ryan, T. E., Erickson, M. L., Brizendine, J. T., Young, H. J., & McCully, K. K. (2012, Jul). Noninvasive evaluation of skeletal muscle mitochondrial capacity with near-infrared spectroscopy: correcting for blood volume changes. *J Appl Physiol (1985)*, *113*(2), 175-183. https://doi.org/10.1152/japplphysiol.00319.2012

Simpson, L. P., Jones, A. M., Skiba, P. F., Vanhatalo, A., & Wilkerson, D. (2015, Feb). Influence of hypoxia on the power-duration relationship during high-intensity exercise. *Int J Sports Med*, *36*(2), 113-119. https://doi.org/10.1055/s-0034-1389943

Soloviev, A. I., & Basilyuk, O. V. (1993, May). Evidence for decrease in myofilament responsiveness to Ca2+ during hypoxia in spontaneously active vascular smooth muscle in rats. *Exp Physiol*, *78*(3), 395-402. https://doi.org/10.1113/expphysiol.1993.sp003693

Sousa, A. C., Millet, G. P., Viana, J., Milheiro, J., & Reis, V. (2021, Jun). Effects of Normobaric Hypoxia on Matched-severe Exercise and Power-duration Relationship. *Int J Sports Med*, *42*(8), 708-715. https://doi.org/10.1055/a-1236-3953

Staiano, W., Bosio, A., de Morree, H. M., Rampinini, E., & Marcora, S. (2018). The cardinal exercise stopper: Muscle fatigue, muscle pain or perception of effort? *Prog Brain Res*, *240*, 175-200. https://doi.org/10.1016/bs.pbr.2018.09.012

Szubski, C., Burtscher, M., & Loscher, W. N. (2007, Jun). Neuromuscular fatigue during sustained contractions performed in short-term hypoxia. *Med Sci Sports Exerc*, *39*(6), 948-954. https://doi.org/10.1249/mss.0b013e3180479918

Therien, A. G., & Blostein, R. (2000, Sep). Mechanisms of sodium pump regulation. *Am J Physiol Cell Physiol*, *279*(3), C541-566. https://doi.org/10.1152/ajpcell.2000.279.3.C541

Thorsteinsdottir, H., Diseth, T. H., Lie, A., Tangeraas, T., Matthews, I., Asberg, A., & Bjerre, A. (2018, Jun 19). Small effort, high impact: Focus on physical activity improves oxygen uptake (VO(2peak)), quality of life, and mental health after pediatric renal transplantation. *Pediatr Transplant*, e13242. https://doi.org/10.1111/petr.13242

Tschakovsky, M. E., & Hughson, R. L. (1999, Aug). Ischemic muscle chemoreflex response elevates blood flow in nonischemic exercising human forearm muscle. *Am J Physiol*, *277*(2), H635-642. https://doi.org/10.1152/ajpheart.1999.277.2.H635

Van Cutsem, M., Feiereisen, P., Duchateau, J., & Hainaut, K. (1997, Dec). Mechanical properties and behaviour of motor units in the tibialis anterior during voluntary contractions. *Can J Appl Physiol*, *22*(6), 585-597. https://doi.org/10.1139/h97-038

van der Zee, P., Cope, M., Arridge, S. R., Essenpreis, M., Potter, L. A., Edwards, A. D., Wyatt, J. S., McCormick, D. C., Roth, S. C., Reynolds, E. O., & al., e. (1992). Experimentally measured optical pathlengths for the adult head, calf and forearm and the head of the newborn infant as a function of inter optode spacing. *Adv Exp Med Biol*, *316*, 143-153. https://doi.org/10.1007/978-1-4615-3404-4_17

Vanhatalo, A., Doust, J. H., & Burnley, M. (2007, Mar). Determination of critical power using a 3-min all-out cycling test. *Med Sci Sports Exerc*, *39*(3), 548-555. https://doi.org/10.1249/mss.0b013e31802dd3e6

Vanhatalo, A., Fulford, J., DiMenna, F. J., & Jones, A. M. (2010, Apr). Influence of hyperoxia on muscle metabolic responses and the power-duration relationship during severe-intensity exercise in humans: a 31P magnetic resonance spectroscopy study. *Exp Physiol*, *95*(4), 528-540. https://doi.org/10.1113/expphysiol.2009.050500

Vanhatalo, A., Poole, D. C., DiMenna, F. J., Bailey, S. J., & Jones, A. M. (2011, Mar). Muscle fiber recruitment and the slow component of O2 uptake: constant work rate vs. all-out sprint exercise. *Am J Physiol Regul Integr Comp Physiol*, *300*(3), R700-707. https://doi.org/10.1152/ajpregu.00761.2010

Venhorst, A., Micklewright, D., & Noakes, T. D. (2018a, Nov). Perceived Fatigability: Utility of a Three-Dimensional Dynamical Systems Framework to Better Understand the Psychophysiological Regulation of Goal-Directed Exercise Behaviour. *Sports Med*, *48*(11), 2479-2495. https://doi.org/10.1007/s40279-018-0986-1

Venhorst, A., Micklewright, D., & Noakes, T. D. (2018b, Aug). Towards a three-dimensional framework of centrally regulated and goal-directed exercise behaviour: a narrative review. *Br J Sports Med*, *52*(15), 957-966. https://doi.org/10.1136/bjsports-2016-096907

Vigotsky, A. D., Halperin, I., Lehman, G. J., Trajano, G. S., & Vieira, T. M. (2017). Interpreting Signal Amplitudes in Surface Electromyography Studies in Sport and Rehabilitation Sciences. *Front Physiol*, *8*, 985. https://doi.org/10.3389/fphys.2017.00985

Walker, K. L., Saunders, N. R., Jensen, D., Kuk, J. L., Wong, S. L., Pyke, K. E., Dwyer, E. M., & Tschakovsky, M. E. (2007, Nov). Do vasoregulatory mechanisms in exercising human muscle compensate for changes in arterial perfusion pressure? *Am J Physiol Heart Circ Physiol*, *293*(5), H2928-2936. https://doi.org/10.1152/ajpheart.00576.2007

Wasserman, D. (2019, Jun). Physical activity improves mental health. *Acta Paediatr*, *108*(6), 984-985. https://doi.org/10.1111/apa.14772

Westerblad, H., & Allen, D. G. (1996, Apr). The effects of intracellular injections of phosphate on intracellular calcium and force in single fibres of mouse skeletal muscle. *Pflugers Arch*, *431*(6), 964-970. https://www.ncbi.nlm.nih.gov/pubmed/8927516

Westerblad, H., Duty, S., & Allen, D. G. (1993, Jul). Intracellular calcium concentration during low-frequency fatigue in isolated single fibers of mouse skeletal muscle. *J Appl Physiol (1985)*, *75*(1), 382-388. https://doi.org/10.1152/jappl.1993.75.1.382

Wilson, D. F., & Erecinska, M. (1985, Oct). Effect of oxygen concentration on cellular metabolism. *Chest*, *88*(4 Suppl), 229S-232S. https://doi.org/10.1378/chest.88.4_supplement.229s

Wilson, D. F., Erecinska, M., Drown, C., & Silver, I. A. (1979, Jul). The oxygen dependence of cellular energy metabolism. *Arch Biochem Biophys*, *195*(2), 485-493. https://doi.org/10.1016/0003-9861(79)90375-8

Wright, J. R., McCloskey, D. I., & Fitzpatrick, R. C. (1999, Mar). Effects of muscle perfusion pressure on fatigue and systemic arterial pressure in human subjects. *J Appl Physiol (1985)*, *86*(3), 845-851. https://doi.org/10.1152/jappl.1999.86.3.845

Wright, J. R., McCloskey, D. I., & Fitzpatrick, R. C. (2000, Apr). Effects of systemic arterial blood pressure on the contractile force of a human hand muscle. *J Appl Physiol (1985)*, *88*(4), 1390-1396. https://doi.org/10.1152/jappl.2000.88.4.1390

Zajac, F. E., & Faden, J. S. (1985, May). Relationship among recruitment order, axonal conduction velocity, and muscle-unit properties of type-identified motor units in cat plantaris muscle. *J Neurophysiol*, *53*(5), 1303-1322. https://doi.org/10.1152/jn.1985.53.5.1303

Appendix A – Changes to Proposed Thesis

Significant changes from the originally proposed thesis occurred, however, they were not documented via the thesis proposal amendment form process. See below for undocumented changes.

Date of thesis proposal:

04/2020.

Thesis Advisory Committee:

Supervisor: Michael Tschakovsky

Committee Member: Brendon Gurd

Committee Member: Chris McGlory

Thesis study 1, undocumented methodology design changes:

1. Because of COVID related personnel limitations, the experimental model was changed from the lower leg (tibialis anterior) to the forearm (flexor digitorum superficialis).

2. Because of a malfunction of laboratory equipment, we did not make electroencephalography measurements.

Appendix B – Control of Oxidative Phosphorylation

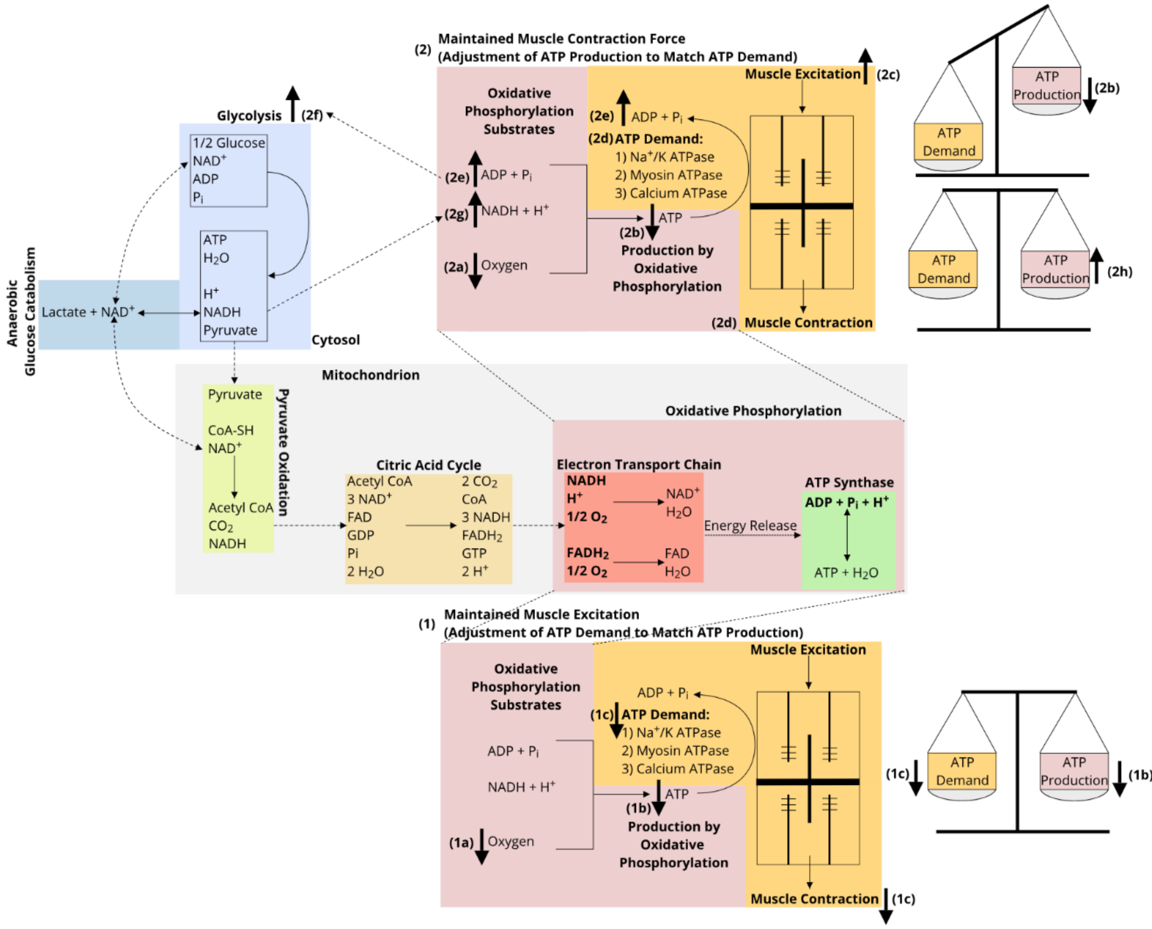

Figure 6-1. (1) Under conditions of maintained muscle excitation, exercising muscle ATP demand adjusts to changes in ATP production. A decrease in oxygen delivery (1a) leads to a decrease in ATP production by oxidative phosphorylation (1b). Without a compensatory increase in muscle excitation, ATP demand decreases to match ATP production (1c). (2) Under conditions of maintained muscle contraction force, exercising muscle ATP production is adjusted to match ATP demand. A decrease in oxygen delivery (2a) leads to a decrease in ATP production via oxidative phosphorylation (2b). Muscle excitation is increased (2c) to prevent a decrease in muscle contraction force and therefore ATP demand is necessarily maintained (2d). ATP demand now exceeds ATP production, causing an increase in ADP and P_i (2e). Increased ADP and P_i in combination with reduced ATP causes increased glycolytic flux. Increased glycolytic flux increases NADH and H^+ needed to drive oxidative phosphorylation (2g). Combined, the increase in in ADP, P_i, NADH and H^+ restores the rate of ATP production via oxidative phosphorylation – matching ATP production to demand (2h).

Appendix C – Additional Experimental Design Information

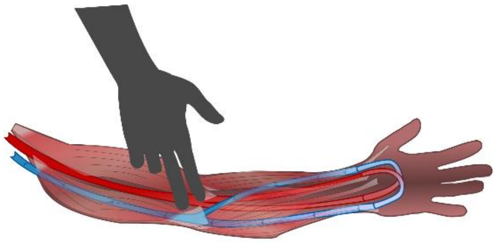

Figure 6-2. In thesis study 1 (Chapter 3 – Experimental Design), manual brachial artery compression was completed for 4-min to reduce brachial artery mean blood velocity by 50% of steady state measures (i.e., hypoperfusion condition). Under the control condition, manual compression was completed just next to the brachial artery to simulate compression discomfort without causing a decrease in forearm blood flow.

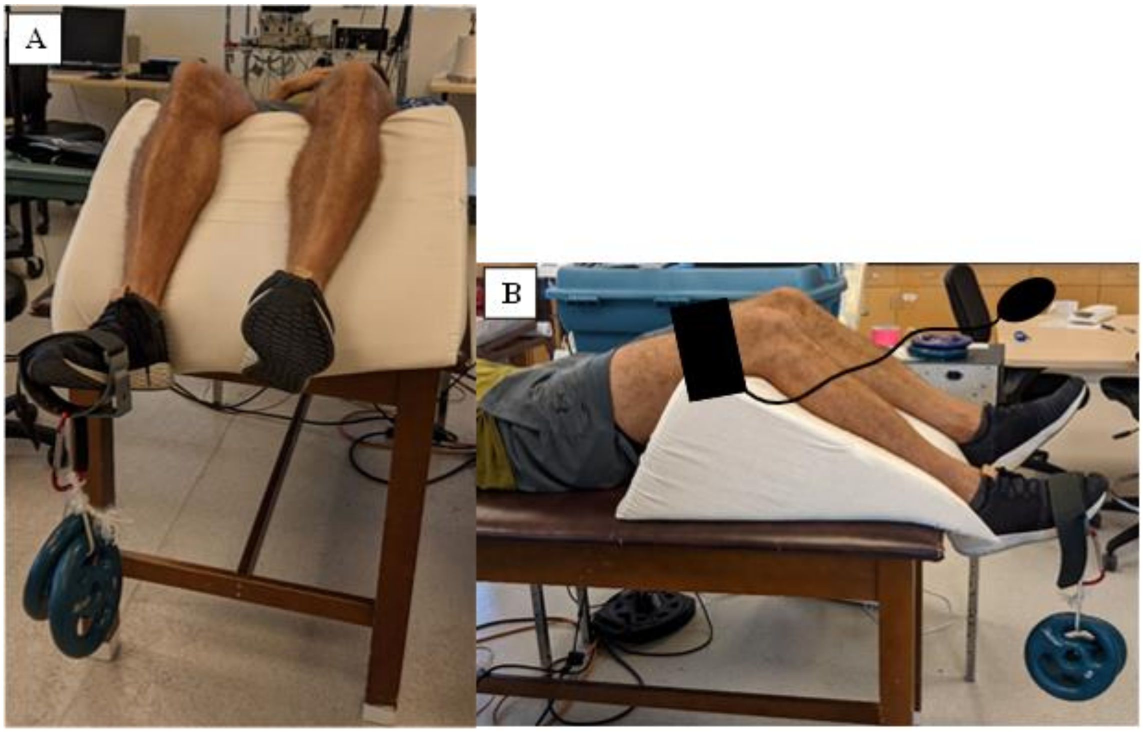

Figure 6-3. In thesis study 2 (Chapter 4 – Metaboreflex protocol), metaboreflex stimulation was achieved by inflating blood pressure cuffs (~200-220 mmHg) positioned bi-laterally just above the knees and then asking participants to complete rhythmic bi-lateral dorsiflexion exercise in rhythm with handgrip contractions. A ten-pound weight was secured bi-laterally to the participants feet during dorsiflexion exercise. Dorsiflexion exercise was stopped after 2-min though the blood pressure cuff remained inflated for 4-min.

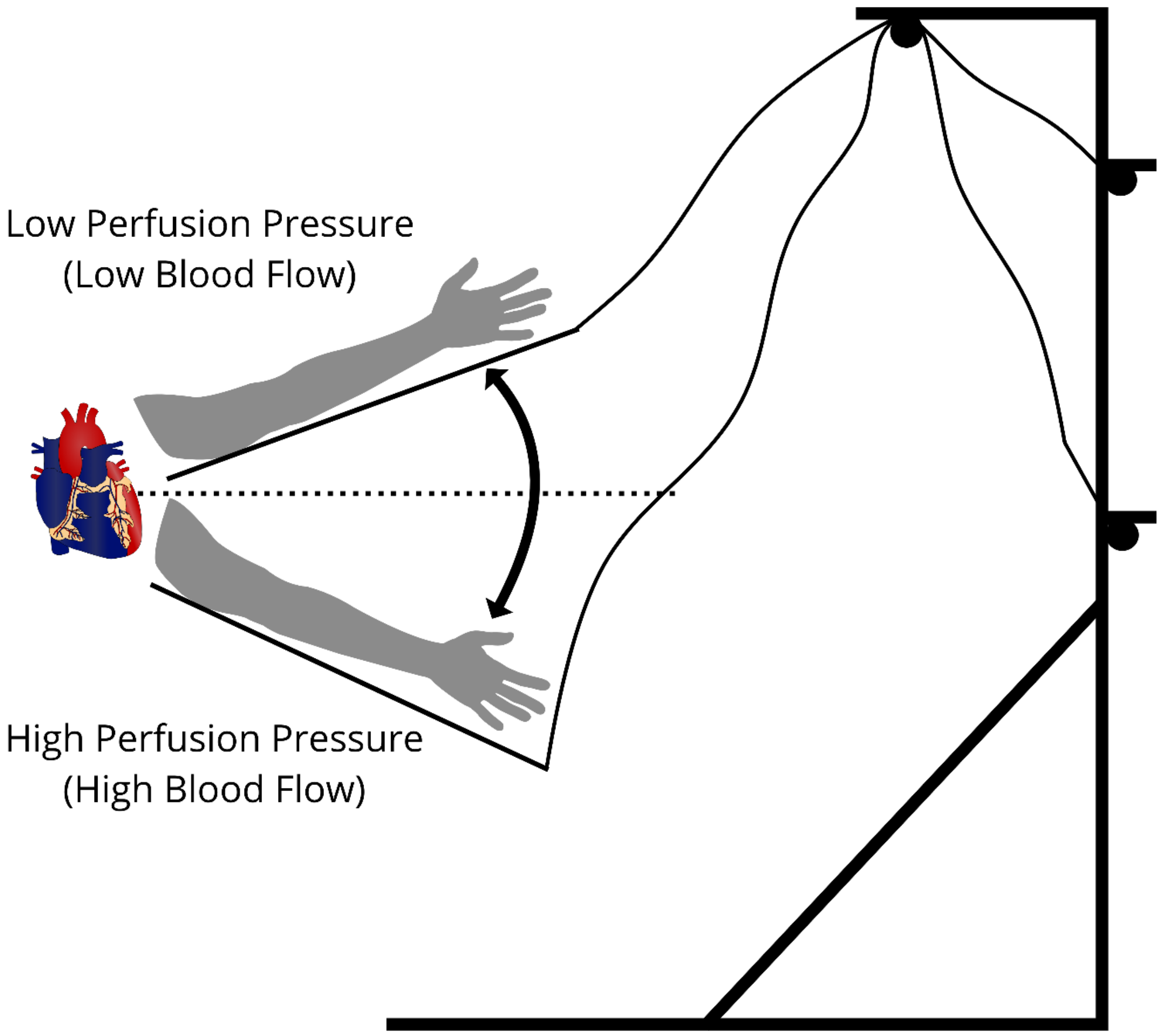

Figure 6-4. In thesis study 3 (Chapter 5 – Experimental Design and Conditions), to create perfusion pressure changes we used a pulley system to rapidly move the exercising arm – taking advantage of hydrostatic pressure differences. To create a low perfusion pressure condition the arm is started in an above heart position. Next, the arm is lowered to below heart level to increase perfusion pressure to match that of the high perfusion pressure condition. And finally, the arm is returned to an above heart position to restore low perfusion pressure.